Technical Report Documentation Page

1. Report No.	2. Government Accession No.	3. Recipient's Catalog No.
FHWA/TX-05/0-4196-2		

4. Title and Subtitle	5. Report Date
DEVELOPMENT OF GUIDELINES FOR IDENTIFYING AND TREATING LOCATIONS WITH A RED-LIGHT-RUNNING PROBLEM	September 2004
	6. Performing Organization Code

7. Author(s)	8. Performing Organization Report No.
James Bonneson and Karl Zimmerman	Report 0-4196-2

9. Performing Organization Name and Address	10. Work Unit No. (TRAIS)
Texas Transportation Institute The Texas A&M University System College Station, Texas 77843-3135	11. Contract or Grant No. Project No. 0-4196

12. Sponsoring Agency Name and Address	13. Type of Report and Period Covered
Texas Department of Transportation Research and Technology Implementation Office P.O. Box 5080 Austin, Texas 78763-5080	Technical Report: September 2002 - August 2004
	14. Sponsoring Agency Code

15. Supplementary Notes

Project performed in cooperation with the Texas Department of Transportation and the Federal Highway Administration.
Project Title: Safety Impact of Red-Light-Running in Texas: Where is Enforcement Really Needed?

16. Abstract

The problem of red-light-running is widespread and growing; its cost to society is significant. However, the literature is void of quantitative guidelines that can be used to identify and treat problem locations. Moreover, there has been concern voiced over the validity of various methods used to identify problem locations, especially when automated enforcement is being considered. The objectives of this research project were to: (1) quantify the safety impact of red-light-running at intersections in Texas, and (2) provide guidelines for identifying truly problem intersections and whether enforcement or engineering countermeasures are appropriate.

This report documents the work performed and conclusions reached as a result of a two-year research project. During the first year, the researchers determined that about 37,700 red-light-related crashes occur each year in Texas. Of this number, 121 crashes are fatal. These crashes have a societal cost to Texans of about $2.0 billion dollars annually. During the second year, red-light-related crash and violation prediction models were developed. These models were used to quantify the effect of various intersection features on crash and violation frequency. The insights obtained were used to identify effective engineering countermeasures. The models were also used to quantify the effectiveness of officer enforcement. Procedures were developed to identify and rank problem locations. The models and procedures were incorporated in a *Red-Light-Running Handbook* that is intended to serve as a guide to help engineers reduce red-light-related crashes.

17. Key Words	18. Distribution Statement
Signalized Intersection, Red-Light-Running, Right Angle Collisions	No restrictions. This document is available to the public through NTIS: National Technical Information Service Springfield, Virginia 22161 http://www.ntis.gov

19. Security Classif.(of this report)	20. Security Classif.(of this page)	21. No. of Pages	22. Price
Unclassified	Unclassified	136	

DEVELOPMENT OF GUIDELINES FOR IDENTIFYING AND TREATING LOCATIONS WITH A RED-LIGHT-RUNNING PROBLEM

by

James Bonneson, P.E.
Research Engineer
Texas Transportation Institute

and

Karl Zimmerman, P.E.
Assistant Research Engineer
Texas Transportation Institute

Report 0-4196-2
Project Number 0-4196
Project Title: Safety Impact of Red-Light-Running in Texas:
Where is Enforcement Really Needed?

Performed in cooperation with the
Texas Department of Transportation
and the
Federal Highway Administration

September 2004

TEXAS TRANSPORTATION INSTITUTE
The Texas A&M University System
College Station, Texas 77843-3135

DISCLAIMER

The contents of this report reflect the views of the authors, who are responsible for the facts and the accuracy of the data published herein. The contents do not necessarily reflect the official view or policies of the Federal Highway Administration (FHWA) and/or the Texas Department of Transportation (TxDOT). This report does not constitute a standard, specification, or regulation. It is not intended for construction, bidding, or permit purposes. The engineer in charge of the project was James Bonneson, P.E. #67178.

NOTICE

The United States Government and the State of Texas do not endorse products or manufacturers. Trade or manufacturers' names appear herein solely because they are considered essential to the object of this report.

ACKNOWLEDGMENTS

This research project was sponsored by the Texas Department of Transportation and the Federal Highway Administration. The research was conducted by Drs. James Bonneson and Karl Zimmerman with the Texas Transportation Institute.

The researchers would like to acknowledge the support and guidance provided by the project director, Mr. Wade Odell, and the members of the Project Monitoring Committee, including: Mr. Punar Bhakta, Mr. Mike Jedlicka, Mr. Danny Magee, Mr. Ismael Soto (all with TxDOT), and Mr. Walter Ragsdale (with the City of Richardson). In addition, the researchers would like to acknowledge the valuable assistance provided by Dr. Dominique Lord, Mr. George Balarezo, Mr. Ho Jun Son, and Mr. Greg Morin during the conduct of the field studies and the subsequent data reduction activities. Their efforts are greatly appreciated.

TABLE OF CONTENTS

TABLE OF CONTENTS (Continued)

LIST OF FIGURES

Figure **Page**

LIST OF TABLES

Table **Page**

CHAPTER 1. INTRODUCTION

OVERVIEW

Retting et al. (*1*) found that drivers who disregard traffic signals are responsible for an estimated 260,000 "red-light-running" crashes each year in the U.S., of which about 750 are fatal. These crashes represent about 4 percent of all crashes and 3 percent of fatal crashes. Retting et al. also found that red-light-running crashes accounted for 5 percent of all injury crashes. This over-representation (i.e., 5 percent injury vs. 4 percent overall) led to the conclusion that red-light-related crashes are typically more severe than other crashes.

A recent review of the Fatality Analysis Reporting System (FARS) database by the Insurance Institute for Highway Safety indicated that an average of 95 motorists die each year on Texas streets and highways as a result of red-light violations (*2*). A ranking of red-light-related fatalities on a "per capita" basis indicates that Texas has the fourth highest rate in the nation. Only the states of Arizona, Nevada, and Michigan experienced more red-light-related fatalities per capita. Moreover, the cities of Dallas, Corpus Christi, Austin, Houston, and El Paso were specifically noted to have an above-average number of red-light-related crashes (on a "per capita" basis) relative to other U.S. cities with populations over 200,000.

An examination of the Texas Department of Public Safety crash database by Quiroga et al. (*3*) revealed that the reported number of persons killed or injured in red-light-related crashes in Texas has grown from 10,000 persons/yr in 1975 to 25,000 persons/yr in 1999. They estimate that these crashes currently impose a societal cost on Texans of $1.4 to $3.0 billion annually.

The problem of red-light-running is widespread and growing; its cost to society is significant. A wide range of potential countermeasures to the red-light-running problem exist. These countermeasures are generally divided into two broad categories: engineering countermeasures and enforcement countermeasures. A study by Retting et al. (*4*) has shown that countermeasures in both categories are effective in reducing the frequency of red-light violations.

Unfortunately, guidelines are not available for identifying intersections with the potential for safety improvement (i.e., "problem" intersections) and whether engineering or enforcement is the most appropriate countermeasure at a particular intersection. Moreover, there has been concern voiced over the validity of various methods used to identify problem locations, especially when automated enforcement is being considered (*5, 6*). There has also been concern expressed that engineering countermeasures are sometimes not fully considered prior to the implementation of enforcement (*5, 6, 7*).

RESEARCH OBJECTIVE

The objectives of this research project were to: (1) quantify the safety impact of red-light-running at intersections in Texas, and (2) provide guidelines for identifying truly problem intersections and whether enforcement or engineering countermeasures are appropriate. These objectives were achieved through the satisfaction of the following goals:

- Identify the frequency of crashes caused by red-light-running at intersections on the Texas highway system and in the larger Texas cities.
- Develop guidelines for identifying intersections with abnormally high rates of red-light violations and related crashes.
- Develop guidelines for identifying the most effective countermeasure (or countermeasures) for application at a given intersection.

The research conducted in pursuit of these goals is documented in this report. The findings were used to develop a handbook for use by engineers when addressing red-light-related problems.

RESEARCH SCOPE

This research project addressed red-light violations that occur at signalized intersections on Texas streets and highways. The focus was on red-light violations by drivers traveling through the intersection (as opposed to those that turn at the intersection). Guidelines were developed that consider both violation and crash frequency as indicators of a red-light-related problem.

RESEARCH APPROACH

This project's research approach was based on a 2-year program of field investigation, data analysis, and guideline development. The research findings were used to develop a guideline document to assist in the identification of problem locations and the implementation of countermeasures to reduce red-light-related crashes. During the first year of the research, the frequency of red-light violations on the Texas highway system and in the larger Texas cities was quantified. In the second year, area-wide officer enforcement was evaluated as a treatment for red-light-related safety problems. Research in the second year also produced models for estimating the expected frequency of violations and crashes. The findings from both years of research were combined to develop guidelines for identifying and treating problem locations on an area-wide and a local intersection basis.

The main product of this research is the *Red-Light-Running Handbook: An Engineer's Guide to Reducing Red-Light-Related Crashes*. This document provides technical guidance for engineers who desire to locate and treat intersections with red-light-related safety problems. It also provides quantitative information on the effectiveness of the more promising countermeasures. The analytic procedures in the *Handbook* are implemented in an Excel ® spreadsheet. The spreadsheet is available at http://tti.tamu.edu/documents/0-4196-treat.xls.

CHAPTER 2. INTERSECTION RED-LIGHT-RELATED CRASH FREQUENCY

OVERVIEW

This chapter describes the development of a procedure for identifying intersections with the potential for red-light-related safety improvement (i.e., "problem" intersections). The application of this procedure identifies intersections likely to need some type of improvement and for which the treatment is likely to be cost-effective. To this end, the procedure can be used to identify and rank intersections with an above average frequency of red-light-related crashes. The procedure focuses on the individual approach to a signalized intersection. It considers crashes caused by through vehicles on the approach. It does not address intersection approaches that terminate at the intersection (i.e., the stem approach of a "T" intersection).

A review of the literature on the topics of problem location identification and crash prediction is described in the next section. Then, a site selection and data collection plan is described. Next, the assembled database is examined and used to calibrate a crash prediction model. Finally, the calibrated model is used to develop the procedure for identifying problem intersection approaches.

LITERATURE REVIEW

This section reviews the literature related to procedures for identifying problem intersections. It is not an exhaustive review. Rather, it references two key documents that describe the findings of a comprehensive review of site "screening" techniques. This section also summarizes recent research in the area of red-light-related crash prediction models and factors correlated with red-light violation frequency.

Procedures for Identifying Problem Intersections

Hauer (*8*) examined alternative techniques for identifying locations for potential safety improvement. He identified eight techniques that are, or could be, used to identify problem locations. These techniques are listed in Table 2-1.

Several of the techniques listed in Table 2-1 are based on the use of crash frequency and others are based on the use of crash rate. Those based on frequency tend to direct the search for problem locations to high-volume locations. These techniques may not find the most unsafe (i.e., risky) locations; however, improvements to locations with frequent crashes tend to be the most efficient in terms of the cost-effective reduction in crashes. In contrast, techniques based on rate tend to direct the search to locations where the risk of a crash is highest, regardless of crash frequency. Improvements to locations with a high crash rate tend to be most sensitive to the level of motorist safety but may not be cost-effective to provide.

Table 2-1. Alternative Techniques for Quantifying Improvement Potential.

No.	Technique	Rationale
1	Reported crash frequency, F_o	Treat sites with the most frequently observed crashes.
2	Reported crash rate, R_o	Treat sites where the reported crash risk is highest.
3	Expected crash frequency, F_n	Treat sites with the highest expected frequency of crashes.
4	Expected crash rate, R_n	Treat sites where the expected crash risk is highest.
5	Difference in crash frequency, $F_o - F_n$	Treat sites with the highest potential for crash reduction.
6	Difference in crash rate, $R_o - R_n$	Treat sites with the highest potential for risk reduction.
7	Scaled difference in frequency[1], $(F_o - F_n)/s_F$	Same as 5 but weigh by degree of uncertainty in potential benefit.
8	Scaled difference in rate[2], $(R_o - R_n)/s_R$	Same as 6 but weigh by degree of uncertainty in potential benefit.

Notes:
1 - s_F = standard deviation of the difference in crash frequency.
2 - s_R = standard deviation of the difference in crash rate.

As noted by Hauer (*8*), present practice is to use Technique 1, 2, or both to identify problem locations. However, these two techniques can mistakenly identify sites as problem locations when, in fact, their recent association with a relatively frequent number of crashes is due only to the randomness in crash occurrence (and not to a degradation in safety). Techniques 3 through 8 are intended to overcome these deficiencies.

Techniques 3 and 4 use the *expected* (or average) crash frequency or rate to identify problem locations. Hauer (*9*) has advocated the use of the empirical Bayes method to compute the expected crash frequency or crash rate. This method estimates an expected crash frequency (or rate) by computing a weighted average of the reported crash frequency (or rate) and a predicted frequency (or rate). The predicted frequency is obtained from a model that is calibrated using crash data from several sites with similar geometry and traffic control. The expected frequency (or rate) is preferred to the reported frequency (or rate) for locating problem locations because the misleading effects of randomness in crash occurrence are minimized.

The difference in crash frequency (or rate) used in Techniques 5 and 6 is a further improvement on Techniques 3 and 4. This difference is intended to identify sites where the potential for safety improvement is greatest. In this regard, the difference identifies sites with "above average" crash frequencies (or rates). The rationale follows that these sites are most likely to demonstrate the most significant reduction in crashes as a result of treatment. Sites that have "below average" crash frequencies (or rates) are not likely to realize as large a reduction in crashes (or risk) and, hence, are not likely to be cost-effective to treat.

Techniques 7 and 8 represent one final enhancement to Techniques 5 and 6. Specifically, the enhancement is that of computing the standard deviation of the estimated difference in frequency (or rate) and using it to "scale," or weigh, this difference based on the degree of uncertainty

associated with it. In this manner, locations with a large difference might not be identified as being a problem location if there is considerable uncertainty associated with the estimated difference in crash frequency (or rate).

Persaud et al. (*10*) evaluated the efficiency of Techniques 1, 2, 3, and 5. They found that Technique 5 was the most efficient at identifying intersections with treatable crashes. Technique 2 was the least efficient technique.

Challenges of Identifying Red-Light-Related Crashes

There are several challenges to the accurate identification of red-light-related crashes. Such crashes are not explicitly identified on the crash report forms used by most states (including Texas). As a result, the identification of red-light-related crashes requires a thorough review of the crash report with consideration given to the following crash attributes: contributing cause, crash type, traffic control, and offense charged. The officer narrative and crash diagram also provide important clues to the cause of the crash.

Unfortunately, the narrative and diagram are rarely available in a coded crash database. This sole use of a coded database can lead to errors. The extent of these errors was recently investigated by Bonneson et al. (*11*). They identified the attributes commonly used to identify red-light-related crashes using coded databases. They found that various combinations of the following three attributes were commonly used:

- intersection relationship: "at" the intersection,
- crash type: "right-angle," and
- first contributing factor: "disregard of stop and go signal."

To test the accuracy of these three attributes, Bonneson et al. (*11*) used them to identify the red-light-related crashes at 70 signalized intersections in three Texas cities during a 3-year period. A total of 274 crashes satisfied these three attributes. However, after the acquisition and review of the peace officer reports for all 3338 crashes that occurred in the vicinity of these intersections, it was found that four crashes in the pool of 274 were not truly red-light-related and that 232 red-light-related crashes were *not* identified (i.e., they were missed). In summary, crash attributes commonly thought to be useful for identifying red-light-related crashes may identify only about 54 percent (= [274 − 4]/[274 − 4 + 232] ×100) of those that actually occur. Bonneson et al. (*11*) found that the following attributes would identify 79 percent of the red-light-related crashes:

- intersection relationship: "at" the intersection, and
- first contributing factor: "disregard of stop and go signal" or "disregard stop sign or light."

Red-Light-Related Safety Prediction Models

Mohamedshah et al. (*12*) used crash data obtained from the State of California to develop a model for predicting the frequency of red-light-related crashes on an intersection approach. Their database included 4709 red-light-related crashes that occurred during a 4-year period at 1756 four-legged, urban intersections.

A variety of factors were considered in the calibration of a prediction model. These factors included: annual average daily traffic (AADT) on both intersecting streets, number of lanes crossed, presence of left-turn bays, and type of traffic control (i.e., pretimed, actuated, or semi-actuated). Other factors were also considered; however, only the factors listed were found to be statistically significant. The data reported by Mohamedshah et al. (*12*) were used to examine the effect of AADT and lanes crossed on red-light-related crashes. The results of this examination are shown in Figure 2-1. The number of lanes crossed was converted to an equivalent distance required by the red-light-running driver to clear the intersection.

The trends shown in Figure 2-1a indicate that the annual crash frequency on the major-street intersection approach ranges from 0.2 to 0.6 crashes per year over the range of AADTs. Figure 2-1b indicates that crashes are somewhat insensitive to clearance distance for distances up to 130 ft. However, crashes were found to increase with clearance distances in excess of 130 ft. This effect of distance was found to be significant only for vehicles on the cross-street approaches.

Recent research by Bonneson et al. (*13*) found that there was a positive correlation between red-light violations and related crashes. Hence, it is logical that factors that influence violations may also influence crash frequency. This section reviews several factors found by Bonneson et al. and others to be correlated with red-light violations.

Review of Factor Effects

Bonneson et al. (*13*) found that the following factors were correlated with violation frequency: approach flow rate, cycle length, yellow interval duration, running speed, clearance path length, platoon ratio, use of signal head back plates, and use of advance detection. Their effect on red-light violation frequency is illustrated in Table 2-2 for specified changes in the factor value.

The information in Table 2-2 illustrates the individual effect of each factor on red-light violation frequency. The magnitude of the effect is dependent on the change of the associated factor. Specific changes are listed in Table 2-2; different changes may yield different effects on violation frequency. In general, a decrease in violations was found to be associated with a decrease in flow rate, an increase in yellow duration, a decrease in speed, an increase in clearance path length (i.e., a wider intersection), a decrease in platoon density, and the addition of signal head back plates.

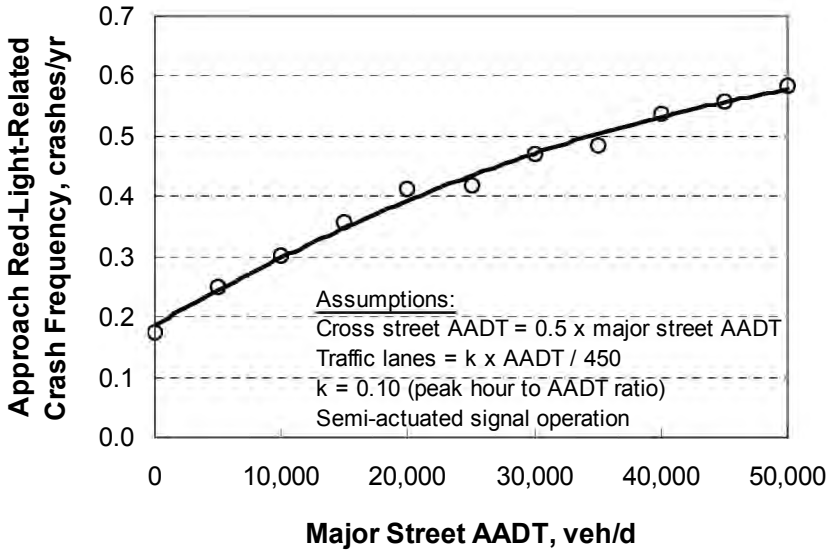

a. Effect of Major Street Traffic Volume.

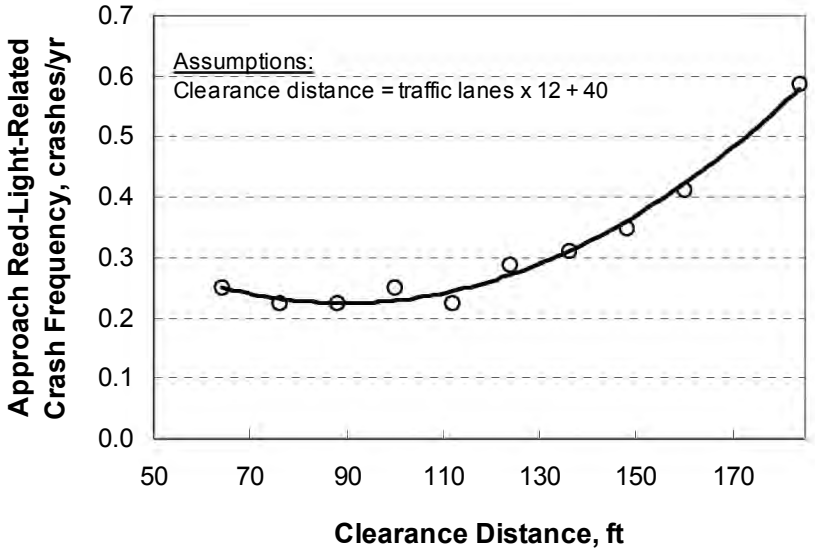

b. Effect of Clearance Distance.

Figure 2-1. Effect of Traffic Volume and Clearance Distance on Crash Frequency.

Table 2-2. Effect of Selected Factors on Red-Light Violation Frequency.

Factor	Effect of a Reduction in the Factor Value [1]		Effect of an Increase in the Factor Value [1]	
	Factor Change	Violation Freq. Change	Factor Change	Violation Freq. Change
Approach flow rate	-1.0 %	-1.0 %	+1.0 %	+1.0 %
Cycle length	from 90 to 70 s	+29 %	from 90 to 110 s	-18 %
Yellow interval duration	-1.0 s	+110 %	+1.0 s	-53 %
Running speed	-10 mph	-33 %	+10 mph	+45 %
Clearance path length	-40 ft	+81 %	+40 ft	-48 %
Platoon ratio	-1	-18 %	+1	+21 %
Use of back plates	remove back plates	+33 %	add back plates	-25 %

Note:
1 - Negative changes represent a reduction in the associated factor.

Examination of a Common Yellow Interval Equation

One equation for calculating the yellow interval duration is that proposed by Technical Committee 4A-16 working under the direction of the Institute of Transportation Engineers (ITE) (*14*). The equation recommended by this committee is:

$$Y = T_{pr} + \frac{V_a}{2\,d_r + 2\,g\,G_r} \quad \textbf{(1)}$$

where,
Y = yellow interval duration, s;
d_r = deceleration rate, use 10 ft/s^2;
g = gravitational acceleration, use 32.2ft/s^2;
G_r = approach grade, ft/ft;
T_{pr} = driver perception-reaction time, use 1.0 s; and
V_a = 85th percentile approach speed, ft/s.

The relationship between Equation 1 and red-light violation frequency was evaluated by Bonneson et al. (*13*). A "yellow interval difference" was estimated by subtracting the yellow interval computed with Equation 1 from the observed yellow interval at several intersection approaches. The relationship between this difference and the observed violation frequency is shown in Figure 2-2. The data in this figure indicate that there is a trend toward more red-light violations when the observed yellow duration is shorter than the computed duration. A regression analysis of the relationship between yellow interval difference and red-light violation frequency indicated that the relationship is statistically significant (i.e., $p = 0.001$). A similar finding was previously reported by Retting and Greene (*15*) in an examination of red-light violations at several intersections.

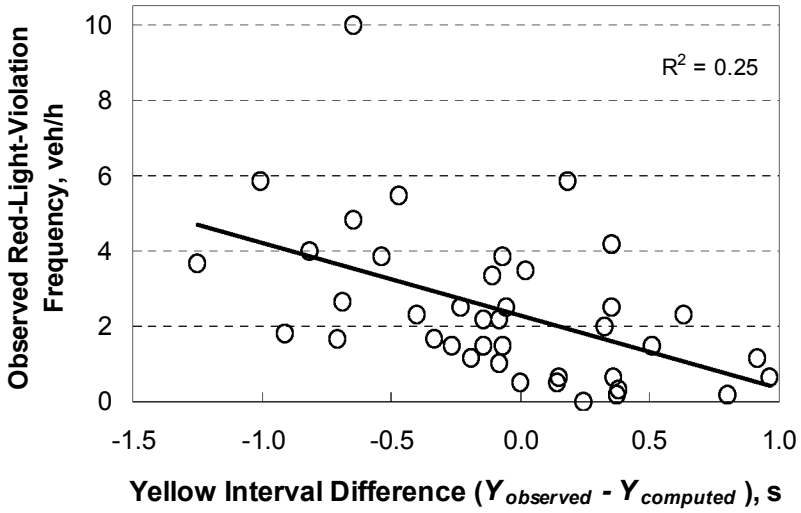

Figure 2-2. Red-Light Violation Frequency as a Function of Yellow Interval Difference.

SITE SELECTION AND DATA COLLECTION PLAN

This section describes the assembly of a database to be used in the development of a model for estimating red-light-related crash frequency. Specifically, it describes the field study sites, the criteria for their selection, and a data collection plan. Included in this description are the procedures used to acquire and process the data. The database includes the traffic volume, geometry, traffic control, and crash data for several intersection approaches in Texas. A field study "site" is defined herein to be one signalized intersection approach.

Site Selection Criteria

The intersection approaches selected for inclusion in the database were intended to be "typical" such that they collectively reflected a cross section of intersections in Texas. The specific criteria used to select these intersections included:

- signalized intersection (actuated or semi-actuated),
- moderate to high volumes,
- randomly selected intersection,
- speed limits between 30 and 50 mph,
- approaching drivers have a clear view of signal heads,
- intersection is in an urban or suburban area, and
- no significant changes in geometry (e.g., added lane), speed limit, or phasing in last 3 years.

In addition to the above criteria, it was essential that AADTs and crash reports were available from the cities within which the intersections were located.

Field Study Site Characteristics

A total of 47 intersections in three Texas cities (Corpus Christi, Garland, and Irving) were selected for further investigation. These intersections represent 181 approach study sites. Preliminary geometry, traffic control, and traffic volume data were obtained for each approach to ensure reasonable representation of several factors believed to be correlated with red-light-related crashes. The characteristics of these study sites are summarized in Table 2-3.

Table 2-3. General Site Characteristics–Intersection Approach Crash Analysis.

Characteristic	Statistic or Category	Location			Overall (all cities)
		City 1	City 2	City 3	
Intersections	Count	22	12	13	47
Approach study sites[1]	Count	87	44	50	181
Annual average daily traffic[2], veh/d	Average	19,528	25,374	20,329	21,170
	Standard deviation	8685	9065	11,578	9898
Approach speed limit[3], mph	Average	36	42	34	37
	Range	30 to 45	40 to 45	30 to 40	30 to 45
Through lanes on the approach[3]	Sites with 1 lane	10	0	4	14
	Sites with 2 lanes	71	28	37	136
	Sites with 3 lanes	6	16	9	31
Red signal light source[3]	Sites with bulb	58	44	50	152
	Sites with LED[4]	29	0	0	29
Signal head back plate[3]	Sites with back plates	6	44	50	100
	Sites w/o back plates	81	0	0	81

Notes:
1 - A field study site is defined as one intersection approach.
2 - AADT volumes listed represent an average for years 1999, 2000, and 2001.
3 - Data reflect conditions observed in 2003.
4 - LED: light-emitting diode. Signal indication utilizes LEDs as the light source in lieu of an incandescent lamp.

With few exceptions, all four approaches were studied at each intersection. In City 1, one approach had a relatively high posted speed limit so it was eliminated. In City 2, two intersections had a "T" configuration. In City 3, one intersection had a "T" configuration. At these intersections, only the two major-street approaches were included in the database. Protected-only left-turn phasing was used at 15 percent of the study sites. This percentage is consistent among each of the three cities.

Traffic volumes, speed limits, and through lane distributions were fairly consistent among cities. In contrast, the use of red LED signal indications and signal head back plates tended to be city-specific. This trend reflects the preferences of the city transportation agencies and was impossible to avoid during site selection. It resulted in a potential for confounding of the effect of these two characteristics with other city-related differences in driver behavior. With the exception of four sites, all sites used incandescent bulbs to illuminate the yellow indications.

Data Collection Plan

Crash reports for each of the study sites for the years 1999, 2000, and 2001 were requested from the traffic engineering departments of the three Texas cities. All total, 1018 crash reports were obtained for the 47 intersections. AADT volumes were also obtained for each intersection approach for the range of years 1998 to 2002. These volumes were adjusted (by extrapolation or interpolation) to obtain an estimate of the AADT for 2000.

Field visits were scheduled for each city during the Fall of 2003. During the visit, the intersection geometry and traffic control devices were measured or inventoried. Data collected for each approach study site included:

- street names and route numbers;
- designation as major or minor route;
- speed limit;
- number of through lanes;
- number of left-turn lanes;
- clearance path length;
- approach width;
- approach grade category (less than -2.0 percent, level, more than 2.0 percent);
- red and yellow signal lens illumination (LED, bulb);
- left-turn phasing (protected-only, protected-permitted, permitted-only, none);
- skew angle; and
- yellow interval duration (for through movement phases).

Each of the approach study sites was examined in the field to verify that it had not undergone significant physical change during the previous 4 years. Agency records were not readily available to confirm whether the yellow interval duration or speed limits had been changed during the previous 4 years. However, there was no evidence or indication from city staff that such changes had occurred.

The duration of the all-red interval for the through movement phases was estimated in the field by observation of the signal operation. These estimates indicated that an all-red interval in the range of 0.5 to 1.5 s was used at each site. Given the narrow range in these data, it was determined that a relationship between all-red duration and crash frequency would not likely be quantifiable. As a result, no further effort was expended to precisely quantify the all-red duration at each site. A

similar conclusion was reached with regard to grade because only a few sites in one city had grades in excess of 2.0 percent (up or down).

DATA ANALYSIS

This section characterizes the field study sites through a summary of the volume, geometry, traffic control, and crash databases assembled. It also describes the development and calibration of a crash prediction model. In the last section, a sensitivity analysis is conducted that describes the relationship between red-light-related crash frequency and various influential factors.

Database Summary

The database assembled for this research is summarized in this section. It includes the traffic volume, geometry, traffic control, and crash data for 181 approach study sites at 47 intersections. Initially, selected traffic characteristics are described. Then, the crash data are summarized.

Descriptive Statistics

Table 2-4 lists several statistics that describe conditions at the study sites. Path length was combined with speed limit to obtain a clearance time estimate. Clearance time represents the time required to traverse the intersection when traveling at the posted speed limit. An "implied" deceleration rate is computed by algebraically manipulating Equation 1 to yield deceleration rate as a function of speed limit, reaction time, and yellow duration.

Table 2-4. Speed-Based Site Characteristics–Intersection Approach Crash Analysis.

Characteristic	Statistic	Location			Overall (all cities)
		City 1	City 2	City 3	
Approach study sites	Count	87	44	50	181
Clearance path length[1], ft	Average	110	122	97	109
	Standard deviation	18	15	20	20
Clearance time[2], s	Average	2.1	2	1.9	2
	Standard deviation	0.4	0.3	0.4	0.4
Yellow interval duration[1], s	Average	3.7	4.3	4.8	4.1
	Range	3.1 to 4.7	4.0 to 4.7	4.1 to 5.3	3.1 to 5.3
Deceleration rate[3], ft/s^2	Average	9.9	9.5	6.7	8.9
	Standard deviation	0.8	0.4	0.7	1.5

Notes:
1 - Data reflect conditions observed in 2003.
2 - Clearance time = clearance path length/approach speed limit (in ft/s).
3 - Deceleration rate = 0.5 × approach speed limit (in ft/s)/(yellow – 1.0).

The statistics in Table 2-4 indicate reasonable balance in clearance path length and clearance path time among the study sites. The sites in City 3 have a tendency toward longer yellow intervals and lower deceleration rates. The lower deceleration rate results from the tendency of City 3 to have slower speeds and longer yellow intervals, relative to the other two cities.

Crash Characteristics

The crash reports were manually reviewed to determine the crash type, contributing factors, and whether the crash was a result of a red-light violation. The officer's narrative opinion and diagram were critical to this determination. Only those crashes that were definitively a result of a red-light violation were identified as such in the database. It was not possible to determine whether a crash was related to a red-light violation for 2 percent of the reports reviewed in this manner.

Each crash was assigned to one intersection approach based on the direction of travel of "vehicle 1," as specified on the crash report. The convention followed by the officers filling out the report is to identify vehicle 1 as the vehicle that was most likely the cause of the crash. In the case of red-light-related left-turn-opposed crashes, the through vehicle was identified as "vehicle 1."

A summary of the crash database is provided in Table 2-5. The crashes tabulated in this table correspond to crashes that occurred at the intersection (and not on its approaches). All total, 296 red-light-related crashes were reported during a 3-year period. These crashes represent 29 percent of all the crashes that occurred at the 47 intersections. About 44 percent of the red-light-related crashes were categorized as property-damage-only (PDO) crashes. The average crash rate is 0.55 red-light-related crashes per year per approach.

Table 2-5. Database Summary–Intersection Approach Crash Analysis.

Characteristic	Statistic	Location			Total (all cities)
		City 1	City 2	City 3	
Approach study sites	Count	87	44	50	181
Red-light-related crashes, crashes/3 years	Severe (i.e., injury or fatal)	71	67	27	165
	Property damage only	85	34	12	131
	Total:	156	101	39	296
	Average (cr/yr/app):	0.60	0.77	0.26	0.55
	Percent PDO [1]:	54	34	31	44
All crashes at intersection and associated with the approach, crashes/3 years	Severe (i.e., injury or fatal)	270	172	79	521
	Property damage only	327	107	63	497
	Total:	597	279	142	1018
	Average (cr/yr/app):	2.29	2.11	0.95	1.87
	Percent PDO [1]:	55	38	44	49

Note:
1 - PDO: property-damage-only crash.

Typical PDO percentages among cities for red-light-related crashes are in the range of 50 to 60 percent (*11*). An examination of the PDO percentages listed in Table 2-5 indicates that many PDO crashes in Cities 2 and 3 are not being reported. This problem makes it difficult to compare total crashes (i.e., PDO, injury, and fatal) among cities.

Model Development

This section describes the development of a crash prediction model. This model is developed using only severe crash data because of previously noted problems related to unreported PDO crashes in two of the three cities. Initially, the relationship between selected intersection factors and red-light-related crash frequency is examined. Then, the statistical analysis methodology used to calibrate the model is described. Finally, the calibrated model is presented.

Analysis of Factor Effects

The relationship between selected factors and red-light-related crash frequency is analyzed in this section. In general, the analysis of factor effects considered a wide range of factors and factor combinations; they include: intersection leg AADT, speed limit, yellow interval duration, clearance path length, clearance time, back plate presence, red signal light source, skew angle, grade, deceleration rate, left-turn phasing, number of lanes, major versus minor street designation, and city (unless otherwise indicated, all factors apply to the subject approach). Those factors and combinations that were found to be most highly correlated (in a relative sense) are discussed in this section. The crash data analyzed in this section include all crashes (i.e., PDO, injury, and fatal).

The effect of intersection leg AADT on red-light-related crash frequency is illustrated in Figure 2-3. The pattern in the data indicates that crash frequency increases with an increase in volume. This trend is similar to that shown previously in Figure 2-1a. A similar analysis of cross street AADT did not reveal a significant relationship with crash frequency.

There are only 18 data points shown in Figure 2-3. In fact, each data point in this figure (and in subsequent figures in this section) represents an average for 10 approach study sites. This aggregation was needed because plots with 181 data points tended to obscure the portrayal of trends in the data. To overcome this problem, the site data were sorted by the independent variable (e.g., leg AADT), placed in sequential groups of 10, and averaged over the group for both the independent and dependent variables. This procedure was only used for graphical presentation; the 181 site-based data points were used for all statistical analyses.

Figure 2-4 illustrates the relationship between yellow interval duration and crash frequency. The trend line indicates that crash frequency decreases with increasing yellow duration. It is likely that an increase in yellow duration has the most influence on crashes between left-turning vehicles (turning as a "permitted" movement at the end of the adjacent through phase) and opposing through vehicles. In this situation, a longer yellow time provides additional time for the last left-turning driver to find a gap through which to safely turn at the end of the phase. Bonneson et al. (*11*) report

that about 15 percent of all red-light-related crashes include a left-turning vehicle. The trend shown in Figure 2-4 is similar to that noted previously in Figure 2-2 with regard to red-light violations.

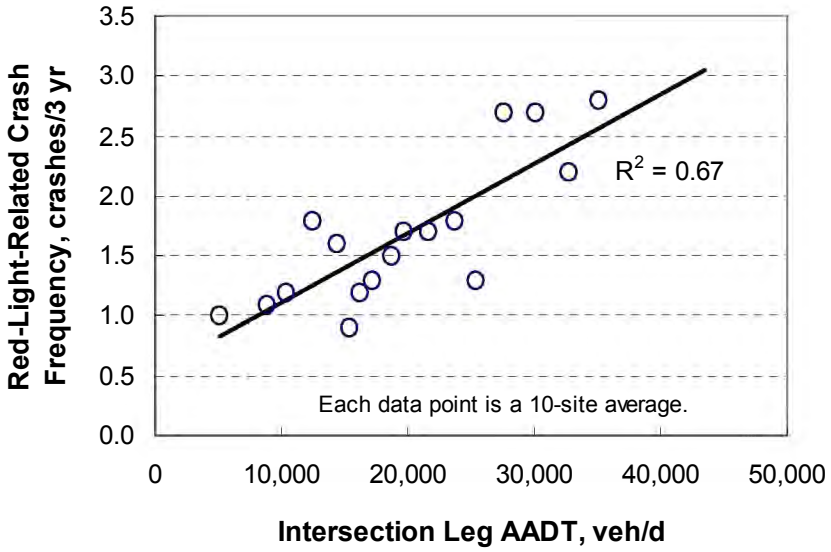

Figure 2-3. Crash Frequency as a Function of Leg AADT.

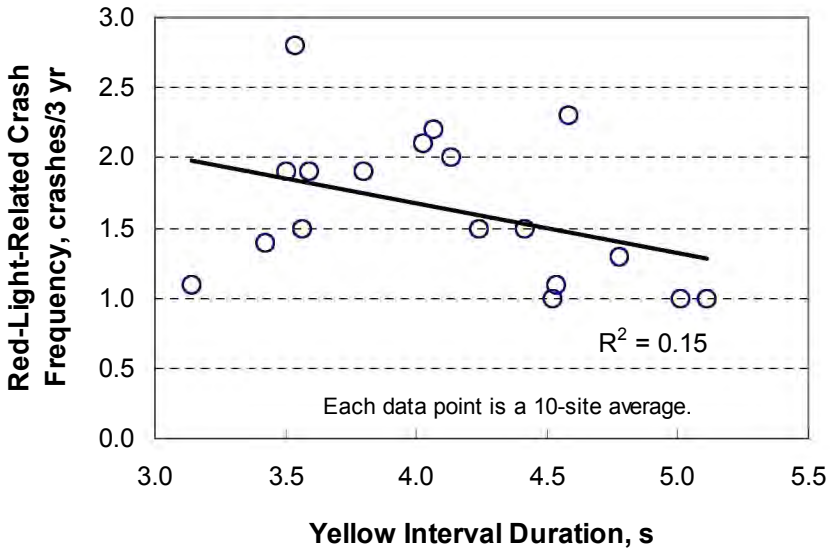

Figure 2-4. Crash Frequency as a Function of Yellow Interval Duration.

Figure 2-5 illustrates the relationship between approach speed limit and crash frequency. The trend shown in this figure indicates that crash frequency increases significantly with speed. Again,

the trend shown in this figure is similar to that noted previously in Table 2-2 with regard to the effect of speed on red-light violations.

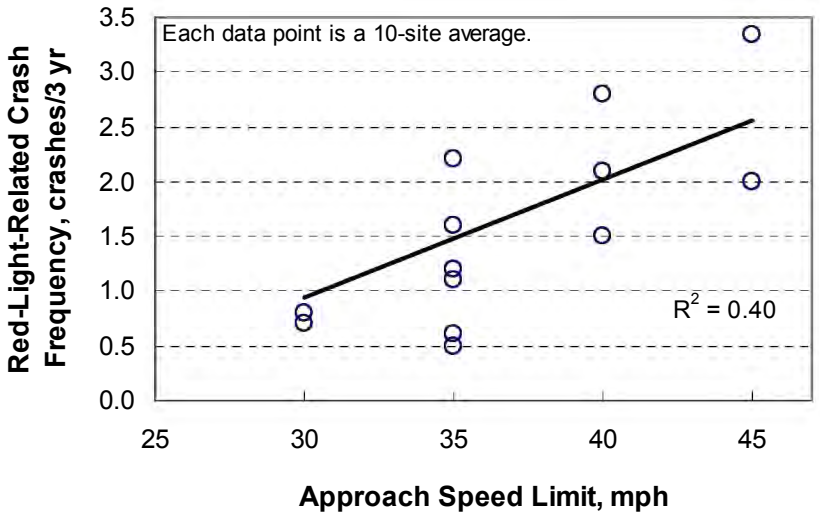

Figure 2-5. Crash Frequency as a Function of Approach Speed Limit.

The combined effect of both yellow duration and speed was examined in terms of the effect of "implied" deceleration rate on crash frequency. The result of this examination indicated that deceleration rate is highly correlated with crash frequency (e.g., $R^2 = 0.41$). Crash frequency was higher on those approaches where the yellow interval was associated with a higher deceleration rate.

The effect of clearance path length and clearance time on crash frequency was also examined. The effect of clearance time was more highly correlated than clearance path length. Its relationship with crash frequency is shown in Figure 2-6. The trend line indicates that crash frequency is lower on approaches with longer clearance times. It is similar to the trend noted previously in Table 2-2 with regard to the effect of clearance path length on red-light violations. It suggests that drivers are less likely to violate a red indication at wide intersections.

Further examination of the database indicates that almost all of the study sites have a clearance time in the range of 1.5 to 2.5 s. These times correspond to clearance path lengths in the range of 80 to 130 ft. In Figure 2-1b, path lengths in this range were not found to have a significant effect on crash frequency. Hence, the negative slope associated with the trend line in Figure 2-6 is somewhat contrary to that shown in Figure 2-1b.

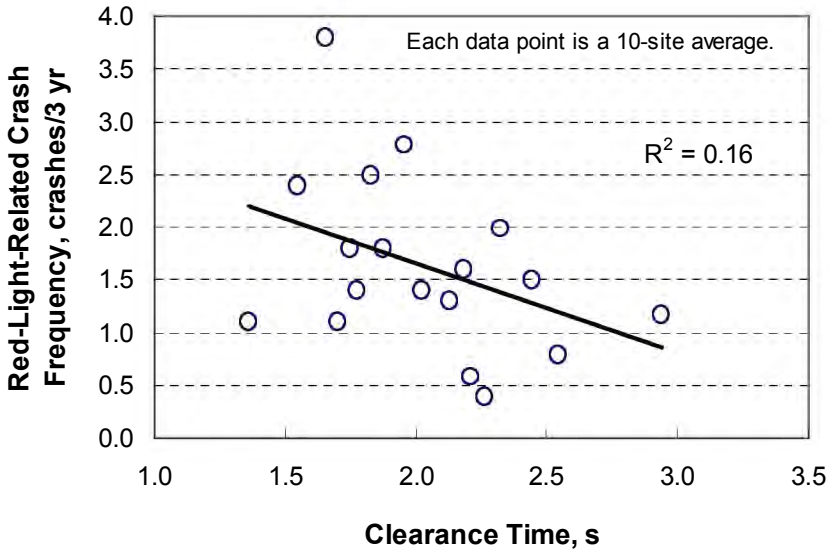

Figure 2-6. Crash Frequency as a Function of Clearance Time.

Statistical Analysis Method

A preliminary examination of the crash data indicated that they are neither normally distributed nor of constant variance, as is assumed when using traditional least-squares regression. Under these conditions, the generalized linear modeling technique, described by McCullagh and Nelder (*16*), is appropriate because it accommodates the explicit specification of an error distribution using maximum-likelihood methods for coefficient estimation.

The distribution of crash frequency can be described by the family of compound Poisson distributions. In this context, there are two different sources of variability underlying the distribution. One source of variability stems from the differences in the mean crash frequency m among the otherwise "similar" intersection approaches. The other source stems from the randomness in crash frequency at any given site, which likely follows the Poisson distribution.

Abbess et al. (*17*) have shown that if event occurrence at a particular location is Poisson distributed then the distribution of events of a group of locations can be described by the negative binomial distribution. The variance of this distribution is:

$$V(x) = E(m) + \frac{E(m)^2}{k} \quad \textbf{(2)}$$

where,

x = reported crash frequency for a given approach having an expected frequency of $E(m)$; and
k = dispersion parameter.

The Nonlinear Regression procedure (NLIN) in the SAS software was used to estimate the model coefficients (*18*). The benefits of using this procedure are: (1) nonlinear model forms can be evaluated, and (2) the dispersion parameter *k* can be held fixed during the model building process (as described in the next paragraph). The "loss" function associated with NLIN was specified to equal the log likelihood function for the negative binomial distribution. The procedure was set up to estimate model coefficients based on maximum-likelihood methods.

The goal of the regression model development was to build a parsimonious model. This type of model explains as much of the systematic variability as possible using the fewest number of variables. The procedure described by Sawalha and Sayed (*19*) was used to achieve this goal. It is based on a forward building procedure where one variable is added to the model at a time. The dispersion parameter *k* is held fixed at the best-fit value for a model with *p* variables while evaluating alternative models with *p*+1 variables (i.e., models where one candidate variable has been added). Only those variables that are: (1) associated with a calibration coefficient that is significant at a 95 percent confidence level, and (2) that reduce the scaled deviance by at least 3.84 ($= \chi^2_{0.05,1}$) are considered as candidates for inclusion. Of all candidate variables, the one that reduces the scaled deviance by the largest amount is incorporated into an "enhanced" model. A best-fit *k* is computed for the enhanced model and the process repeated until no candidate variables can be identified.

The advantage of the NLIN procedure is that *k* can be held fixed during the search for candidate variables. The disadvantage of this procedure is that it is not able to compute the best-fit value of *k* for the enhanced model. This disadvantage is overcome by using the Generalized Modeling (GENMOD) procedure in SAS with the enhanced model. GENMOD automates the *k*-estimation process using maximum-likelihood methods. Thus, GENMOD is used to regress the relationship between the reported and predicted crash frequencies (where the natural log of the predicted values is specified as an offset variable and the "log" link function is used). This new estimate of *k* from GENMOD is then used in a second application of NLIN and the process repeated until convergence is achieved between the *k* value used in NLIN and that obtained from GENMOD. Convergence is typically achieved in two iterations.

Model Calibration

The regression analysis revealed that crash frequency is correlated with leg AADT, yellow interval duration, speed limit, and clearance time. A separate examination of the "implied" deceleration rate (i.e., combining yellow duration and speed) indicated that it is a more accurate and logical predictor of crash frequency so it was substituted for the yellow duration and speed variables.

The analysis of clearance time was initially assumed to be linear (based on the trend in Figure 2-6). However, a more detailed analysis comparing the model predictions (without a clearance time term) with the observed clearance times indicated a non-linear relationship. The best-fit function for clearance time indicated that crash frequency decreased with increasing clearance times up to 2.5 s. Crash frequency then increased for clearance times in excess of 2.5 s. This latter effect is supported by the trend in Figure 2-1b. Several model forms were evaluated to reflect this

trend; however, the best fit was found using the positive deviation in clearance time from 2.5 s. An absolute-value function was used to quantify this deviation.

The best-fit crash prediction model was specified using the following equation:

$$E[r] = \left(\frac{Q_d}{1000}\right)^{b_1} e^{(b_0 + b_2 d_i + b_3 T_c)} \quad \textbf{(3)}$$

with,

$$d_i = \frac{1.47\ V_{sl}}{2\,(Y-1)} \quad \textbf{(4)}$$

$$T_c = \left| \frac{L_p}{1.47\ V_{sl}} - 2.5 \right| \quad \textbf{(5)}$$

where,

$E[r]$ = expected severe red-light-related crash frequency for the subject approach, crashes/yr;
d_i = deceleration rate implied by speed limit and yellow duration, ft/s^2;
T_c = clearance time deviation, s;
Q_d = intersection leg AADT (two-way total), veh/d;
V_{sl} = approach speed limit, mph;
Y = yellow interval duration, s;
L_p = clearance path length, ft; and
b_i = calibration coefficients (i = 0, 1, 2, 3).

The statistics related to the calibrated model are shown in Table 2-6. The calibration coefficient values shown can be used with Equations 3, 4, and 5 to estimate the severe red-light-related crash frequency for a given intersection approach.

A dispersion parameter k of 4.0 was found to yield a scaled Pearson χ^2 of 1.01. The Pearson χ^2 statistic for the model is 179, and the degrees of freedom are 177 (= $n - p - 1$ = 181 − 3 − 1). As this statistic is less than $\chi^2_{0.05,\,177}$ (= 209), the hypothesis that the model fits the data cannot be rejected. The R^2 for the model is 0.11. An alternative measure of model fit that is better suited to negative binomial error distributions is R_K^2, as developed by Miaou (*20*). The R_K^2 for the calibrated model is 0.45.

Table 2-6. Calibrated Model Statistical Description–Intersection Approach Crash Analysis.

Model Statistics		Value		
R^2 (R_K^2):		0.11 (0.45)		
Scaled Pearson χ^2:		1.01		
Pearson χ^2:		179 ($\chi^2_{0.05,\,177}$ = 209)		
Dispersion Parameter k:		4		
Observations n_o:		181 sites (165 crashes during a 3-year period)		
Standard Error:		±1.1 crashes/yr		
Range of Model Variables				
Variable	**Variable Name**	**Units**	**Minimum**	**Maximum**
Q_d	Intersection leg AADT	veh/d	1347	49,233
Y	Yellow interval duration	s	3.1	5.3
V_{sl}	Approach speed limit	mph	30	45
L_p	Clearance path length	ft	65	166
Calibrated Coefficient Values				
Variable	**Definition**	**Value**	**Std. Dev.**	**t-statistic**
b_0	Intercept	-4.70	0.85	-5.5
b_1	Effect of leg AADT	0.509	0.180	2.8
b_2	Effect of deceleration rate	0.186	0.065	2.9
b_3	Effect of clearance time deviation	0.533	0.287	1.9

The regression coefficients for the calibrated model are listed in the last rows of Table 2-6. The *t*-statistics shown indicate that all coefficients are significant at a 94 percent level of confidence or higher. A positive coefficient indicates that crashes increase with an increase in the associated variable value. Thus, approaches with higher deceleration rates are likely to have a higher frequency of red-light-related crashes. The use of clearance time *deviation* requires some caution when interpreting the coefficient sign. With this variable, crashes are found to *decrease* with increasing clearance time up to 2.5 s; thereafter, they *increase* with increasing clearance time.

The calibrated coefficients were inserted into Equation 3 to yield the following model:

$$E[r] = \left(\frac{Q_d}{1000}\right)^{0.509} e^{(-4.70 \,+\, 0.186\, d_i \,+\, 0.533\, T_c)} \qquad \textbf{(6)}$$

This model can be used with Equations 4 and 5 to estimate the severe red-light-related crash frequency for an intersection approach.

One means of assessing a model's fit is through the graphical comparison of the observed and predicted red-light-related crash frequencies. This comparison is provided in Figure 2-7. The trend line in this figure does *not* represent the line of best fit; rather, it is a "$y = x$" line. The data

would lie on this line if the model predictions exactly equaled the observed data. The clustering of the data around this line indicates that the model is able to predict crash frequency without bias.

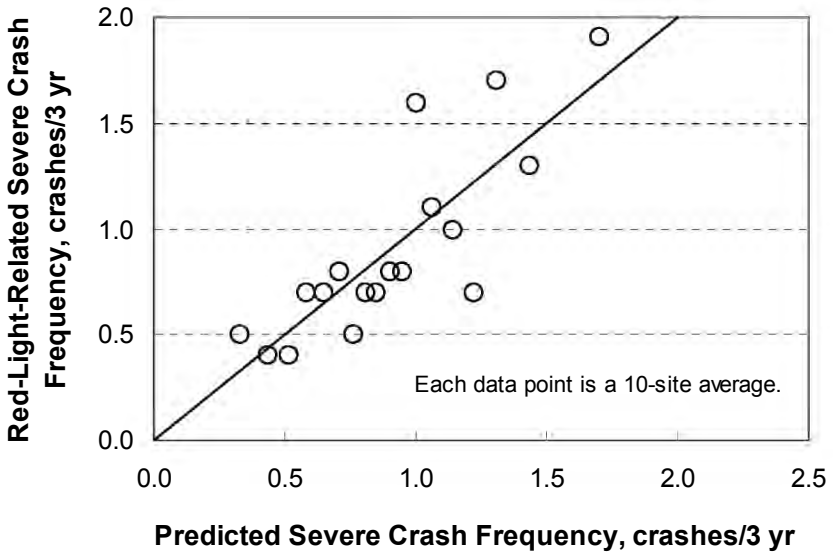

Figure 2-7. Comparison of Reported and Predicted Intersection Crash Frequency.

Sensitivity Analysis

This section describes the findings from a sensitivity analysis of the calibrated model. Examined are the effect of yellow interval duration, approach speed limit, and clearance path length on crash frequency.

Analysis Approach

The approach taken in this analysis was to examine the effect of a change in one variable on crash frequency while the other variables held constant. For a given variable, the relative effect of a small change (or deviation) from a "base" value was computed using Equation 6 twice, once using the "new" value and once using the base value. The ratio of the expected red-light violation frequencies was then computed as:

$$MF = \frac{E[r]_{new}}{E[r]_{base}} \quad \textbf{(7)}$$

where, *MF* represents a "modification factor" indicating the extent of the change in red-light-related crashes due to a change in the base value.

Yellow Interval Duration

The effect of a change in yellow interval duration on the frequency of red-light-related severe crashes is shown in Figure 2-8. Speed limit is also indicated in this figure because it was found to have a secondary influence on the effect of yellow duration. Equation 1 was used to compute a base yellow duration for each speed limit evaluated.

The trend in Figure 2-8 indicates that an increase in yellow interval duration decreases severe crashes. For example, an increase in yellow duration of 1.0 s is associated with an *MF* of about 0.6, which corresponds to a 40 percent reduction in crashes. This reduction is consistent with the effect of yellow interval duration on red-light violation frequency shown in Table 2-2.

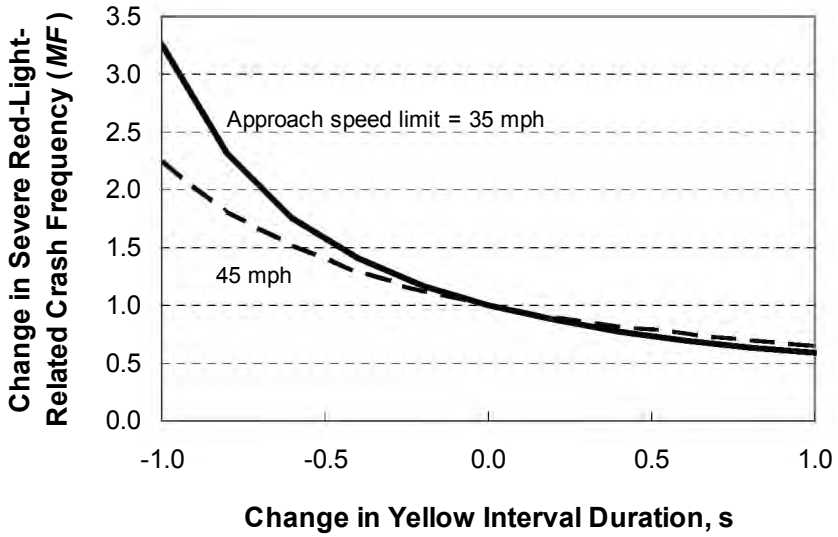

Figure 2-8. Effect of a Change in Yellow Interval Duration on Crash Frequency.

Approach Speed Limit

The effect of a change in speed limit on the frequency of severe red-light-related crashes is shown in Figure 2-9. This effect was found to be dependent on the actual speed limit. Equation 1 was used to compute a base yellow duration for each speed limit evaluated.

In general, the trend in Figure 2-9 indicates that an increase in speed limit is associated with an increase in crashes. For example, a 10-mph increase in the speed limit (where the base speed limit is 35 mph and clearance path length is 90 ft) is associated with an *MF* of 2.09. This *MF* corresponds to a 109 percent increase in crashes. A similar effect of speed change on red-light violations was identified in Table 2-2.

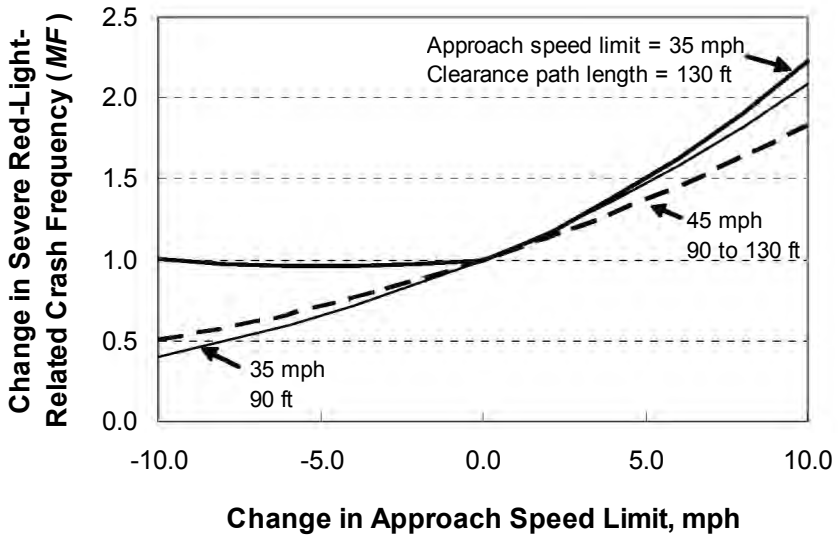

Figure 2-9. Effect of a Change in Speed Limit on Crash Frequency.

The thick solid line in Figure 2-9 illustrates the effect of exceptionally wide intersections on crash frequency. This line corresponds to a path length of 130 ft and a speed limit of 35 mph. It is effectively horizontal for speed reductions from 1 to 10 mph. In this range, crashes will not be decreased by a speed reduction because of the resulting increase in clearance time. In effect, the benefit of speed reduction is offset by increased exposure to crash, as measured by the increased time required to traverse the intersection.

Length of Clearance Path

The effect of a change in clearance path length on crash frequency is shown in Figure 2-10. In general, the trend in this figure indicates that an increase in path length is associated with a decrease in severe crashes. For example, if approach "B" has a clearance path of 90 ft and speed limit of 35 mph and approach "A" has a path that is 130 ft (40 ft longer), then the *MF* is about 0.68. This value indicates that approach "A" should have about 32 percent fewer crashes than approach "B" (all other factors being the same). This trend is consistent with that noted in Table 2-2 and reflects a decrease in red-light violations with increasing clearance path length.

The thick solid line in Figure 2-10 illustrates the effect of exceptionally wide intersections on crash frequency. This line corresponds to a path length of 130 ft and a speed limit of 35 mph. The "V" shape to this trend line indicates that increasing or decreasing the 130-ft path length will increase crashes. This breakpoint coincides with a clearance time of 2.5 s. It effectively defines an optimal intersection width for a given approach speed (or, alternatively, an optimum speed limit for a given width). These optimal widths are 110, 120, 150, and 165 ft for speed limits of 30, 35, 40, and 45 mph, respectively. The "V" shape is consistent with the trend line shown in Figure 2-1b.

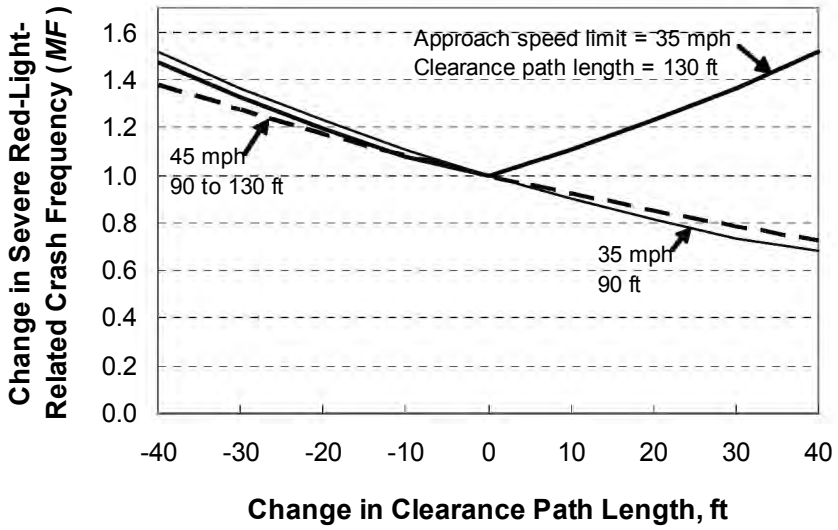

Figure 2-10. Effect of a Change in Clearance Path Length on Crash Frequency.

MODEL EXTENSIONS

Examination of a Common Yellow Interval Equation

This section examines the relationship between red-light-related crashes and the yellow interval duration computed using Equation 1. The approach taken in this examination was to compare the recorded crash frequency on an approach with the difference between the yellow duration observed at the approach and that computed for it using Equation 1. All crashes (i.e., PDO, injury, and fatal) were used for this examination. The results are shown in Figure 2-11.

The data in Figure 2-11 indicate that there is a trend toward fewer red-light-related crashes when the observed yellow duration is longer than the computed duration. A regression analysis of the relationship between yellow interval difference and crash frequency indicated that the relationship is statistically significant (i.e., $p = 0.001$). A similar finding with respect to red-light violations was shown in Figure 2-2.

Identify Sites with Potential for Red-Light-Related Safety Improvement

Hauer (*9*) and others have observed that intersections selected for safety improvement are often in a class of "high-crash" locations. As a consequence of this selection process, these intersections tend to exhibit significant crash reductions after specific improvements are implemented. While the observed reduction is factual, it is not typical of the benefit that could be derived from the improvement if it were applied to other locations. Hauer (*9*) advocates the use of

the empirical Bayes method to more accurately quantify the true crash reduction potential of a specific improvement or countermeasure.

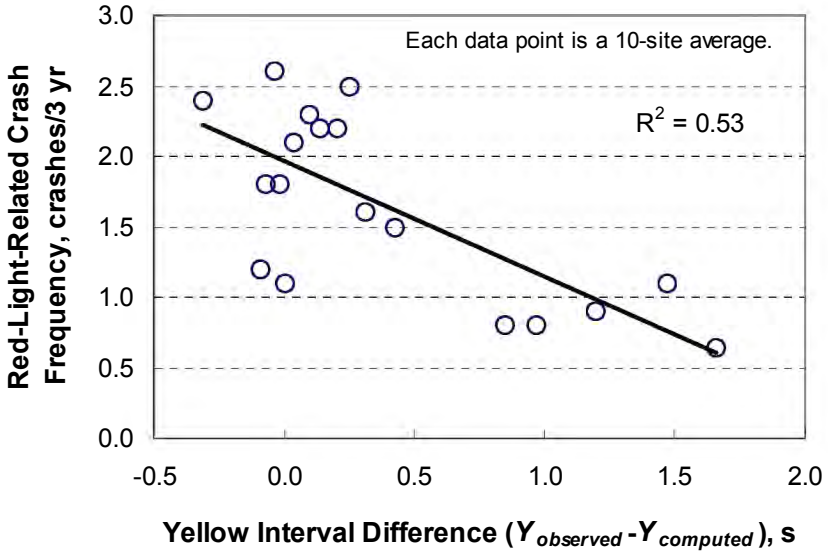

Figure 2-11. Crash Frequency as a Function of Yellow Interval Difference.

The empirical Bayes method can be used to obtain an unbiased estimate of the red-light-related crash frequency for a specific intersection approach. This estimate is based on a weighted combination of the reported frequency of red-light-related crashes x on the subject approach and the predicted red-light-related crash frequency $E[r]$ of similar approaches. The unbiased estimate (i.e., $E[r|x]$) is a more accurate estimate of the expected red-light-related crash frequency on the subject approach than either of the individual values (i.e., $E[r]$ or x). The following equations can be used to compute $E[r|x]$:

$$E[r|x] = E[r] \times weight + \frac{x}{y} \times (1 - weight) \quad \textbf{(8)}$$

with,

$$weight = \left(1 + \frac{E[r]\, y}{k} \right)^{-1} \quad \textbf{(9)}$$

where,

$E[r|x]$ = expected red-light-related crash frequency given that x crashes were reported in y years, crashes/yr;

x = reported red-light-related crash frequency, crashes;
y = time interval during which x crashes were reported, yr; and
weight = relative weight given to the prediction of expected red-light-related crash frequency.

The estimate obtained from Equation 8 can also be used (with Equation 6) to identify problem intersection approaches. Initially, Equation 6 is used to compute the expected red-light-related crash frequency for a "typical" approach. Then, Equation 8 is used to compute the expected red-light-related crash frequency *given* that x crashes were reported for the subject approach. These two estimates are then used to compute the following index:

$$Index = \frac{E[r|x] - E[r]}{\sqrt{\sigma_{r|x}^2 + \sigma_r^2}} \quad \textbf{(10)}$$

with,

$$\sigma_{r|x}^2 = (1 - weight)\ \frac{E[r|x]}{y} \quad \textbf{(11)}$$

$$\sigma_r^2 = \frac{E[r]^2}{k\ n_o} \quad \textbf{(12)}$$

where,
$\sigma_{r|x}^2$ = variance of $E[r|x]$;
σ_r^2 = variance of $E[r]$ for the typical intersection approach; and
n_o = number of observations used in the development of the model used to predict $E[r]$.

The values of k and n_o are provided in Table 2-6.

If the reported red-light-related crash frequency x, when expressed on an annual basis (i.e., as the quotient of x/y), is less than the expected crash frequency $E[r]$, then the index will be negative. If this situation occurs, the subject approach is not likely to have a red-light-related crash problem. However, the red-light violation frequency should also be evaluated to confirm this finding.

The index value is an indicator of the extent of the red-light-related crash problem for a given intersection approach. It is consistent with the "scaled difference in frequency" statistic identified in Table 2-1. In general, intersection approaches associated with a positive index value have more red-light-related crashes than the "typical" approach. An approach with an index of 2.0 is likely to have a greater problem than an approach with an index of 1.0. Greater certainty in the need for treatment can be associated with higher index values.

Occasionally, an intersection approach may not have its yellow interval or approach speed limit in conformance with agency policy. When this occurs, the computed index value should reflect

the deviation from agency policy. In this situation, two values of *E[r]* should be computed (i.e., *E[r, existing]* and *E[r, policy]*. The first value (i.e., *E[r, existing]*) is obtained using Equation 6 with variable values that reflect conditions on the subject intersection approach. This value is used in Equations 8 and 9 to estimate *E[r|x]* and *weight*, respectively.

The second value (i.e., *E[r, policy]*) represents the expected red-light-related crash frequency of the typical intersection approach having yellow intervals timed in accordance with agency policy and a speed limit established in accordance with agency policy. If agency policy does not address yellow interval timing, then Equation 1 should be used to compute the value of *Y* in Equation 4. If agency policy does not address procedures for establishing speed limits, then the 85th percentile approach speed should be used for V_{sl} in Equations 4 and 5. The value of *E[r, policy]* is then used in Equations 10 and 12 to estimate the *index* and σ_r^2, respectively.

CHAPTER 3. AREA-WIDE RED-LIGHT-RELATED CRASH FREQUENCY AND ENFORCEMENT EFFECTIVENESS

OVERVIEW

This chapter examines the effectiveness of officer enforcement at reducing red-light-related crashes. In this program, the enforcement agency specifically targets traffic control violations at signalized intersections using a heightened level of enforcement relative to that previously employed. The program is sustained for a period of time that can range from several months to 1 year. The objective of the program is to encourage drivers to be compliant with traffic control laws and more aware of traffic control devices; the overarching goal is to make the road safer, as evidenced by fewer crashes. This type of targeted enforcement is often coupled with a public awareness campaign that is intended to inform drivers and garner public support for the program.

The next section briefly reviews the various types of enforcement activities used to deter red-light violations and reduce the associated crashes. Then, a data collection plan is described. The plan is devised to provide the data needed to evaluate the effectiveness of enforcement programs using before-after methods. Next, the data collected are used to develop a model for predicting the annual number of reported red-light-related crashes within a city. This model is then used with the before-after data to quantify the effectiveness of enforcement. Finally, a procedure is described wherein the crash prediction model is used to identify cities with potential for safety improvement.

LITERATURE REVIEW

This section reviews the types of enforcement programs being used to address red-light violation problems. Initially, the goals of these programs are reviewed. Then, the characteristics of the officer enforcement program and the camera enforcement program are described. Finally, the effectiveness of these two programs are synthesized from findings reported in the research literature.

Program Goals

The need to establish specific goals for an enforcement program is an important, and early, step in the process of treating problem intersections. These goals provide a benchmark by which program success can be measured. They should be based on achieving a level of reduction in crashes or violations that: (1) is cost-effective in its use of enforcement, (2) recognizes that a small number of violations will always occur, and (3) is reasonable and acceptable to both the engineer and the public. The use of citation data as a measure of program effectiveness should be avoided because the number of citations issued in a period of time is strongly correlated with enforcement strategy and effort expended (i.e., productivity). It is not a strong indicator of a change in driver behavior.

There is little doubt that increasing enforcement will reduce red-light violations and related crashes. However, it is also likely that there is a point of diminishing returns where further increases

in enforcement effort bring little additional safety benefit. In this context, the cost of providing sufficient enforcement to eliminate red-light violations could exceed the financial resources of most cities. Even if these resources were available, it could be reasonably argued that they could be more cost-effectively applied to other road safety problems. This argument suggests that elimination of red-light violations may be an unreasonable goal for most cities.

Types of Enforcement

Enforcement activities used to treat safety problems can be categorized as one of two types: officer and camera. Typical methods by which each of these two types are used to deal with red-light violations is described in this section.

Officer Enforcement

Many enforcement agencies use a team enforcement technique to address red-light violations and other intersection traffic control violations. With this technique, one officer is stationed upstream of the signalized intersection, and a second officer is located downstream of the intersection. When the "upstream" officer observes a violation, he or she sends a radio message to the "downstream" officer, who then proceeds to stop and cite the violator. This technique is generally regarded as successful in reducing violations but is labor-intensive.

Some agencies use enforcement lights as an alternative to team enforcement. An enforcement light can be attached to the signal head or to the signal mast arm. The latter type of installation is shown in Figure 3-1. These lights are illuminated while the traffic signal indication is red. They allow a single officer stationed downstream of the signal to observe vehicles entering the intersection and note whether the signal indication is red. Enforcement lights eliminate the need for team enforcement and, therefore, have a lower operating cost.

Camera Enforcement

Red-light enforcement cameras are typically deployed upstream of, and facing toward, the intersection. Figure 3-2 illustrates a typical camera location. Pavement sensors detect the speed of the vehicle as it crosses the stop line. If its speed exceeds a specified threshold value during the red indication, it is assumed that it is in violation, and the camera takes a sequence of two photos of the vehicle. A red-light camera at a typical intersection can cost from $50,000 to $60,000, with installation adding from $10,000 to $25,000 (*21*). Operating costs are reported by Maccubbin et al. (*22*) to be in the vicinity of $5000 per month.

A red-light violation may be treated as a civil or criminal offense, depending on the relevant state statutes (it is a criminal offense in Texas). Tickets for civil offenses can be sent by mail to violators. Prosecution of the violation as a criminal offense requires proof that the individual committed the offense (e.g., a frontal photograph of the driver at the time of the violation) and is adjudicated in a criminal court with a fine levied by a judge. Fines can range from $50 to $270 (*22*).

Figure 3-1. Enforcement Light.

Figure 3-2. Enforcement Camera.

A short period of time is often allowed to lapse between the start of red and camera activation. This time is referred to herein as the "grace period." A recent review of grace period values used throughout the world revealed that 0.5 s is the "international standard" and that 0.3 s is commonly used in the U.S. (*6*). A similar review by Milazzo et al. (*7*) of U.S. practice indicated a range of 0.1 to 0.3 s. They recommended the use of a 0.4-s grace period, with a possible increase for intersection approaches having significant downgrade.

Program Effectiveness

Officer Enforcement Effectiveness

Officer enforcement is generally recognized as having an immediate, positive effect of reducing red-light violations. The extent of this impact varies depending on whether the officer (and vehicle) is visible to potential offenders (i.e., overt/visible vs. covert/hidden deployment). The impact also varies depending on whether the enforcement is targeting specific, problem locations

or it is deployed at random times and locations (i.e., targeted vs. random enforcement tactic). Finally, the impact is likely to decrease over time since the enforcement activity ended.

Overt versus Covert Enforcement. Officer enforcement is generally recognized as having an immediate, positive effect of reducing red-light violations. The extent of this impact will likely vary, depending on whether the officer (and vehicle) is visible. Logically, visible officers are likely to have a more significant impact on violation frequency than hidden officers. In fact, Cooper (*23*) found that visible police presence significantly reduced traffic control violations. On the other hand, Krulikowski and Holman (*24*) found that officers that remain mostly hidden from view were ineffective at reducing red-light-related crash frequency.

Targeted versus Random Selection of Intersection. Because of the labor-intensive nature of officer enforcement, most agencies target intersections with a high frequency of red-light violations or red-light-related crashes. The rationale for this approach is that the return on the officers' time will be maximized because they will likely issue a large number of citations. This approach is also viewed as being responsive to public concerns because it can have an immediate impact on the frequency of red-light violations.

An alternative to the targeted enforcement approach is random enforcement. The random selection of location and time for a short-term (i.e., 1 or 2 hours) enforcement activity should increase the officers' citywide effect on violations. This approach has the advantage of allowing enforcement agencies to cover a larger geographic area with limited staff resources. The random enforcement approach was implemented in Queensland, Australia, and studied by Newstead et al. (*25*). An analysis of before-after crash data indicated that random enforcement reduced crashes by 11 percent.

Temporal Effectiveness. Cooper (*23*) conducted an evaluation of the effects of increased enforcement on driver behavior at seven intersections in Toronto, Canada. Each location received a different duration of enforcement. The officers were highly visible at all times during the enforcement activity. Cooper observed a 28 percent reduction in the number of intersection violations while enforcement was taking place (and provided that enforcement was sustained for at least 1 hour each day). However, the effectiveness of the enforcement diminished rapidly once the officers left the intersection. This effect is shown in Figure 3-3 using the post-enforcement violation data reported by Cooper.

The trend in Figure 3-3 suggests that violation rates increase by 19 percent after about 10 hours and 38 percent after about 6 days. Given that the original reduction due to officer presence was 28 percent, this trend implies that one-half the benefit of officer presence was lost after 10 hours, and all of it was lost after 6 days. The trend in Figure 3-3 can be used to estimate the average reduction in daily violations based on the number of enforcement hours each day and typical weekday hourly volume patterns. For example, if the enforcement is repeated during the peak traffic hour each day, then a 16 percent reduction in daily violations is realized. This value would increase to 17 percent if an additional hour of enforcement was provided.

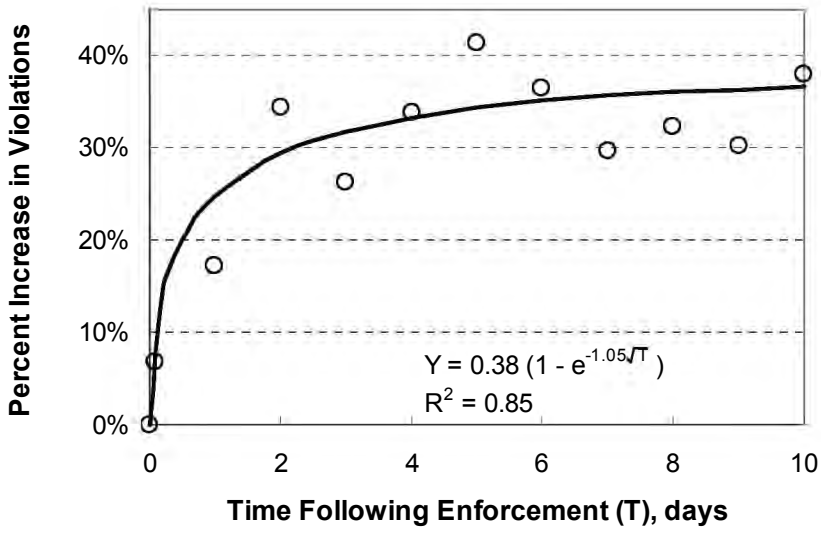

Figure 3-3. Increase in Violations Following an Overt Officer Enforcement Activity.

Camera Enforcement Effectiveness

The effectiveness of camera enforcement at reducing red-light violations has been widely reported. A review of this literature by Bonneson et al. (*11*) indicates that camera enforcement reduces red-light violations at the treated intersection between 40 and 59 percent. Camera enforcement reduces red-light-related crashes between 20 and 36 percent at the treated intersection. However, rear-end crashes have been found to increase between 20 and 37 percent at these intersections. A comprehensive investigation of the impact of camera enforcement on total crashes (including right-angle and rear-end crashes) found that camera enforcement reduced total crashes by 7 percent on a citywide basis (*26*).

Several studies have examined the effect of camera enforcement on other, non-camera-enforced intersections in the same city. Data reported by the California state auditor indicated that the application of camera enforcement at selected intersections in six cities coincided with a 10 percent reduction in red-light-related crashes on a citywide basis (*6*).

Summary of Findings

The literature review revealed that little is known about the effectiveness of area-wide officer enforcement efforts that target specific types of violations. The limited amount of data found suggest that: (1) 1 or 2 hours of officer enforcement at a specific intersection reduces crashes by only a few percentage points when averaged over a 24-hour period, (2) covert deployments are likely ineffective at significantly reducing violations, and (3) the reductions due to targeted enforcement are often short-lived (i.e.,violation rates return to pre-enforcement levels within a day or so after the officer

leaves the intersection). The more successful officer enforcement efforts are likely those that: (1) are implemented on an area-wide basis with innovative enforcement strategies (e.g., visible officer presence and random location selection), and (2) include a public awareness campaign (e.g., media advertisement, public meetings, posters, etc.).

DATA COLLECTION PLAN

The review of the literature revealed that little is known about the effectiveness of officer enforcement. Evidence was offered to suggest that long-term, area-wide enforcement is likely to have a more lasting effect than short-term enforcement of a problem intersection. Other elements of the enforcement activity (e.g., overt vs. covert and temporal effectiveness) were also discussed but their influences reasoned to be more of academic interest because it is unlikely that enforcement agencies will alter their enforcement activities as related to visible/hidden or enforcement duration.

The objective of this research was to quantify the effect of area-wide officer enforcement of intersection traffic control on red-light-related crashes. This type of enforcement targets traffic control violations at signalized intersections located throughout a jurisdiction. TxDOT's Traffic Safety Section, in cooperation with local law enforcement agencies, has funded area-wide enforcement activities of this type since 1997. The program is titled "Selective Traffic Enforcement Program (STEP);" it is described in more detail in a subsequent section.

Activities directed at achieving the objective were focused on the TxDOT STEP. A database was established that included crash and enforcement data for several cites that participated in the program. The findings from a before-after analysis of these data should provide quantitative evidence of the effectiveness of area-wide enforcement in terms of a measurable reduction in red-light-related crashes.

The next section describes TxDOT's selective enforcement program. Then, the composition of the database is described. Finally, the cities included in the database are identified.

TxDOT Selective Traffic Enforcement Program

Through its Traffic Safety Section, TxDOT has awarded grants, called Intersection Traffic Control STEPs (ITC-STEPs), to facilitate heightened enforcement of traffic laws at intersections. Eighteen Texas cities have participated in the ITC-STEP since it started in 1997. Each city identified about 10 percent of its intersections for heightened enforcement. Presumably, these intersections were selected because they had a disproportionately high number of crashes.

As part of the ITC-STEP, each city also schedules a public awareness campaign to coincide with the heightened enforcement activity. Most programs last for 1 or 2 fiscal years. The participating agency submits reports periodically that document program activities and measures of productivity. Items listed in the report include:

- number and type of citations/arrests issued as part of STEP-funded enforcement;
- number and type of citations/arrests issued by participating agency;
- number of STEP enforcement hours worked;
- number of intersection traffic-control-related crashes;
- number of presentations conducted in support of the grant;
- number of persons attending presentations;
- number of community events in which STEP officers participated (i.e., health fairs, booths);
- number of media exposures (i.e., news releases and interviews); and
- number of public information and education materials distributed (e.g., key tags).

The STEP enforcement hours represent additional hours beyond those routinely provided by the city. Hence, STEP hours are paid to the officers as overtime from the program funds.

STEP funds enable enforcement agencies to focus their efforts on particular types of violations (e.g., intersection traffic control) and reduce the frequency of these violations through a combination of heightened enforcement and public awareness. The disadvantages of this type of "area-wide" enforcement are: (1) that it is costly to implement, and (2) the simultaneous use of targeted enforcement and public awareness activities makes it impossible to determine the relative effectiveness of any one activity. With rare exception, the program is not continued by the local agency after the STEP grant funding is expended.

Database Composition

The database developed for this research describes the history of enforcement activities, public awareness events, and red-light-related crashes for selected cities. The observational unit in the database is a 1-year record of activities, events, and crashes. The "year" is defined by the beginning and ending dates of the STEP funding year (i.e., October 1 through September 30).

A 2- or 3-year crash history for each city was gathered for the years prior to implementation of the STEP. The city's crash history was also gathered for each year that it participated in the program. All crash data were obtained from the Texas Department of Public Safety (DPS) crash database. The data include all severe (i.e., injury or fatality) red-light-related crashes. A red-light-related crash was defined as a crash occurring "at" a signalized intersection where the first contributing factor identified in the officer report is designated as "disregard of stop and go signal" or "disregard of stop sign or light." These attributes were found by Bonneson et al. (*11*) to be the most accurate for identifying red-light-related crashes.

Quantitative data describing the enforcement strategies and public awareness activities conducted as part of the STEP were obtained from the evaluation reports submitted by the program participants. These data were identified in the previous section. All reports were obtained from TxDOT's Traffic Safety Section.

Demographic information for each city represented in the database was also gathered. As with the crash data, the observational unit was the 1-year period defined by the STEP funding year. These data include:

- population of the city,
- number of registered vehicles in the city,
- number of licensed drivers in the city, and
- full-time equivalent (FTE) police officers assigned to traffic control enforcement.

These data were gathered from the DPS and the city police departments, as appropriate.

Cities Represented in Database

Table 3-1 identifies eight Texas cities that participated in the ITC-STEP between the years 1997 and 2000. These cities were selected for this investigation because their participation occurred during one or more years for which crash data were also available from the DPS database.

Table 3-1. Texas Cities Represented in Enforcement Database.

City	STEP Funding Year			
	1997	1998	1999	2000
Austin	Before	Before	Before	✔
Bryan	Before	Before	✔	✔
Dallas	Before	Before	Before	✔
Denton	Before	Before	Before	✔
Fort Worth	Before	Before	Before	✔
Garland	Before	Before	✔	✔
Midland	Before	Before	Before	✔
Plano	Before	Before	✔	✔
Participation Dates:	10/1/96 to 9/30/97	10/1/97 to 9/30/98	10/1/98 to 9/30/99	10/1/99 to 9/30/00

Note:
✔ - participated in ITC-STEP. "Before" - year for which data represent the "before ITC-STEP" condition.

DATA ANALYSIS

This section summarizes an analysis of the effectiveness of area-wide enforcement coupled with a public awareness campaign, as implemented for the ITC-STEP. The analysis begins with a summary of the data associated with each of the cities participating in the program. Then, a crash prediction model is developed using regression techniques. This model is used to estimate the expected number of red-light-related crashes that would have occurred in each city had it not

participated in the program. Finally, the reported crash frequency is compared with the expected crash frequency to determine the percent reduction in crashes due to the enforcement effort.

Database Summary

The database assembled for this research is summarized in this section. It includes data describing the enforcement effort expended during the ITC-STEP, population, and crash data for years 1997 to 2000 for each of the eight Texas cities listed in Table 3-1. The enforcement and population data are listed in Table 3-2.

Each row in Table 3-2 represents a period of time (measured in months) during the years 1997 through 2000. Some rows of data represent the "before ITC-STEP" period, and some represent the "during ITC-STEP" period. Whenever possible, each row represents one calendar year; however, the ITC-STEP's fiscal-year basis required division of one calendar year into two rows (one for the "before" period and one for the "during" period in that year). In those instances where there are less than 12 months represented for a calendar year in Table 3-2, the reason is due to a delayed start of the program by the enforcement agency.

The data in Table 3-2 indicate the level of enforcement activity expended in each city. A total of 33,769 officer-hours were expended as part of the ITC-STEP. The number of hours logged varied from 568 (= 387 + 181) for Denton to 13,694 for Dallas. A total of 31,615 citations for red-light violation were issued during the program period. Again, there was a wide range in the number of citations among cities. This variation was partly a reflection of differences in emphasis area among the various cities. The program encouraged enforcement of "child seat" and "seat belt" laws concurrently with red-light violations. In fact, about two citations for "other" violations were issued for every one red-light violation during the course of the program.

The number of media exposure events is also listed in Table 3-2. The number of events sponsored was relatively modest for most cities. Dallas, Garland, and Plano were the most aggressive in using media. Each of these cities held more than 20 events during the course of their program.

The population of the participating cities is illustrated in the last column of Table 3-2. The population estimates for each year were obtained by interpolation using the1990 and 2000 census estimates (*27*). The variation in population among cities is quite wide, ranging from about 64,000 persons in Bryan to more than a million persons in Dallas.

Table 3-2. General Site Characteristics–Area-Wide Crash Analysis.

City	Analysis Period	Time Period		STEP Enforcement Effort		STEP Media Exposures, events	Population,[1] persons
		Months	Calendar Year	Time, officer-hrs	Red-Light Citations		
Austin	Before	12	1997	--	--	--	599,280
		12	1998	--	--	--	618,374
		9	1999	--	--	--	637,468
	During	3	1999	1005	1485	2	637,468
		8	2000	4024	5160	5	656,562
Bryan	Before	12	1997	--	--	--	62,463
		12	1998	--	--	--	63,528
		1	1999	--	--	--	64,594
	During	10	1999	1292	904	1	64,594
		9	2000	487	406	1	65,660
Dallas	Before	12	1997	--	--	--	1,134,069
		12	1998	--	--	--	1,152,239
		12	1999	--	--	--	1,170,410
		4	2000	--	--	--	1,188,580
	During	5	2000	13,694	7397	36	1,188,580
Denton	Before	12	1997	--	--	--	76,257
		12	1998	--	--	--	77,684
		9	1999	--	--	--	79,110
	During	3	1999	387	898	2	79,110
		9	2000	181	445	8	80,537
Fort Worth	Before	12	1997	--	--	--	508,572
		12	1998	--	--	--	517,279
		10	1999	--	--	--	525,987
	During	2	1999	286	not reported	0	525,987
		9	2000	1737	not reported	0	534,694
Garland	Before	12	1997	--	--	--	205,233
		11	1998	--	--	--	208,744
	During	1	1998	192	226	2	208,744
		10	1999	2043	3780	18	212,256
		8	2000	2675	5415	2	215,768
Midland	Before	12	1997	--	--	--	93,330
		12	1998	--	--	--	93,885
		10	1999	--	--	--	94,441
	During	1	1999	54	13	2	94,441
		9	2000	1229	347	0	94,996
Plano	Before	12	1997	--	--	--	194,035
		11	1998	--	--	--	203,367
	During	1	1998	187	202	3	203,367
		9	1999	2599	2899	0	212,689
		8	2000	1701	2038	18	222,030

Note:
1 - Based on 2000 census (*27*).

Table 3-3 summarizes the number of severe crashes that occurred at the signalized intersections in each of the participating cities. The crash frequency listed in column 5 represents the number of crashes at signalized intersections that have "disregard stop and go signal" or "disregard stop sign or light" listed as the first contributing factor on the officer report. Bonneson et al. (*11*) have shown that crashes with these attributes (i.e., "signalized" intersection, "at" intersection, and "disregard") are most likely to be exclusively red-light related. However, they also reported that these attributes do not identify all red-light-related crashes. They recommended that the number of crashes found using the aforementioned attributes should be inflated by 32 percent to estimate the actual red-light-related crash frequency.

The last column of Table 3-3 represents the estimated number of severe red-light-related crashes, as expressed in terms of crashes per month. The estimate in any one row was obtained by inflating the reported frequency of severe "disregard" crashes by 32 percent and then converting this product into a monthly rate by dividing by the corresponding number of months listed in column 3. The relationship between the red-light-related crash frequency and city population is shown in Figure 3-4.

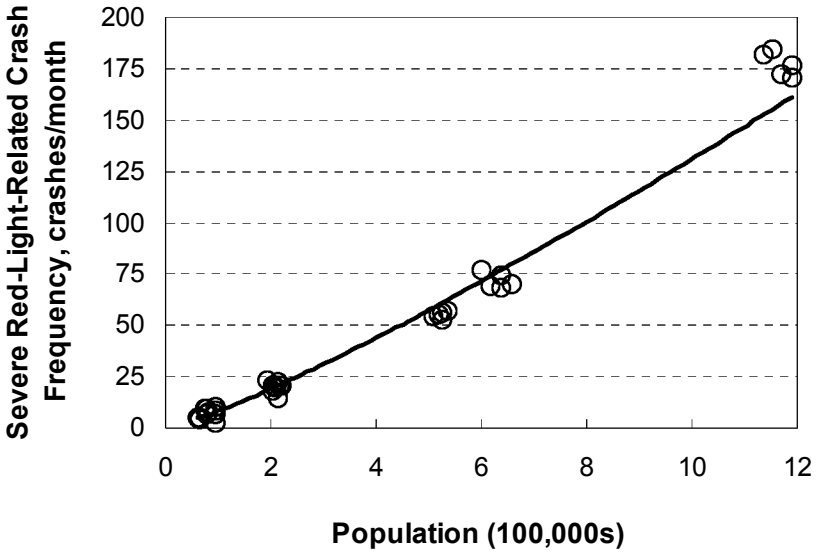

Figure 3-4. Relationship between City Population and Crash Frequency.

The data shown in Figure 3-4 indicate the existence of a strong correlation between city population and severe crash frequency. Each data point in the figure represents one time period (i.e., row) in Table 3-3. It should not be inferred from this figure that "population" is a cause for red-light-related crashes. Rather, population is a surrogate for the driver behavior, traffic conditions, road network capacity, and level of enforcement present in each city. This relationship will be explored further in the next section.

Table 3-3. Site Crash Characteristics–Area-Wide Crash Analysis.

City	Analysis Period	Time Period		Severe "Disregard" Crashes at Intersections			Severe Red-Light-Related Crash Freq., crashes/month
		Months	Calendar Year	Frequency, crashes/period	Freq., cr/month/ 100,000 persons	Relative Change *RC*, %	
Austin	Before	12	1997	703	8.9	-6.1	77
		12	1998	631			69
		9	1999	469			69
	During	3	1999	170	8.3		75
		8	2000	426			70
Bryan	Before	12	1997	49	6.4	-7.9	5
		12	1998	49			5
		1	1999	3			4
	During	10	1999	37	5.9		5
		9	2000	36			5
Dallas	Before	12	1997	1652	11.7	-4.0	182
		12	1998	1677			184
		12	1999	1567			172
		4	2000	517			171
	During	5	2000	668	11.2		176
Denton	Before	12	1997	84	7.3	9.5	9
		12	1998	54			6
		9	1999	49			7
	During	3	1999	21	8.0		9
		9	2000	56			8
Fort Worth	Before	12	1997	498	8.1	-1.4	55
		12	1998	501			55
		10	1999	426			56
	During	2	1999	80	8.0		53
		9	2000	389			57
Garland	Before	12	1997	181	7.1	6.5	20
		11	1998	155			19
	During	1	1998	15	7.5		20
		10	1999	162			21
		8	2000	128			21
Midland	Before	12	1997	94	7.6	-34.5	10
		12	1998	82			9
		10	1999	65			9
	During	1	1999	2	5.0		3
		9	2000	45			7
Plano	Before	12	1997	211	8.3	-10.4	23
		11	1998	170			20
	During	1	1998	14	7.5		18
		9	1999	153			22
		8	2000	124			20

The severe crash frequency in column 5 of Table 3-3 was used to explore relative trends in the crash data during the "before" and "during" time periods. In light of the strong correlation between population and crash frequency, a normalized crash frequency was computed in terms of monthly severe crashes per 100,000 persons. A separate crash frequency was computed for the "before" and the "during" periods. These frequencies are listed in column 6. The relative change in crashes was then computed using these frequencies in the following equation:

$$RC = \left(\frac{r_{during}}{r_{before}} - 1 \right) \times 100 \qquad \textbf{(13)}$$

where,

RC = relative change in crash frequency due to treatment, %;
r_{during} = crash frequency during treatment period, crashes/period; and
r_{before} = crash frequency before treatment, crashes/period.

A negative value for the relative change indicates a reduction in crash frequency.

The computed value of relative change for each city is listed in column 7 of Table 3-3. These values are shown graphically in Figure 3-5. The trends in this figure indicate that six of the cities experienced a reduction in severe red-light-related crashes in the period during the area-wide enforcement activity. The amount of reduction varied from 1.4 to 34 percent.

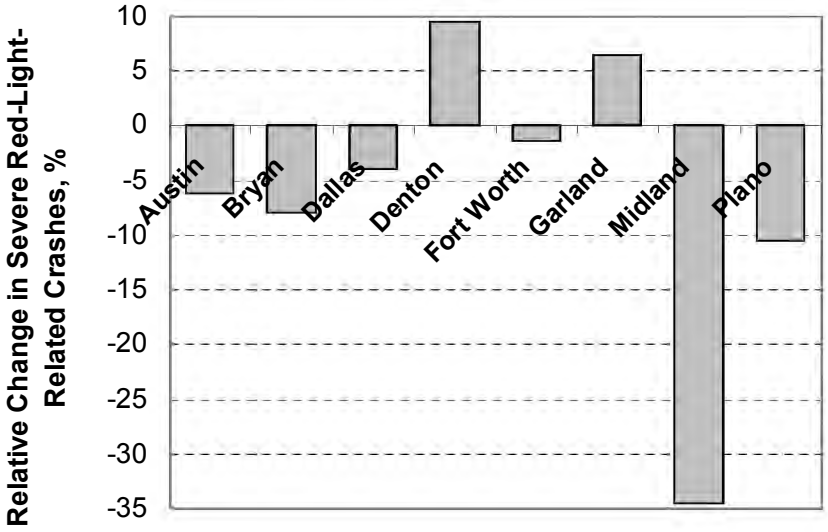

Figure 3-5. Relative Change in Crash Frequency Following Area-Wide Enforcement.

As indicated in Figure 3-5, crash frequency increased in Denton and Garland during the conduct of the enforcement program. This increase is illogical as it is unlikely that the increased officer presence and associated media events precipitated an increase in crashes. Possible explanations for this increase were considered, and a variety of cause-effect relationships were evaluated but none proved useful.

Officials with Denton and Garland were contacted but could offer no additional information, in part because the events took place several years prior to the conduct of this research. For Garland, the researchers noted that major freeway reconstruction occurred during the years 1999 and 2000 in the vicinity of Garland, and that a significant portion of freeway traffic was diverted through the city to avoid work-zone-related congestion. It is possible that this diversion could have resulted in an increase in crashes by an amount larger than the reduction achieved due to the enforcement program.

Model Development

This section describes the development of a model for estimating the citywide frequency of severe red-light-related crashes as a function of population. The likely existence of this relationship was noted in the discussion associated with Figure 3-4. The next section describes the statistical analysis methodology used to calibrate the model. Then, the calibrated model is presented and its fit to the data discussed.

Database Summary

A database was assembled of cities in Texas with a population of 15,000 or more persons. The database included crash data for the years 1997 through 2000 and city population for year 2000. The data were screened to include only severe crashes occurring at signalized intersections and for which the first contributing factor cited in the peace officer report was "disregard stop and go signal" or "disregard stop sign or light." The crash frequency obtained for each city was then inflated by 32 percent to obtain an accurate estimate of the frequency of severe red-light-related crashes.

A total of 135 cities satisfied the minimum population criteria. Cities with less than 15,000 persons were noted to frequently have no severe red-light-related crashes during the 4-year period. Hence, they were excluded to avoid a possible bias in the regression analysis due to an excessive number of observations with zero crashes.

Statistical Analysis Method

A preliminary examination of the crash data indicated that they are neither normally distributed nor of constant variance, as is assumed when using traditional least-squares regression. Under these conditions, the generalized linear modeling technique, described by McCullagh and Nelder (*16*), is appropriate because it accommodates the explicit specification of an error distribution using maximum-likelihood methods for coefficient estimation.

The distribution of crash frequency can be described by the family of compound Poisson distributions. In this context, there are two different sources of variability underlying the distribution. One source of variability stems from the differences in the mean crash frequency *m* among the otherwise "similar" cities. The other source stems from the randomness in crash frequency at any given city, which likely follows the Poisson distribution.

Abbess et al. (*17*) have shown that if event occurrence at a particular location is Poisson distributed then the distribution of events of a group of locations can be described by the negative binomial distribution. The variance of this distribution is:

$$V(x) = E(m) + \frac{E(m)^2}{k} \quad \textbf{(14)}$$

where,

x = reported crash frequency for a given city having an expected frequency of $E(m)$; and
k = dispersion parameter.

The Nonlinear Regression procedure (NLIN) in the SAS software was used to estimate the model coefficients (*18*). The benefits of using this procedure are: (1) nonlinear model forms can be evaluated, and (2) the dispersion parameter *k* can be held fixed during the model building process (as described in the next paragraph). The "loss" function associated with NLIN was specified to equal the log likelihood function for the negative binomial distribution. The procedure was set up to estimate model coefficients based on maximum-likelihood methods.

The goal of the regression model development was to build a parsimonious model. This type of model explains as much of the systematic variability as possible using the fewest number of variables. The procedure described by Sawalha and Sayed (*19*) was used to achieve this goal. It is based on a forward building procedure where one variable is added to the model at a time. The dispersion parameter *k* is held fixed at the best-fit value for a model with *p* variables while evaluating alternative models with *p*+1 variables (i.e., models where one candidate variable has been added). Only those variables that are: (1) associated with a calibration coefficient that is significant at a 95 percent confidence level, and (2) that reduce the scaled deviance by at least 3.84 ($= \chi^2_{0.05,1}$) are considered as candidates for inclusion. Of all candidate variables, the one that reduces the scaled deviance by the largest amount is incorporated into an "enhanced" model. A best-fit *k* is computed for the enhanced model and the process repeated until no candidate variables can be identified.

The advantage of the NLIN procedure is that *k* can be held fixed during the search for candidate variables. The disadvantage of this procedure is that it is not able to compute the best-fit value of *k* for the enhanced model. This disadvantage is overcome by using the Generalized Modeling (GENMOD) procedure in SAS with the enhanced model. GENMOD automates the *k*-estimation process using maximum-likelihood methods. Thus, GENMOD is used to regress the relationship between the reported and predicted crash frequencies (where the natural log of the predicted values is specified as an offset variable and the "log" link function is used). This new

estimate of k from GENMOD is then used in a second application of NLIN and the process repeated until convergence is achieved between the k value used in NLIN and that obtained from GENMOD. Convergence is typically achieved in two iterations.

Model Calibration

The regression analysis revealed that city population was strongly correlated with severe red-light-related crash frequency. The relationship was initially assumed to be continuous over the range of population, as suggested by the trend line in Figure 3-4. However, subsequent analyses indicated that the relationship between population and crash frequency was different for cities with a small population compared to those having a large population. Several model forms were evaluated to reflect these differences. The best fit was obtained by including an indicator variable in the regression model that changed the curve slope for cities with a population in excess of $b_3 \times 100{,}000$ persons. The best-fit prediction model was specified using the following equation:

$$E[r] = e^{b_0} b_3^{-I_p b_2} \left(\frac{P_a}{100{,}000} \right)^{(b_1 + I_p b_2)} \quad \textbf{(15)}$$

where,

$E[r]$ = expected severe red-light-related crash frequency for the subject city, crashes/yr;
I_p = indicator variable for population (= 1.0 if population exceeds $b_3 \times 100{,}000$ persons; and 0.0 otherwise);
P_a = area population, persons; and
b_i = calibration coefficients (i = 0, 1, 2, 3).

The statistics related to the calibrated model are shown in Table 3-4. The calibration coefficient values shown can be used with Equation 15 to estimate the annual severe red-light-related crash frequency for a given city or jurisdiction of known population.

A dispersion parameter k of 2.66 was found to yield a scaled Pearson χ^2 of 1.02. The Pearson χ^2 statistic for the model is 134, and the degrees of freedom are 131 (= $n - p - 1 = 135 - 3 - 1$). As this statistic is less than $\chi^2_{0.05,\,131}$ (= 159), the hypothesis that the model fits the data cannot be rejected. A measure of model fit that is appropriate for negative binomial error distributions is R_K^2, as developed by Miaou (*20*). R_K^2 for the calibrated model is 0.84.

The regression coefficients for each model are listed in the last rows of Table 3-4. The t-statistics shown indicate that, with one exception, all coefficients are significant at a 95 percent level of confidence or higher. The coefficient associated with b_3 is significant at a 90 percent level. A positive coefficient indicates that crashes increase with an increase in the associated variable value. Thus, cities with a larger population are likely to have a higher frequency of red-light-related crashes.

Table 3-4. Calibrated Model Statistical Description–Area-Wide Crash Analysis.

Model Statistics		Value		
R_K^2:		0.84		
Scaled Pearson χ^2:		1.02		
Pearson χ^2:		134 ($\chi^2_{0.05,\,131}$ = 159)		
Dispersion Parameter k:		2.66		
Observations n_o:		135 cities (68,253 crashes during a 4-year period)		
Range of Model Variables				
Variable	**Variable Name**	**Units**	**Minimum**	**Maximum**
P_a	Area population	persons	15,132	1,953,631
Calibrated Coefficient Values				
Variable	**Definition**	**Value**	**Std. Dev.**	**t-statistic**
b_0	Intercept	4.79	0.15	31.9
b_1	Effect of population when $\leq b_3 \times 100{,}000$	1.458	0.118	12.4
b_2	Incremental effect of population $>b_3 \times 100{,}000$	-0.376	0.189	-2.0
b_3	Population threshold in 100,000s	1.013	0.631	1.6

The indicator variable I_p adapts Equation 15 to cities with a population in excess of 101,300 persons. The resulting form of the calibrated equation is:

$$E[r] = \begin{cases} 120\left(\dfrac{P_a}{100{,}000}\right)^{1.458} & : \; Population \leq 101{,}300 \\ 121\left(\dfrac{P_a}{100{,}000}\right)^{1.082} & : \; Population > 101{,}300 \end{cases} \quad \textbf{(16)}$$

The fit of the calibrated model to the data is illustrated in Figure 3-6. The trends shown are logical and similar to those noted for Figure 3-4. The frequency of severe crashes is higher in cities with higher populations.

The slope of the line in Figure 3-6 is steepest for cities in the range of 60,000 to 101,300 persons. This trend may be related to the characteristics associated with these cities, as may differ from those with smaller or larger populations. These cities tend not to have relatively high traffic demands on their urban street network, relative to cities with smaller populations. On the other hand, they do not have as extensive a network of urban freeways as do cities with a larger population and are likely to have notable peak-hour traffic demands at major intersections. Hence, the concentration of drivers at intersections is likely to be high in cities of 60,000 to 101,300 during peak hours. There will likely be some anxiety associated with peak-hour delays, and the drivers will typically have few alternative routes that include controlled-access highways. These factors may combine to explain the slightly steeper slope of the trend line for cities of 60,000 to 101,300 persons.

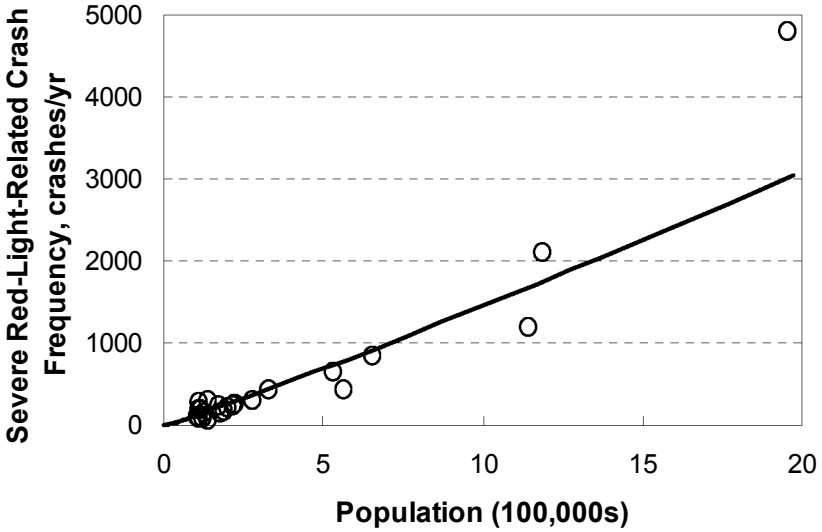

a. Cities with a Population in Excess of 200,000 Persons.

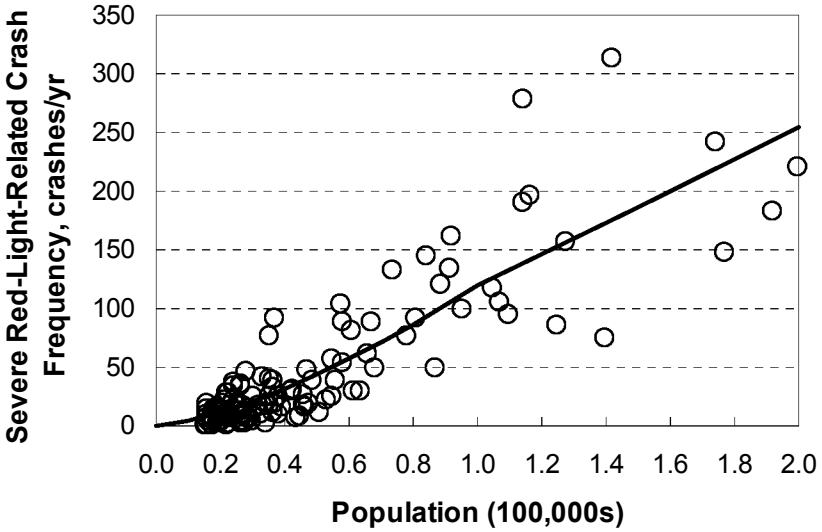

b. Cities with a Population Relationship between 15,000 and 200,000 Persons.

Figure 3-6. Predicted Relationship between City Population and Crash Frequency.

ENFORCEMENT EFFECTIVENESS EVALUATION

This section describes the analysis and evaluation of the effectiveness of area-wide enforcement (in combination with a public awareness campaign). Initially, the statistical analysis

methods used for the before-during evaluation are described. Then the findings from the evaluation are summarized.

Statistical Analysis Method

A before-after evaluation method was used to evaluate the crash data and quantify the effectiveness of area-wide enforcement. The empirical Bayes-based method described by Hauer (*9*) was used for the analysis. This method yields an unbiased estimate of the crash frequency in the "before" period. This estimate is then extrapolated to the "after" period (hereafter referred to as the "during" period to be consistent with the experimental design) to obtain an estimate of the crashes that would have occurred in the "during" period had additional enforcement not been implemented. This extrapolated estimate is then compared with the crashes that actually occurred with the enforcement to determine if crashes were truly reduced.

The estimate of the crashes in the "before" period is based on a weighted combination of the reported frequency of crashes during the "before" period x and the predicted crash frequency $E[r]$, obtained from Equation 16. The estimate obtained in this manner $E[r|x]$ is a more accurate estimate of the expected crash frequency in the subject city than either of the individual values (i.e., $E[r]$ or x). The following equations were used to compute $E[r|x]$:

$$E[r|x] = E[r] \times weight + \frac{x}{y} \times (1 - weight) \quad \textbf{(17)}$$

with,

$$weight = \left(1 + \frac{E[r]\, y}{k} \right)^{-1} \quad \textbf{(18)}$$

where,

$E[r|x]$ = expected red-light-related crash frequency given that x crashes were reported in y years, crashes/yr;
x = reported red-light-related crash frequency, crashes;
y = time interval during which x crashes were reported, yr; and
$weight$ = relative weight given to the prediction of expected red-light-related crash frequency.

Table 3-5 illustrates the application of Equations 17 and 18 to the "before" data. Column 4 lists the severe red-light-related crash frequency x_i estimated to occur during the corresponding time period i in each city. This estimate is obtained by multiplying the data in the last column of Table 3-3 by the number of months represented by the time period. The sum of these estimates for any given city represents the reported red-light-related crash frequency in the "before" period x (i.e., $x = \sum x_i$).

Table 3-5. Expected Annual Area-Wide Crashes in "Before" Period.

City	Time Period		Severe Red-Light-Related Crash Freq. *x*, crashes/period	Expected Crash Freq. *E[r]*, crashes/period	Equivalent Years Relative to 1997 *y*	Weight Given to $E[r_{1997}]$, *weight*	Expected Crash Freq. *E[r|x]*, crashes/yr
	Months	Calendar Year					
Austin	12	1997	928	837	1.00	0.0011	839
	12	1998	833	866	1.03		
	9	1999	619	671	0.80		
	Total:		**2380**		**2.83**		
Bryan	12	1997	65	60	1.00	0.0204	63
	12	1998	65	62	1.02		
	1	1999	4	5	0.09		
	Total:		**134**		**2.11**		
Dallas	12	1997	2181	1669	1.00	0.0005	2100
	12	1998	2214	1698	1.02		
	12	1999	2068	1727	1.03		
	4	2000	682	585	0.35		
	Total:		**7145**		**3.40**		
Denton	12	1997	111	81	1.00	0.0116	87
	12	1998	71	83	1.03		
	9	1999	65	64	0.79		
	Total:		**247**		**2.82**		
Fort Worth	12	1997	657	701	1.00	0.0013	653
	12	1998	661	714	1.02		
	10	1999	562	606	0.86		
	Total:		**1880**		**2.88**		
Garland	12	1997	239	262	1.00	0.0052	230
	11	1998	205	245	0.93		
	Total:		**444**		**1.93**		
Midland	12	1997	124	108	1.00	0.0085	111
	12	1998	108	109	1.01		
	10	1999	86	92	0.85		
	Total:		**318**		**2.86**		
Plano	12	1997	279	247	1.00	0.0055	256
	11	1998	224	238	0.96		
	Total:		**503**		**1.96**		

Each row of column 5 represents the expected severe red-light-related crash frequency $E[r_i]$ for a specific time period *i*. This value is obtained by converting *E[r]* from Equation 16 into an

equivalent number of crashes for the specified time period. This conversion is achieved by dividing $E[r]$ by 12 and then multiplying it by the number of months in the corresponding time period.

The values in column 6 represent the ratio of expected crashes in any given time period i to that estimated for 1997 (i.e., $y_i = E[r_i]/E[r_{1997}]$). This ratio represents an equivalent number of years, relative to 1997, for the corresponding time period and reflects the increase in population that occurred each year after 1997. For any given city, the total number of equivalent years represents an equivalent time interval y during which the x crashes were reported (i.e., $y = \sum y_i$).

As suggested in the preceding paragraph, the base year for the analysis is 1997 with all subsequent time periods adjusted for population growth using the concept of "equivalent years." Hence, the weight computed using Equation 18 is based on the expected red-light-related crash frequency for 1997 $E[r_{1997}]$, as listed in the first row of column 5 for each city. Thus, the value of *weight* for Austin (= 0.0011) was computed from Equation 18 using the following values: $E[r] = E[r_{1997}] = 837$, $y = 2.83$, and $k = 2.66$.

The last column in Table 3-5 represents an unbiased estimate of the red-light-related crash frequency for the "before" period. It is computed from Equation 17. For example, the value of $E[r|x]$ for Austin was computed using the following values: $E[r] = E[r_{1997}] = 837$, $y = 2.83$, and $x = 2380$.

The value of $E[r|x]$ in the last column of Table 3-5 is an unbiased estimate of the red-light-related crash frequency. However, it is not directly comparable to the reported crash frequency in the "during" period. This incompatibility stems from the fact that population increased between the two analysis periods. The procedure recommended by Hauer (*9*) to remove this bias is described in the following paragraphs. The discussion that follows references the values shown in Table 3-6.

As described by Hauer (*9*), an unbiased estimate of treatment effectiveness requires a prediction of the crash frequency that would have occurred had the treatment not been applied. As a first step in computing this predicted quantity, Equation 16 is used to estimate the expected severe red-light-related crash frequency $E[r_i]$ for each time period i. This estimate is shown in column 5 of Table 3-6 and is computed in the same manner as column 5 of Table 3-5.

The next step is to compute the equivalent number of years in the "during" period $y_{a,i}$, relative to 1997, for each time period i. This value is shown in column 6 of Table 3-6 and is computed in the same manner as column 6 of Table 3-5.

Finally, the crash frequency that would have occurred had the treatment not been applied rlr_i^* is computed for each time period i. These estimates are listed in each row of column 7 in Table 3-6. The values shown were computed as the product of $E[r|x]$ (from Table 3-5) and the corresponding equivalent number of years $y_{a,i}$. For example, in Table 3-6, the estimate of rlr_{1999}^* for Austin in 1999 (= 224 crashes/period) is based on the following values: $E[r|x] = 839$ and $y_{a,1999} = 0.27$.

Table 3-6. Expected Annual Area-Wide Crashes in "During" Period.

Crashes That...			...Occurred With Enforcement	...Would Have Occurred Without Enforcement			
City	Time Period		Severe Red-Light-Related Crash Freq. λ, crashes/period	Expected Crash Freq. *E[r]*, crashes/period	Equivalent Years Relative to 1997 y_a	Expected Crash Freq. rlr^*, crashes/period	Variance $\sigma^2_{rlr^*i}$, (cr/period)^2
	Months	Calendar Year					
Austin	3	1999	224	224	0.27	224	21
	8	2000	562	616	0.74	617	160
	Total:		**786**			**841**	**181**
Bryan	10	1999	49	53	0.88	55	15
	9	2000	48	49	0.81	51	19
	Total:		**97**			**106**	**34**
Dallas	5	2000	882	732	0.44	920	119
	Total:		**882**			**920**	**119**
Denton	3	1999	28	21	0.26	23	2
	9	2000	74	66	0.81	71	20
	Total:		**102**			**94**	**22**
Fort Worth	2	1999	106	121	0.17	113	7
	9	2000	513	555	0.79	517	142
	Total:		**619**			**630**	**149**
Garland	1	1998	20	22	0.08	19	1
	10	1999	214	227	0.87	199	72
	8	2000	169	185	0.70	162	58
	Total:		**403**			**380**	**131**
Midland	1	1999	3	9	0.08	9	0
	9	2000	59	83	0.77	86	23
	Total:		**62**			**95**	**23**
Plano	1	1998	18	22	0.09	22	1
	9	1999	202	205	0.83	212	89
	8	2000	164	191	0.77	197	77
	Total:		**384**			**431**	**167**

For a specified city, the total number of severe red-light-related crashes that would have occurred had the treatment not been applied rlr^* is estimated as the sum of the individual estimates for each time period i (i.e., $rlr^* = \sum rlr_i^*$). This value is then compared with the number of severe red-light-related crashes reported in the "during" period to accurately determine the effectiveness of the treatment. In Table 3-6, the estimate of rlr^* for Austin is 841 crashes. By comparison, only 786 crashes were reported for the same time period. The reduction in crashes is likely due to the enforcement program implemented by the City of Austin.

The variance of the estimate of rlr^* is needed in a subsequent calculation. It can be computed using the following equation:

$$\sigma^2_{rlr,^*i} = \frac{y_{a,i} \; E[r_{1997}] \; rlr^*}{y \; E[r_{1997}] + k} \quad \textbf{(19)}$$

where,

$\sigma^2_{rlr,^*i}$ = variance of rlr_i^* for time period i, (crashes/yr)^2;
$y_{a,i}$ = equivalent years in "during" period, yr;
rlr^* = expected crash frequency that would have occurred had the treatment not been applied, crashes/yr; and
$E[r_{1997}]$ = expected severe red-light-related crash frequency for 1997, crashes/yr.

Column 4 lists the severe red-light-related crash frequency λ_i estimated to occur during the corresponding time period i in each city. This estimate is obtained by multiplying the data in the last column of Table 3-3 by the number of months represented in the corresponding time period. The sum of these estimates for any given city represents the reported red-light-related crash frequency in the "during" period λ (i.e., $\lambda = \sum \lambda_i$).

Evaluation

The data in Table 3-6 were used to evaluate the effectiveness of area-wide enforcement. Specifically, the estimated severe red-light-related crash frequency λ_i in column 4 of Table 3-6 was compared with the expected crash frequency that would have occurred had the additional enforcement not been applied rlr^* (i.e., the last column in Table 3-6). This comparison is shown in Table 3-7.

The effectiveness of the area-wide enforcement is expressed in Table 3-7 in terms of a "crash modification factor" *CMF* and a "relative change" *RC* in crash frequency. The former statistic was computed as:

$$CMF = \frac{\lambda}{rlr^*} \left(1 + \frac{\sigma^2_{rlr,^*i}}{(rlr^*)^2} \right)^{-1} \quad \textbf{(20)}$$

Its standard deviation σ_{CMF} was computed as:

$$\sigma_{CMF} = CMF \left(\frac{1}{\lambda} + \frac{\sigma^2_{rlr,^*i}}{(rlr^*)^2} \right)^{0.5} \left(1 + \frac{\sigma^2_{rlr,^*i}}{(rlr^*)^2} \right)^{-1} \quad \textbf{(21)}$$

Table 3-7. Area-Wide Enforcement Effectiveness.

City	Severe Red-Light-Related Crash Freq. λ, crashes/period	Expected Crash Freq. *rlr**, crashes/period	Variance $\sigma^2_{rlr,*i}$, (cr/period)^2	Crash Modification Factor *CMF*	Factor Standard Deviation	Relative Change *RC*, %
Austin	786	841	181	0.934	0.037	-6.6
Bryan	97	106	34	0.906	0.105	-9.4
Dallas	882	920	119	0.958	0.034	-4.2
Denton	102	94	22	1.077	0.119	7.7
Fort Worth	619	630	149	0.983	0.044	-1.7
Garland	403	380	131	1.060	0.062	6.0
Midland	62	95	23	0.651	0.089	-34.9
Plano	384	431	167	0.889	0.053	-11.1
Total:	3335	3497	826	0.953	0.018	-4.7
Modified Total:[1]	**2830**	**3028**	**674**	**0.936**	**0.019**	**-6.4**

Note:
1 - Modified statistics do not include data for the cities of Denton and Garland.

The relative change was computed as:

$$RC = (CMF - 1) \times 100 \quad \textbf{(22)}$$

As noted in the discussion with Equation 13, a negative value for the relative change indicates a reduction in crash frequency.

The relative change in severe red-light-related crash frequency is listed in the last column of Table 3-7. The values shown are similar with those listed in Table 3-3. The difference between the values in Tables 3-3 and 3-7 is that those in the latter table are based on a more accurate assessment of the crashes that would have occurred in the "during" period based on the increase in population that occurred between the "before" and "during" periods.

The sign associated with the relative change values indicates that crashes were reduced at six of the eight cities. This reduction is likely due to the area-wide enforcement program funded by the ITC-STEP. As discussed previously, the increase in crashes associated with Denton and Garland is illogical and cannot be explained. It is very unlikely that the increase is a result of increased enforcement activities.

The average relative change for all cities is shown in the second to last row of Table 3-7. The analysis indicates that area-wide enforcement (coupled with a public awareness campaign) is likely to reduce severe red-light-related crashes by 4.7 percent. If the data for Denton and Garland are excluded from the analysis, the program reduced crashes by 6.4 percent. Given that a crash increase

in these two cities is illogical in the context of the treatment applied and sharply in contrast to the trends found in the other cities, the reduction of 6.4 percent is believed to represent a more accurate measure of enforcement effectiveness.

A relative change of 6.4 percent corresponds to a crash modification factor of 0.936. The standard deviation of this factor is 0.019. Assuming that the variability in the error of the factor estimate is normally distributed, the 95th percentile confidence interval for the factor was computed as 0.90 to 0.97. This range excludes 1.0 and, thereby, indicates with reasonable confidence that the crash frequency was lower in the "during" period for these six cities than it would have been without the enforcement program.

MODEL EXTENSIONS

The estimate of crash frequency obtained from Equation 17 can also be used (with Equation 16) to identify cities that have an exceptionally high frequency of red-light-related crashes. Initially, Equation 16 is used to compute the expected red-light-related crash frequency for a "typical" city of similar population *E[r]*. Then, Equation 17 is used to compute the expected red-light-related crash frequency *given* that *x* crashes were reported *E[r|x]* for the subject city. These two estimates are then used to compute the following index:

$$Index = \frac{E[r|x] - E[r]}{\sqrt{\sigma^2_{r|x} + \sigma^2_r}} \quad \textbf{(23)}$$

with,

$$\sigma^2_{r|x} = (1 - weight)\ \frac{E[r|x]}{y} \quad \textbf{(24)}$$

$$\sigma^2_r = \frac{E[r]^2}{k\ n_o} \quad \textbf{(25)}$$

where,

$\sigma^2_{r|x}$ = variance of *E[r|x]*;
σ^2_r = variance of *E[r]* for the typical city of similar population; and
n_o = number of observations used in the development of the model used to predict *E[r]*.

The values of *k* and n_o are provided in Table 3-4.

If the reported red-light-related crash frequency *x*, when expressed on an annual basis (i.e., as the quotient of *x*/*y*), is less than the expected crash frequency *E[r]*, then the index will be negative. If this situation occurs, the subject city is not likely to have a red-light-related safety problem.

The index value is an indicator of the extent of the red-light-related safety problem for a given city. In general, cities associated with a positive index value have more severe red-light-related crashes than the "typical" city of similar population. A city with an index of 2.0 is likely to have a greater problem than a city with an index of 1.0. Greater certainty in the need for treatment can be associated with higher index values.

CHAPTER 4. INTERSECTION RED-LIGHT VIOLATION FREQUENCY

OVERVIEW

This chapter describes the findings from an analysis of the causes and effects of red-light violations. The findings presented are the result of a statistical analysis of a red-light violation database originally assembled for TxDOT Research Project 0-4027 but enhanced in this research to include additional factors. A result of this reanalysis is an enhanced model for predicting red-light violation frequency. The findings reported in this chapter represent an update to the material in Chapter 5 of the report *Engineering Countermeasures to Reduce Red-Light-Running* (*13*), as prepared for Project 0-4027.

There were two objectives of this reanalysis of the data and recalibration of the previous model. One objective was to add sites to the database such that it reflected a wider range of key model variables. A second objective was to examine the effect of delay on a driver's propensity to violate the red indication.

The organization of this chapter follows that of Chapter 5 in the Project 0-4027 final report (*13*). Initially, the model described in that report is presented to provide a basis for comparison. Next, the updated database content is summarized and reviewed. Then, the procedures used to develop an enhanced red-light violation prediction model are described. Finally, the findings from a sensitivity analysis using the enhanced model are discussed. The sensitivity analysis illustrates the effects of selected factors on the frequency of red-light violations.

LITERATURE REVIEW

Bonneson et al. (*13*) documented the development of a red-light violation prediction model using data representing 12 hours of traffic observation at each of 20 intersection approaches. These approaches were located in the Texas cities of Mexia, College Station, Richardson, Corpus Christi, and Laredo. The calibrated model they developed has the following form:

$$E[R] = \frac{Q}{C}\,\frac{1}{0.927}\,\ln\left[1 + e^{(2.30 - 0.927\,Y_e - 0.334\,Bp + 0.0435\,V - 0.0180\,L_p + 0.220\,R_p)}\right] e^{(0.745\,I_C + 0.996\,I_L)} \quad \textbf{(26)}$$

with,

$$Y_e = p_x\,Y + (1 - p_x)\max\left[Y, \frac{D}{V}\right] \quad \textbf{(27)}$$

The platoon ratio R_p used in Equation 26 represents the ratio of the flow rate at the end of the phase to the approach flow rate. This ratio is computed as:

$$R_p = \frac{Q_e}{Q} \quad \textbf{(28)}$$

where,

$E[R]$ = expected red-light violation frequency, veh/h;
Q = approach flow rate, veh/h;
C = cycle length, s;
Y_e = effective yellow duration due to advance detector operation, s;
Bp = presence of back plates on the signal heads, (1 if present, 0 if not present);
V = average running speed, mph;
L_p = clearance path length, ft;
R_p = platoon ratio;
p_x = probability of phase termination by max-out (= 1.0 if the movement is pretimed or if it is actuated but does not have advance detection);
Y = yellow interval duration, s;
max $[a,b]$ = the larger of variables a and b;
D = distance between stop line and the most distant upstream detector, ft;
I_C = indicator variable for city of Corpus Christi, (1 if data apply to this city, 0 otherwise);
I_L = indicator variable for city of Laredo, (1 if data apply to this city, 0 otherwise); and
Q_e = phase-end flow rate, veh/h.

Since its publication, two limitations of the model have emerged. First, the effect of delay on motorist propensity to run the red indication is not reflected in the model. The model indicates that an increase in cycle length will result in a decrease in violations. However, it can be reasonably argued that an increase in cycle length will increase motorist delay and that motorists are more likely to run the red when delays are long.

A second limitation of the model is its strong dependency on local calibration. This dependency is illustrated by the two indicator variables included in the model. The calibration coefficients associated with these two variables suggest that intersections in Corpus Christi and Laredo have more than twice the number of violations as those in the other three cities. The need for these indicator variables suggests that either: (1) there are significant differences in enforcement among cities, or (2) there are factors causing red-light violations in these two cities that are not explained by the variables in Equation 26.

In an effort to address the aforementioned limitations, additional field studies were conducted at three intersections in Irving, Texas. The objective of these studies was to add sites to the database such that it reflected a wider range of key model parameters (i.e., traffic volume and yellow duration). Also, the videotapes recorded for Project 0-4027 were reviewed for the purpose of extracting data describing the phase duration (i.e., green interval duration) for each study site. The

phase duration data were used to compute the volume-to-capacity ratio of the phase and its expected uniform control delay (as defined in Chapter 16 of the *Highway Capacity Manual* [*28*]).

SITE SELECTION

Table 4-1 lists the intersections represented in the enhanced database. The first five cities listed represent those cities included in the original database for Project 0-4027. Three intersections in the city of Irving were added for this project. These intersections were selected to add a wider range of volumes and yellow durations in the database. All total, data for 13 intersections are included in the combined database.

Table 4-1. Intersection Characteristics–Intersection Approach Violation Analysis.

City	Intersection[1]	Characteristic			
		Study Sites[2] (Approach)	Cycle Length[3], s	Advance Detection	Enforcement Lights?
Mexia	Bailey St. (F.M. 1365) & Milam St. (U.S. 84)	EB, WB	75	No	No
	S.H. 14 & Tehuacana Hwy. (S.H. 171)	EB, WB	37-66	No	No
College Station	Texas Ave. (S.H. 6) & G. Bush Dr. (F.M. 2347)	NB, SB	89-131	No	No
	College Main & University Dr. (F.M. 60)	EB, WB	110	No	No
Richardson	Plano Road & Belt Line Road	SB, EB	75-108	No	Yes
	Greenville Ave. & Main Street	SB, EB	69-111	No	Yes
Corpus Christi	F.M. 2292 & S.H. 44	EB, WB	57-156	Yes	No
	U.S. 77 & F.M. 665 (City of Driscoll)	NB, SB	42-86	Yes	No
Laredo	Loop 20 & Los Presidentes	NB, SB	90	No	No
	U.S. 83 & Prada Machin	NB, SB	53-90	Yes	No
Irving	MacArthur Blvd. & Royal Lane	NB, SB	103-144	No	No
	Nursery Road & Irving Blvd.	NB, SB	94-109	No	No
	MacArthur Blvd. & Rochelle Road	NB, SB	105-134	No	No

Notes:
1 - North-south street is listed first.
2 - A "site" is defined as one intersection approach. NB: northbound; SB: southbound; EB: eastbound; WB: westbound.
3 - Cycle length range represents the 15th and 85th percentile values observed at the site on 1 day.

At each intersection listed in Table 4-1, two approaches were selected for field study. Each intersection approach represents one study site. The characteristics of each of the 26 approach study sites are listed in Table 4-2. The data in this table indicate that the study sites collectively offer a reasonable range of speeds, grades, all-red interval durations, and signal head support types.

Table 4-2. General Site Characteristics–Intersection Approach Violation Analysis.

City	Study Site	Characteristic					
		Speed Limit, mph	Approach Lanes	Grade, [1] %	Clearance Length, ft [2]	All-Red Interval, s	Signal Head Support
Mexia	EB Milam St.	35	2	-2.8	70	1.0	Mast arm
	WB Milam St.	35	2	2.8	70	1.0	Mast arm
	EB S.H. 171	30	1	-0.5	93	1.0	Span wire
	WB S.H. 171	30	1	0.0	93	1.0	Span wire
College Station	NB Texas Ave.	40	3	0.0	95	1.0	Mast arm
	SB Texas Ave.	40	3	-0.5	102	2.0	Mast arm
	EB University Dr.	35	3	0.5	67	1.0	Mast arm
	WB University Dr.	35	3	0.2	63	1.0	Mast arm
Richardson	SB Plano Road	40	3	0.5	102	2.0	Mast arm
	EB Belt Line Road	35	3	0.0	145	2.5	Mast arm
	SB Greenville Ave.	30	3	0.5	94	2.0	Mast arm
	EB Main Street	30	2	0.0	98	2.0	Mast arm
Corpus Christi	EB S.H. 44	50	2	0.0	95	2.0	Span wire
	WB S.H. 44	50	2	0.0	95	2.0	Span wire
	NB U.S. 77	40	2	0.3	90	2.1	Span wire
	SB U.S. 77	40	2	0.0	90	2.1	Span wire
Laredo	NB Loop 20	40	2	-1.8	89	1.0	Mast arm
	SB Loop 20	40	2	0.9	89	1.0	Mast arm
	NB U.S. 83	55	2	1.5	98	2.0	Mast arm
	SB U.S. 83	55	2	-1.3	98	2.0	Mast arm
Irving	SB MacArthur at Royal	35	3	0.2	119	2.4	Mast arm
	NB MacArthur at Royal	35	3	-0.2	119	2.4	Mast arm
	SB Nursery Road	30	1	0.0	142	2.0	Mast arm
	NB Nursery Road	30	1	0.0	142	2.0	Mast arm
	NB MacArthur at Rochelle	35	2	0.0	89	2.0	Mast arm
	SB MacArthur at Rochelle	35	2	0.0	89	2.0	Mast arm

Notes:
1 - Grade: negative (-) grades are downgrades in a travel direction toward the intersection.
2 - Length of the clearance path measured from the near-side stop line to the far-side stop line.

DATA ANALYSIS

This section summarizes the database assembled for the analysis of factors that may influence red-light violation frequency. Initially, some descriptive statistics are offered that describe the traffic characteristics at each study site. Then, the observed frequency of red-light violations is tabulated for each site and several red-light violation rates quantified.

Database Summary

The database assembled for this research includes the traffic volume, geometry, traffic control, and violation data for 13 intersections. Two approaches were studied at each intersection. Traffic data recorded at each intersection included: vehicle count and classification for each signal cycle, cycle length, number of red-light violations per cycle, average running speed, and flow rate at the end of the phase.

Descriptive Statistics

Summary statistics describing the variables in the database are provided in Tables 4-3 and 4-4. The data in these tables reflect 6 hours of data collection at each intersection approach. The data in Table 4-3 indicate that more than 11,266 signal cycles were observed at 26 intersection approaches. During these cycles, 595 vehicles entered the intersection (as defined by the stop line) after the change in signal indication from yellow to red. Table 4-3 indicates that the sites in Irving had both very low and very high traffic volumes. These extremes in volume added a desired breadth in the range of volumes represented in the database.

Of the 595 vehicles observed to violate the red indication, 84 were heavy vehicles and 511 were passenger cars. Overall, 0.83 percent (= 84/10,160 ×100) of heavy vehicles violated a red indication and 0.32 percent (= 511/160,745 ×100) of passenger cars violated the red indication. A paired test of these two proportions indicates that their difference is significantly different from zero (p = 0.0001). From this test, it is concluded that heavy vehicle operators are more than twice as likely to run the red indication as passenger car drivers. In their examination of two high-speed rural intersections, Zegeer and Deen (*29*) also found that heavy vehicles were more than twice as likely to run the red indication.

Table 4-4 summarizes the statistics associated with selected study site traffic characteristics. In general, these statistics indicate that there is a wide range of flow rates, speeds, yellow-interval durations, volume-to-capacity ratios, heavy-vehicle percentages, clearance path lengths, and cycle lengths represented in the database.

The "platoon ratio" listed in the last row of Table 4-4 represents the ratio of the flow rate at the end of the phase to the average flow rate. Observations during the field studies indicated that red-light violations appeared to be more frequent at intersections with platoons arriving near the end of the green indication.

Violation Rate Statistics

As a first step in the analysis of the data, red-light violation rates were computed for each intersection approach. Two rates were computed. The first rate is expressed in terms of red-light-running events per 1000 vehicles. The second rate represents the number of red-light violations per 10,000 vehicle-cycles, where "cycles" represent the *average* number of cycles per hour during the

period for which vehicles are counted. The use of "vehicle-cycles" is supported by the ratio *Q/C* that appears in Equation 26. Both rates are listed in Table 4-5.

Table 4-3. Site Violation Characteristics–Intersection Approach Violation Analysis.

City	Study Site	Cycles	Heavy Vehicles [1]		All Vehicles [1]	
			Observations	Violations	Observations	Violations
Mexia	EB Milam St.	669	532	7	5003	22
	WB Milam St.	666	483	6	5008	23
	EB S.H. 171	815	48	0	1082	3
	WB S.H. 171	793	91	0	2205	5
College Station	NB Texas Ave.	374	309	1	14,331	31
	SB Texas Ave.	370	321	0	14,180	45
	EB University Dr.	383	277	1	12,802	45
	WB University Dr.	385	541	10	12,176	95
Richardson	SB Plano Road	440	390	0	10,035	8
	EB Belt Line Road	442	160	0	7922	7
	SB Greenville Ave.	484	138	0	3242	5
	EB Main Street	493	278	2	9890	40
Corpus Christi	EB S.H. 44	354	789	4	7026	23
	WB S.H. 44	340	625	1	7667	21
	NB U.S. 77	582	1330	17	5087	36
	SB U.S. 77	590	1160	6	4667	28
Laredo	NB Loop 20	439	568	9	5412	36
	SB Loop 20	432	458	3	5694	38
	NB U.S. 83	574	667	12	4670	43
	SB U.S. 83	525	546	5	4713	32
Irving	SB MacArthur at Royal	175	102	0	8729	6
	NB MacArthur at Royal	175	110	0	7530	0
	SB Nursery Road	207	9	0	1155	0
	NB Nursery Road	207	22	0	979	0
	NB MacArthur at Rochelle	177	100	0	4483	3
	SB MacArthur at Rochelle	175	106	0	5217	0
Total:		**11,266**	**10,160**	**84**	**170,905**	**595**

Note:

1 - "All Vehicles" include both passenger cars and heavy vehicles. A "heavy vehicle" is defined as any vehicle with more than four tires on the pavement, with the exception of a 1-ton pickup truck with dual tires on the rear axle (this truck was considered to be a "passenger car").

Table 4-4. Summary Traffic Characteristics–Intersection Approach Violation Analysis.

Variable	Statistic [1]			
	Average	Std. Deviation	Minimum	Maximum
Approach flow rate, veh/h	637	384	59	1872
Cycle length, s	92	24	47	161
Yellow interval duration, s	4.3	0.60	3.2	5.3
85th percentile speed, mph	43	7.5	32	60
Clearance path length, ft	95	19	63	145
Volume-to-capacity ratio	0.40	0.17	0.13	0.81
Heavy-vehicle percentage, %	7.6	7.4	0	37
Platoon ratio	1.66	0.83	0.13	5.4

Note:

1 - Flow rate, cycle length, volume-to-capacity ratio, heavy-vehicle percentage, and platoon ratio statistics are based on 1 hour observations, with six observations available for each study site and study period combination. Speed statistics are based on one observation for each study site, where each site observation is based on a sample of 100 individual vehicle speeds at each study site. Clearance path length and yellow duration are based on one measurement at each study site.

As shown in the last row of Table 4-5, the overall average rates are 3.5 red-light violations per 1000 vehicles and 0.9 red-light violations per 10,000 veh-cycles. The former rate is similar to that found in the literature. Specifically, data reported by Kamyab et al. (*30*) indicate an average rate of 3.0 violations per 1000 vehicles. Data reported by Baguley (*31*) indicate an average rate of 5.3 violations per 1000 vehicles.

The red-light violation rates listed in Table 4-5 provide some indication of the extent of the problem at the intersections studied. For the purpose of comparing the two rates listed, consider that those approach sites that have a rate that exceeds the average rate by a factor of two or more are "problem" locations. The vehicle-based rates in column 8 indicate that three approaches exceed the average rate of 3.5 violations per 1000 vehicles by a factor of 2.0 or more. These approaches are identified by underline. The vehicle-cycle-based rates in column 9 indicate that four approaches exceed the average rate of 0.9 violations per 10,000 veh-cycles by 2.0 or more. These approaches are also identified by underline.

A comparison of the values in bold font in columns 8 and 9 of Table 4-5 indicate that there is some discrepancy between the two violation rates as to which approaches are problematic. Both rates identify sites with a high number of violations relative to traffic volume. However, the vehicle-cycle-based rate also identifies sites where violation frequency is high relative to the number of signal cycles that occurred. This additional sensitivity illustrates the importance of considering both volume and number-of-cycles when comparing sites based on red-light violation rate.

Table 4-5. Violation Rate Statistics–Intersection Approach Violation Analysis.

City	Study Site	Total Observations					Red-Light Violation Rate[1]	
		Hours of Study	Cycles	Vehicles	Viola-tions	Cycles per Hour	Violations per 1000 veh	Violations[2] per 10,000 veh-cyc
Mexia	EB Milam St.	12	669	5003	22	56	4.4	0.8
	WB Milam St.	12	666	5008	23	56	4.6	0.8
	EB S.H. 171	12	815	1082	3	68	2.8	0.4
	WB S.H. 171	12	793	2205	5	66	2.3	0.3
College Station	NB Texas Ave.	12	374	14,331	31	31	2.2	0.7
	SB Texas Ave.	12	370	14,180	45	31	3.2	1.0
	EB University Dr.	12	383	12,802	45	32	3.5	1.1
	WB University Dr.	12	385	12,176	95	32	7.8	2.4
Richardson	SB Plano Road	12	440	10,035	8	37	0.8	0.2
	EB Belt Line Road	12	442	7922	7	37	0.9	0.2
	SB Greenville Ave.	12	484	3242	5	40	1.5	0.4
	EB Main Street	12	493	9890	40	41	4.0	1.0
Corpus Christi	EB S.H. 44	12	354	7026	23	30	3.3	1.1
	WB S.H. 44	11	340	7667	21	31	2.7	0.9
	NB U.S. 77	12	582	5087	36	49	7.1	1.5
	SB U.S. 77	12	590	4667	28	49	6.0	1.2
Laredo	NB Loop 20	12	439	5412	36	37	6.7	1.8
	SB Loop 20	12	432	5694	38	36	6.7	1.9
	NB U.S. 83	12	574	4670	43	48	9.2	1.9
	SB U.S. 83	12	525	4713	32	44	6.8	1.6
Irving	SB MacArthur at Royal	6	175	8729	6	29	0.7	0.2
	NB MacArthur at Royal	6	175	7530	0	29	0.0	0.0
	SB Nursery Road	6	207	1155	0	35	0.0	0.0
	NB Nursery Road	6	207	979	0	35	0.0	0.0
	NB MacArthur at Rochelle	6	177	4483	3	30	0.7	0.2
	SB MacArthur at Rochelle	6	175	5217	0	29	0.0	0.0
Total Observations & Average Rates:		**275**	**11,266**	**170,905**	**595**	**41**	**3.5**	**0.9**

Notes:
1 - Underlined values exceed the average rate by a factor of 2.0 or more.
2 - Rate computed as: red-light violations/vehicles/cycles per hour × 10,000.

Model Development

This section summarizes the findings from an analysis of the factors associated with red-light violation frequency. The findings presented are the result of a statistical analysis of the database assembled for this research. Initially, the correlation between selected factors and red-light violation

frequency is examined using graphical techniques and simple statistics. Then, a statistical analysis method that is appropriate for developing the violation prediction model is described.

Analysis of Factor Effects

This section describes an analysis of the relationship between red-light violation frequency and selected variables in the database. The analysis considered a wide range of variables; they include: approach flow rate, cycle length, yellow interval duration, speed, clearance path length, volume-to-capacity ratio, heavy-vehicle percentage, use of signal head back plates, platoon ratio, uniform delay, approach grade, number of approach lanes, LED signal indications, use of advance detection, and signal head support. The findings described in this section focus on those variables found to have a significant correlation with red-light violation frequency.

Each variable included in the database represents the events observed during a 1-hour time period. In the case of traffic volume, the observation is the total number of through vehicles traversing the subject approach. Site-specific conditions, such as grade, are a constant for all hours of observation. For most other variables, the observation is an average for the 1-hour period. There are 275 hours of data represented in the database.

The effect of approach flow rate on red-light violation frequency is illustrated in Figure 4-1. This figure indicates that violation frequency increases with increasing flow rate. The pattern in the data indicates that the relationship is linear with negligible violations at zero flow rate.

There are only 28 data points shown in Figure 4-1. In fact, each data point in this figure (and in subsequent figures in this section) represents an average for 10 hours of observation. This aggregation was needed because plots with 275 data points tended to obscure the portrayal of trends in the data. To overcome this problem, the hourly data were sorted by the independent variable (e.g., approach flow rate), placed in sequential groups of 10, and averaged over the group for both the independent and dependent variables. This procedure was only used for graphical presentation; the 275 hour-based data points were used for all statistical analyses.

The ratio of approach flow rate to cycle length was also compared with violation frequency. Figure 4-2 shows the relationship between this ratio and the frequency of red-light violations. Like that found for approach flow rate, violation frequency increases with increasing flow-rate-to-cycle-length ratio. However, the correlation associated with this ratio is larger than that found for approach flow rate alone indicating that both flow rate and cycle length (or its inverse, number of cycles) are correlated with the frequency of red-light violations.

Figure 4-3 illustrates the relationship between yellow interval duration and red-light violation frequency. The best-fit trend line shown suggests that violations decrease with longer yellow intervals. Red-light violations increase significantly for yellow intervals less than 3.5 s. This trend is consistent with that reported by Van der Horst and Wilmink *(32)*.

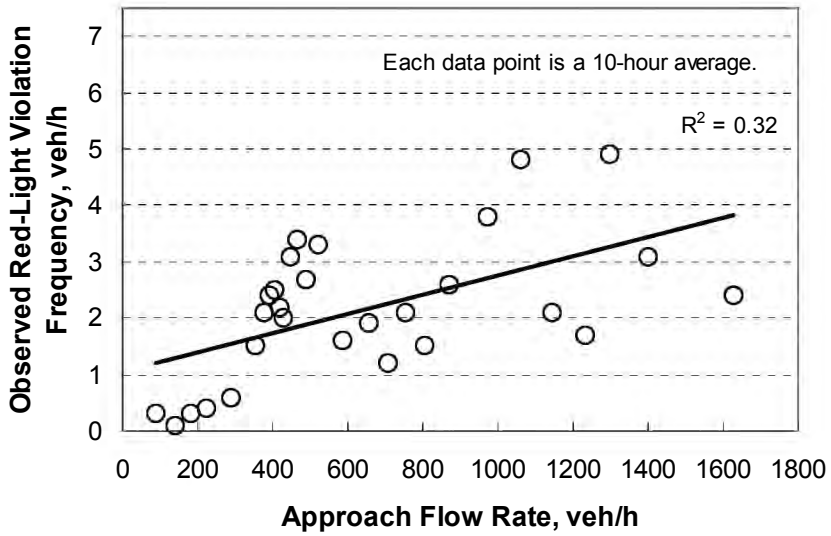

Figure 4-1. Red-Light Violation Frequency as a Function of Approach Flow Rate.

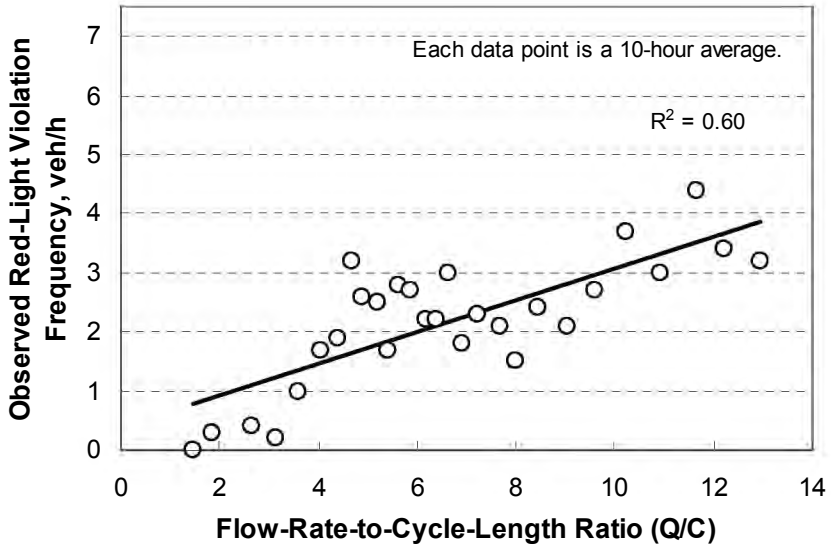

Figure 4-2. Red-Light Violation Frequency as a Function of Flow-Rate-to-Cycle-Length Ratio.

The relationship between approach speed and red-light violation frequency is shown in Figure 4-4. The trend suggests that more red-light violations occur at higher speeds. The scatter in the data suggests that this relationship is not as strong as it is for approach flow rate or yellow interval duration.

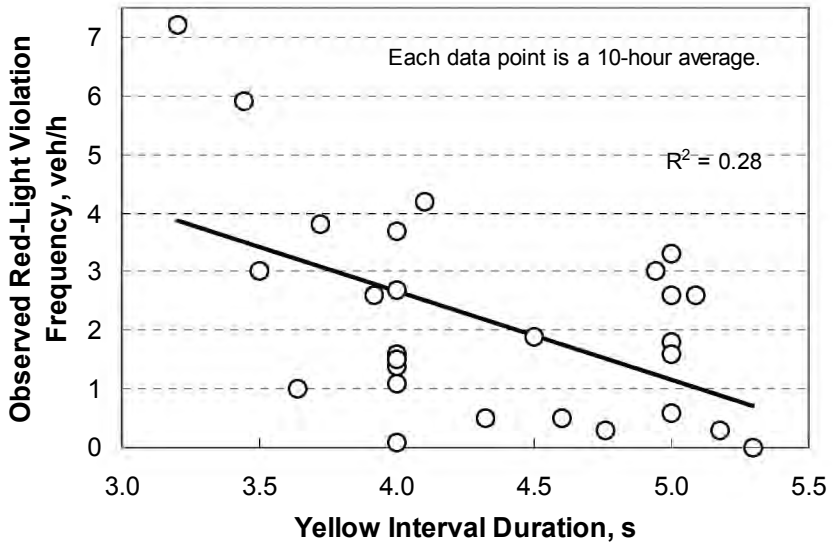

Figure 4-3. Red-Light Violation Frequency as a Function of Yellow Interval Duration.

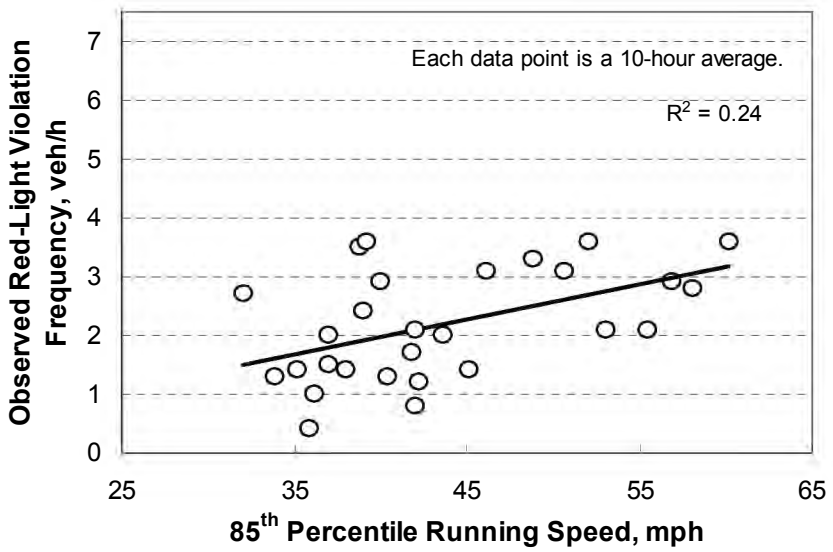

Figure 4-4. Red-Light Violation Frequency as a Function of Speed.

An examination of the relationship between the length of the clearance path through the intersection and red-light violation frequency indicated that violations tended to decrease with increasing path length. Further examination revealed that this effect is more accurately captured by using clearance time (i.e., the ratio of path length to speed). The relationship between clearance time and red-light violation frequency is illustrated in Figure 4-5.

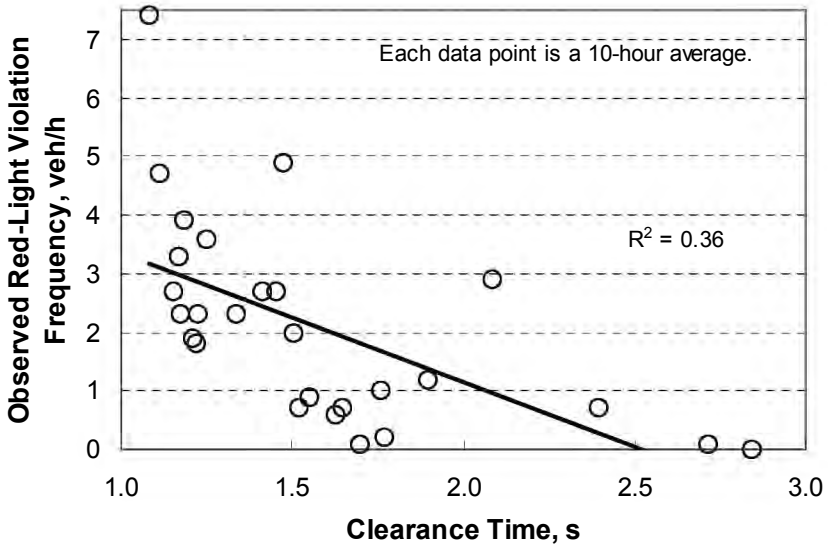

Figure 4-5. Red-Light Violation Frequency as a Function of Clearance Time.

The trend line shown in Figure 4-5 indicates that red-light violations are less frequent at wider intersections. This trend is logical and suggests that drivers are more reluctant to violate the red indication if they believe their "time of exposure" to a right-angle crash is lengthy. This time of exposure directly relates to the time needed by the driver to cross the intersection.

The influence of delay on a driver's propensity to violate the red indication was also examined. This examination focused on two different sources of delay, as defined in the *Highway Capacity Manual* (*28*). One source is due to the periodic presentation of a red indication. This delay is referred to as "uniform delay." It is directly correlated with cycle length and phase duration. A second source of delay stems from cycle failure (or unserved queues at the end of green) that may be due to random arrivals or congestion. This delay is referred to herein as "overflow" delay. It is directly correlated with volume-to-capacity ratio.

The relationship between volume-to-capacity ratio and the frequency of red-light violations is shown in Figure 4-6. The trend line indicates that red-light violations are more frequent at larger volume-to-capacity ratios. This finding suggests that drivers are more likely to violate the red indication (presumably just after the end of the yellow interval) to avoid overflow delay.

The relationship between uniform delay and red-light violation frequency is shown in Figure 4-7. This delay was computed using Equation 16-11 in the *Highway Capacity Manual* (*28*); delay was not measured directly in the field. The scatter in the data is quite large with little change over the range of computed delays. The relatively flat slope of the trend line suggests that uniform delay has a minimal effect on violation frequency. Moreover, the slope of the trend line is illogical because it implies there are *fewer* violations with increasing delay.

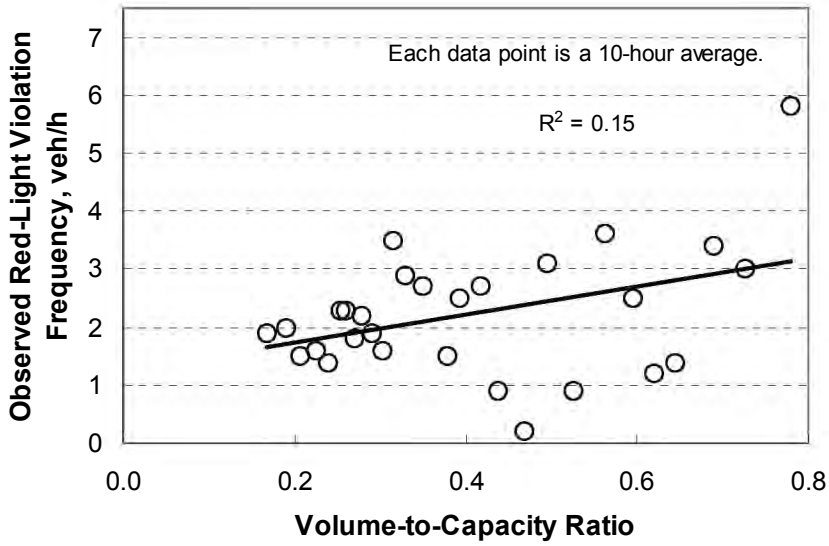

Figure 4-6. Red-Light Violation Frequency as a Function of Volume-to-Capacity Ratio.

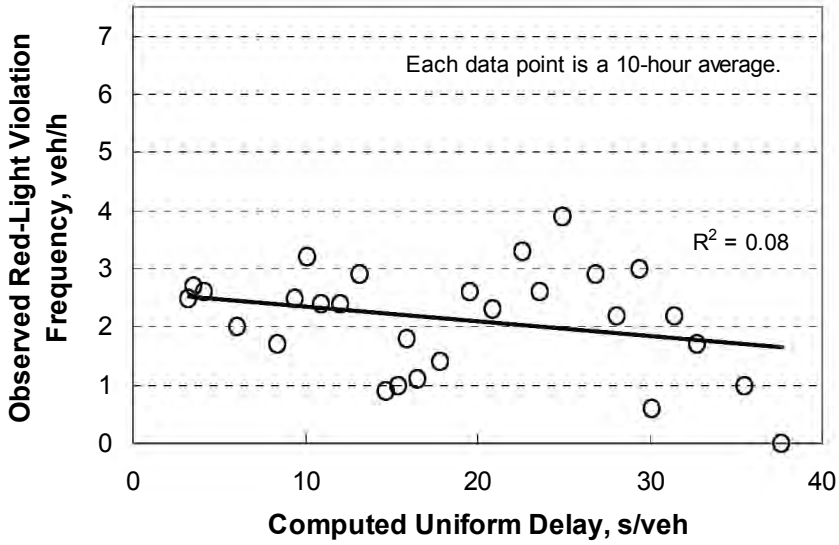

Figure 4-7. Red-Light Violation Frequency as a Function of Uniform Delay.

Figure 4-8 illustrates the relationship between heavy-vehicle percentage and red-light violation frequency. In general, the trends shown suggest that red-light violation frequency increases slightly with heavy-vehicle percentage. A detailed examination of this trend indicated that the increase in violation frequency with increasing heavy-vehicle percentage is explained by an increase in the number of heavy-vehicle violations (and not by the ability of heavy vehicles to indirectly influence nearby car drivers to violate the red).

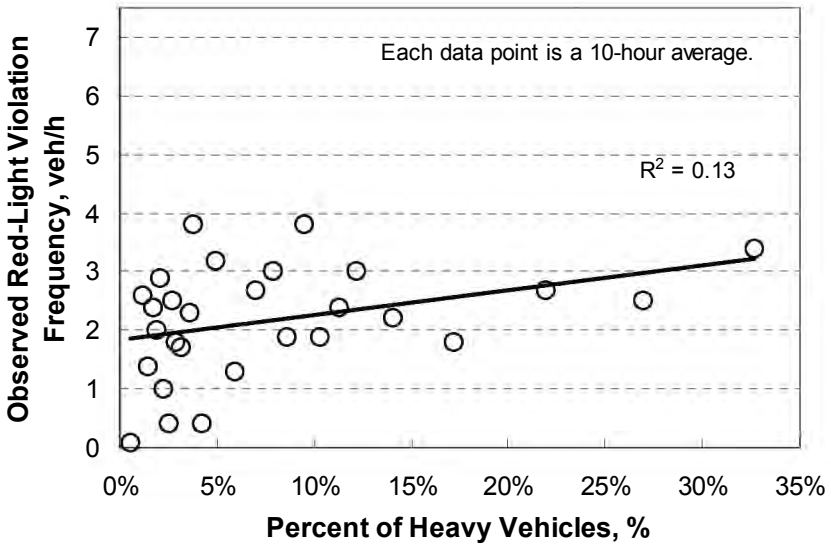

Figure 4-8. Red-Light Violation Frequency as a Function of Heavy-Vehicle Percentage.

The effect of signal head back plates on the frequency of red-light violations is shown in Figure 4-9. Sites with back plates have a lower frequency of red-light violation. The average violation frequency for those sites with back plates was 1.6 veh/h compared to 3.4 veh/h for those sites without back plates (i.e., sites with back plates had only 47 percent of the violations observed at sites without back plates). The standard deviation of each average is shown by the vertical line on the corresponding bar. A statistical analysis indicates that difference between the two averages is statistically significant ($p = 0.01$).

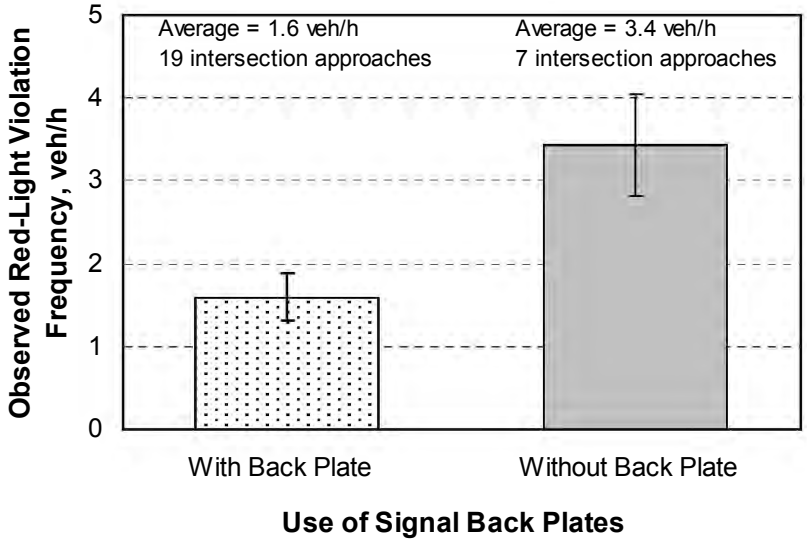

Figure 4-9. Red-Light Violation Frequency as a Function of Back Plate Use.

Statistical Analysis Method

A preliminary examination of the data indicated that they are neither normally distributed nor of constant variance, as is assumed when using traditional least-squares regression. Under these conditions, the generalized linear modeling technique is appropriate because it accommodates the explicit specification of an error distribution using maximum-likelihood methods for coefficient estimation.

The distribution of violation frequency can be described as negative binomial because there are two different sources of variability. One source of variability stems from the differences in the mean frequency *m* among the otherwise "similar" intersection approaches. The other source stems from the randomness in frequency at any given site, which follows the Poisson distribution. The variance of the negative binomial distribution is:

$$V(x) = E(m) + \frac{E(m)^2}{k} \quad \textbf{(29)}$$

where,

x = observed violation frequency for an approach having an expected frequency of $E(m)$; and
k = dispersion parameter.

The Nonlinear Regression procedure (NLIN) in the SAS software was used to estimate the model coefficients (*18*). The benefits of using this procedure are: (1) nonlinear model forms can be evaluated, and (2) the dispersion parameter *k* can be held fixed during the model building process (as described in the next paragraph). The "loss" function associated with NLIN was specified to equal the log likelihood function for the negative binomial distribution. The procedure was set up to estimate model coefficients based on maximum-likelihood methods.

The goal of the regression model development was to build a parsimonious model. This type of model explains as much of the systematic variability as possible using the fewest number of variables. The procedure described by Sawalha and Sayed (*19*) was used to achieve this goal. It is based on a forward building procedure where one variable is added to the model at a time. The dispersion parameter *k* is held fixed at the best-fit value for a model with *p* variables while evaluating alternative models with *p*+1 variables (i.e., models where one candidate variable has been added). Only those variables that are: (1) associated with a calibration coefficient that is significant at a 95 percent confidence level, and (2) that reduce the scaled deviance by at least 3.84 ($= \chi^2_{0.05,1}$) are considered as candidates for inclusion. Larger χ^2 values are used if the subject factor includes two or more parameters. Of all candidate variables, the one that reduces the scaled deviance by the largest amount is incorporated into an "enhanced" model. A best-fit *k* is computed for the enhanced model and the process repeated until no candidate variables can be identified.

The advantage of the NLIN procedure is that *k* can be held fixed during the search for candidate variables. The disadvantage of this procedure is that it is not able to compute the best-fit value of *k* for the enhanced model. This disadvantage is overcome by using the Generalized

Modeling (GENMOD) procedure in SAS with the enhanced model. GENMOD automates the *k*-estimation process using maximum-likelihood methods. Thus, GENMOD is used to regress the relationship between the observed and predicted violation frequencies (where the natural log of the predicted values is specified as an offset variable and the "log" link function is used). This new estimate of *k* from GENMOD is then used in a second application of NLIN and the process repeated until convergence is achieved between the *k* value used in NLIN and that obtained from GENMOD. Convergence is typically achieved in two iterations.

Model Calibration

The regression analysis revealed that mathematic relationships existed between red-light violation frequency and yellow interval duration, use of signal head back plates, speed, clearance path length, heavy-vehicle percentage, and volume-to-capacity ratio. The regression coefficient associated with each of these factors was found to be significant at a level of confidence that exceeded 95 percent. As a result of this analysis, the linear regression terms were specified in the model using the following formulation:

$$E[R] = \frac{Q}{C}\,\frac{1}{b_1}\,\ln\left[1 + e^{(b_0 - b_1 Y_e + b_2 T_{cl} + b_3 HV + b_4 V_{85} + b_5 f_x + b_6 Bp)}\right] \quad \textbf{(30)}$$

with,

$$Y_e = p_x\, Y + (1 - p_x)\max\left[Y, \frac{D}{1.47\, V_{50}}\right] \quad \textbf{(31)}$$

$$T_{ct} = \frac{L_p}{1.47\, V_{85}} \quad \textbf{(32)}$$

$$f_x = \frac{X^2}{1.1 - X} \quad \textbf{(33)}$$

$$X = \frac{Q\,C}{S\,n\,g} \quad \textbf{(34)}$$

where,

E[R] = expected red-light violation frequency, veh/h;

Q = approach flow rate, veh/h;
C = cycle length, s;
Y_e = effective yellow duration due to advance detector operation, s;
T_{ct} = clearance time, s;
HV = heavy-vehicle percentage, %;
V_{85} = 85th percentile speed, mph;
V_{50} = 50th percentile speed (≈0.89 V_{85}), mph;
f_x = overflow delay factor;
Bp = presence of back plates on the signal heads, (1 if present, 0 if not present);
p_x = probability of phase termination by max-out (= 1.0 if the movement is pretimed or if it is actuated but does not have advance detection);
Y = yellow interval duration, s;
max [a,b] = the larger of variables a and b;
D = distance between stop line and the most distant upstream detector, ft;
L_p = clearance path length, ft;
X = volume-to-capacity ratio;
S = saturation flow rate, veh/h/ln;
n = number of lanes serving the approach flow rate; and
g = effective green interval (assumed to equal the green interval duration), s.

The regression analysis indicated that the calibrated model accounted for most of the variability in the data without needing to include city-specific indicator variables. Specifically, differences among the cities are explained by the model variables. Thus, the indicator variables used with Equation 26 are not needed. It is likely that the differences among cities found in the previous model are explained by the overflow-delay and heavy-vehicle-percentage factors included in Equation 30.

The statistics related to the calibrated prediction model are shown in Table 4-6. The calibrated coefficient values can be used with Equations 30 through 34 to predict the hourly red-light violation frequency for a given intersection approach. A dispersion parameter k of 6.1 was found to yield a scaled Pearson χ^2 of 0.99. The Pearson χ^2 statistic for the model is 265, and the degrees of freedom are 268 (= $n - p - 1$ = 275 – 6 – 1). As this statistic is less than $\chi^2_{0.05, 268}$ (= 307), the hypothesis that the model fits the data cannot be rejected. The R^2 for the model is 0.47. An alternative measure of model fit that is better suited to negative binomial error distributions is R_K^2, as developed by Miaou (*20*). R_K^2 for the calibrated model is 0.82.

The regression coefficients for the model are listed in the last rows of Table 4-6. The *t*-statistic shown indicates that all coefficients are significant at a 95 percent level of confidence or higher. A positive coefficient indicates that red-light violations increase with an increase in the associated variable value. Thus, approaches with higher speeds are likely to have a higher frequency of violations. In contrast, violations are less frequent at intersections with wider cross streets or at those with back plates on the signal heads.

Table 4-6. Calibrated Model Statistical Description–Intersection Approach Violation Analysis.

Model Statistics		Value		
R^2 (R_K^2):		0.47 (0.82)		
Scaled Pearson χ^2:		0.99		
Pearson χ^2:		265 ($\chi^2_{0.05,\,268}$ = 307)		
Dispersion Parameter k:		6.1		
Observations n_o:		275 hours		
Standard Error:		±1.8 veh/h		
Range of Model Variables				
Variable	**Variable Name**	**Units**	**Minimum**	**Maximum**
Q	Approach flow rate	veh/h	59	1872
C	Cycle length	s	47	161
Y	Yellow interval duration	s	3.2	5.3
V_{85}	85th percentile speed	mph	32	60
T_{ct}	Clearance time	s	1.1	2.8
X	Volume-to-capacity ratio	--	0.13	0.81
HV	Heavy-vehicle percentage	%	0	37
Calibrated Coefficient Values				
Variable	**Definition**	**Value**	**Std. Dev.**	**t-statistic**
b_0	Intercept	2.47	0.80	3.1
b_1	Effect of effective yellow duration	1.26	0.18	7.1
b_2	Effect of clearance time	-0.855	0.287	-3.0
b_3	Effect of heavy-vehicle percentage	0.0545	0.0114	4.8
b_4	Effect of speed	0.0693	0.0141	4.9
b_5	Effect of overflow delay factor	0.451	0.170	2.7
b_6	Effect of back plates	-0.414	0.163	-2.5

The platoon ratio variable in Equation 26 was not found to be statistically significant during the calibration of Equation 30. Further examination of the data indicated a positive correlation between volume-to-capacity ratio and platoon ratio. Hence, it is likely that the two variables are partially explaining the same variability in the data. However, of the two factors, the overflow delay factor (i.e., volume-to-capacity ratio) was found to explain more of the variability and offers a more plausible explanation for the observed trends.

The fit of the model was assessed through the graphical comparison of the observed and predicted red-light violation frequencies. This comparison is provided in Figure 4-10. The trend line in this figure does *not* represent the line of best fit; rather, it is a "$y = x$" line. The data would fall

on this line if the model predictions exactly equaled the observed data. The trends shown in this figure indicate that the model is able to predict the violation frequency without bias.

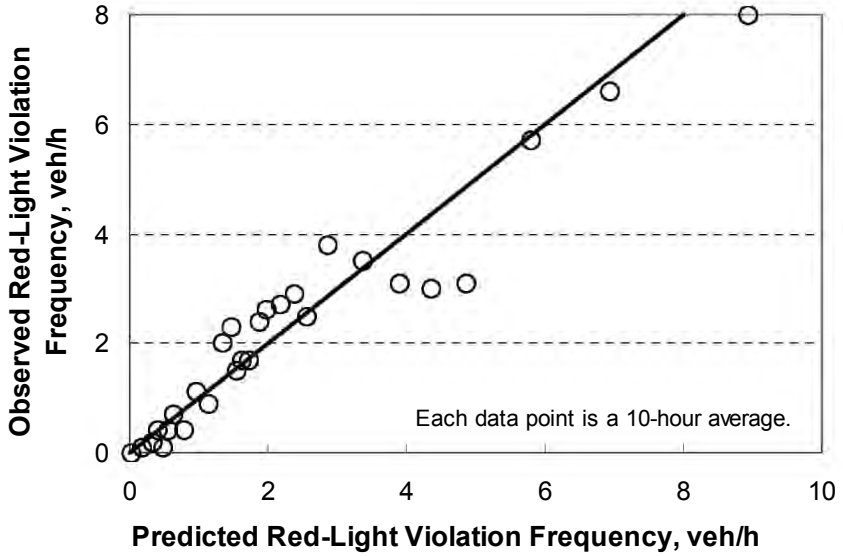

Figure 4-10. Comparison of Observed and Predicted Red-Light Violation Frequency.

The coefficient values were inserted in Equation 30 to yield the following equation:

$$E[R] = \frac{Q}{C}\frac{1}{1.26}\ln\left[1 + e^{(2.47 - 1.26\,Y_e - 0.855\,T_{cl} + 0.0545\,HV + 0.0693\,V_{85} + 0.451\,f_x - 0.414\,Bp)}\right] \quad \textbf{(35)}$$

For actuated approaches with advance detection, the probability of phase termination by max-out was determined from the field data and used in the model calibration process. However, application of the calibrated model to this type of intersection approach will require estimation of the probability of max-out. A procedure described by Bonneson and McCoy (*33*) can be used to compute the probability of max-out. It can also be measured in the field as the portion of cycles for which the subject phase maxes-out. In some instances, it may be sufficient to estimate the probability of max-out using engineering judgment based on familiarity with the operation of the subject intersection approach.

Sensitivity Analysis

This section describes a sensitivity analysis of the calibrated prediction model. Each model variable was analyzed separately from the other variables. Thus, the relative effect of a variable was evaluated with the values of the other model variables held fixed. For this analysis, it was assumed

that the conditions in Equation 31 were such that the effective yellow duration Y_e was equal to the actual yellow interval duration Y.

Analysis Methodology

For a given base variable, the relative effect of a small change (or deviation) from the base value was computed using Equation 35 twice, once using the "new" value and once using the base value. The ratio of the expected red-light violation frequencies was then computed as:

$$MF = \frac{E[R]_{new}}{E[R]_{base}} \quad \textbf{(36)}$$

where, MF represents a "modification factor" indicating the extent of the change in violation frequency due to a change in one variable value. For example, if Equation 35 is evaluated once for a proposed yellow duration of 4.0 s and again for a base yellow duration of 3.0 s, the resulting MF from Equation 36 is about 0.4. Thus, the 1.0-s increase in yellow translates into a 60 percent (= 100 − 0.4 × 100) reduction in violations.

Two trends emerged during the development of the modification factors. First, the value of the modification factor is *not* strongly dependent on the "base" value. Rather, it is only dependent on the magnitude of the change in values. Thus, a 1.0-s increase in yellow duration yields an MF of about 0.4 regardless of whether the change is from 3.0 to 4.0 s, 4.0 to 5.0 s, or any two other values that reflect an increase of 1.0 s.

The second trend that emerged is that the MF is somewhat insensitive to changes in the other variable values. In general, MF values vary less than ±10 percent for the range of typical values for the other variables. For example, a 1.0-s increase in yellow on a 35-mph approach yields an MF of 0.35. If the speed on the approach is 45 mph, then the MF is 0.42 (a 0.07 increase relative to the MF for 35 mph).

Cycle Length

Equation 35 indicates an inverse relationship between a change in cycle length and the frequency of red-light violations. That is, an increase in cycle length corresponds to a decrease in violations. The effect of a change in cycle length is illustrated in Figure 4-11. Trend lines for three "base" cycle lengths are illustrated. A 20-s increase in cycle length from 90 to 110 s is associated with an MF of 0.82, which corresponds to a reduction of 18 percent (= 100 − 0.82 × 100). It should be noted that this change in cycle length assumes no change in any other variable (including the volume-to-capacity ratio).

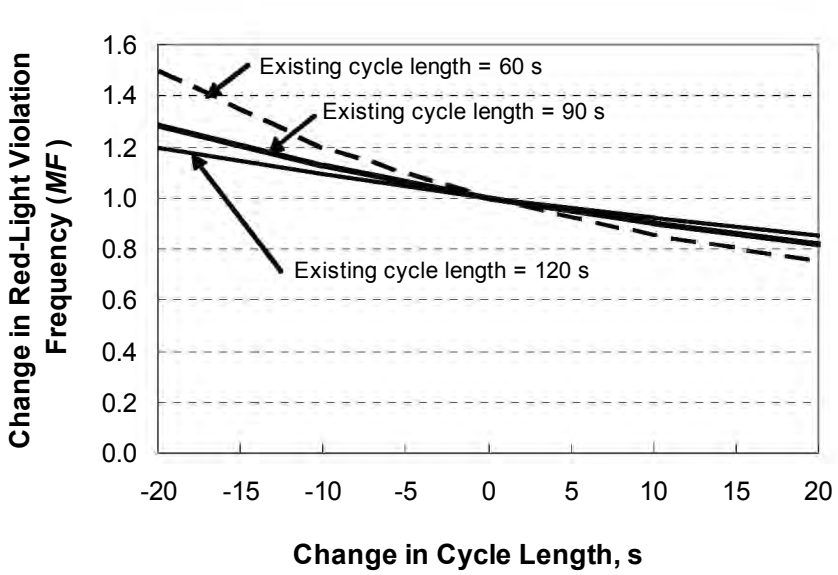

Figure 4-11. Effect of a Change in Cycle Length on Red-Light Violations.

Yellow Interval Duration

The effect of a change in yellow interval duration on the frequency of red-light violations is shown in Figure 4-12. The trend in this figure indicates that an increase in yellow interval duration decreases red-light violations. For example, an increase in yellow duration of 1.0 s is associated with an *MF* of 0.4, which corresponds to a 60 percent reduction.

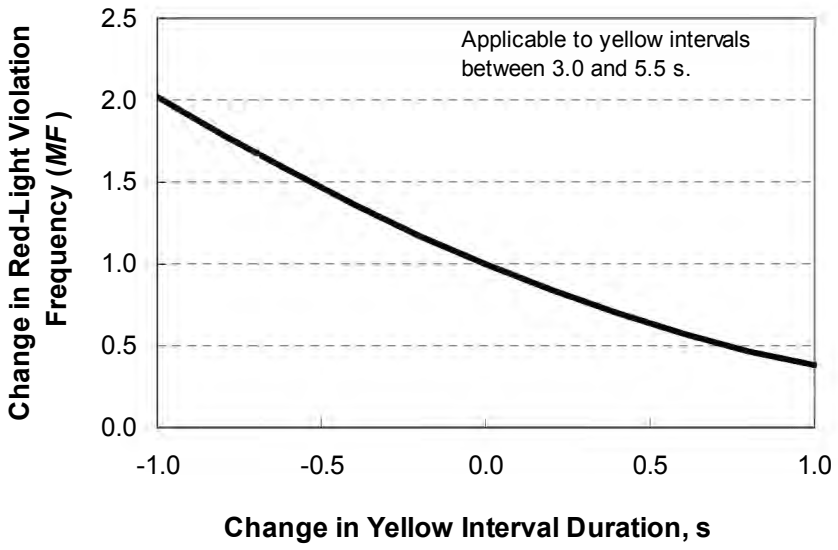

Figure 4-12. Effect of a Change in Yellow Interval Duration on Red-Light Violations.

85th Percentile Speed

The effect of a change in 85th percentile speed on the frequency of red-light violations is shown in Figure 4-13. The trend in this figure indicates that an increase in speed is associated with an increase in red-light violations. For example, an increase in speed of 10 mph is associated with an *MF* of 1.7, which corresponds to a 70 percent increase in red-light violations.

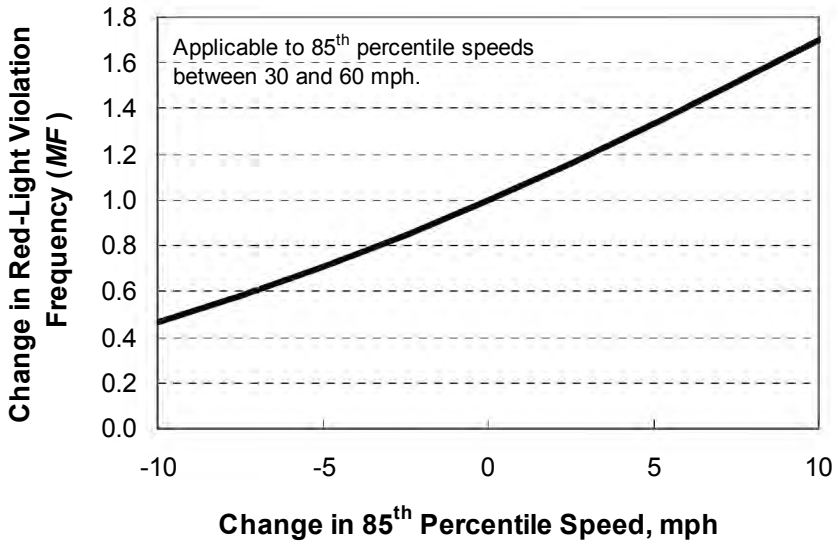

Figure 4-13. Effect of a Change in 85th Percentile Speed on Red-Light Violations.

Length of Clearance Path

The effect of a change in clearance path length on red-light violations is shown in Figure 4-14. The trend in this figure indicates that an increase in path length is associated with a decrease in red-light violations. For example, if approach "A" has a clearance path that is 40 ft longer than approach "B," then its *MF* is 0.7. This value indicates that approach "A" has 30 percent fewer violations than approach "B" (all other factors being the same).

Heavy-Vehicle Percentage

The effect of a change in heavy-vehicle percentage on red-light violations is shown in Figure 4-15. The trend in this figure indicates that an increase in the percentage of heavy vehicles increases the number of violations. As discussed previously, this increase is likely a result of the greater propensity of heavy-vehicle operators to run the red light.

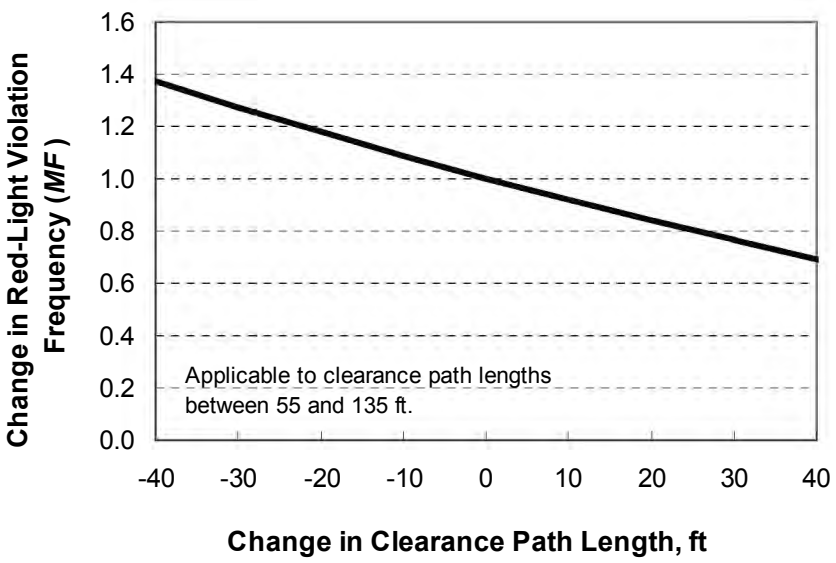

Figure 4-14. Effect of a Change in Clearance Path Length on Red-Light Violations.

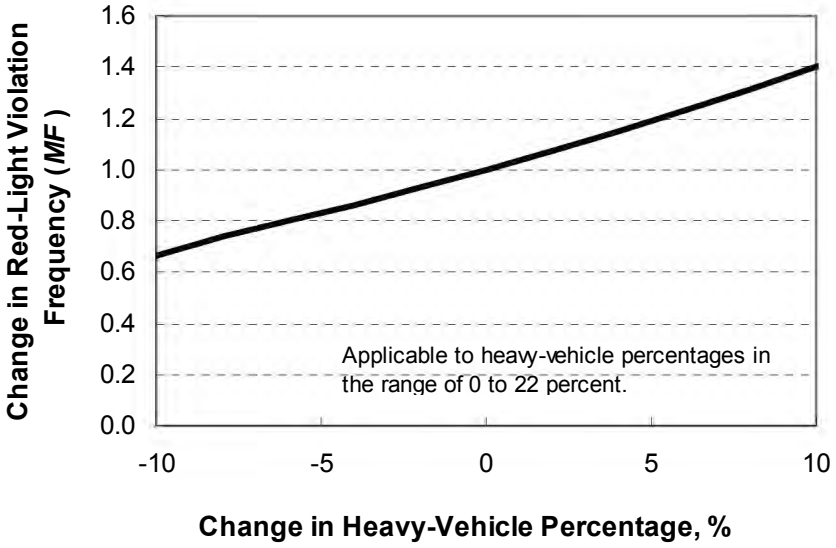

Figure 4-15. Effect of a Change in Heavy-Vehicle Percentage on Red-Light Violations.

Volume-to-Capacity Ratio

The effect of a change in volume-to-capacity ratio on the frequency of red-light violations is shown in Figure 4-16. The trend in this figure indicates that a decrease in volume-to-capacity ratio is associated with a decrease in violations. For example, if the phase duration is increased such that

the existing volume-to-capacity ratio of 0.8 decreased by 0.1, then the *MF* is 0.77, which corresponds to a 23 percent reduction in violations.

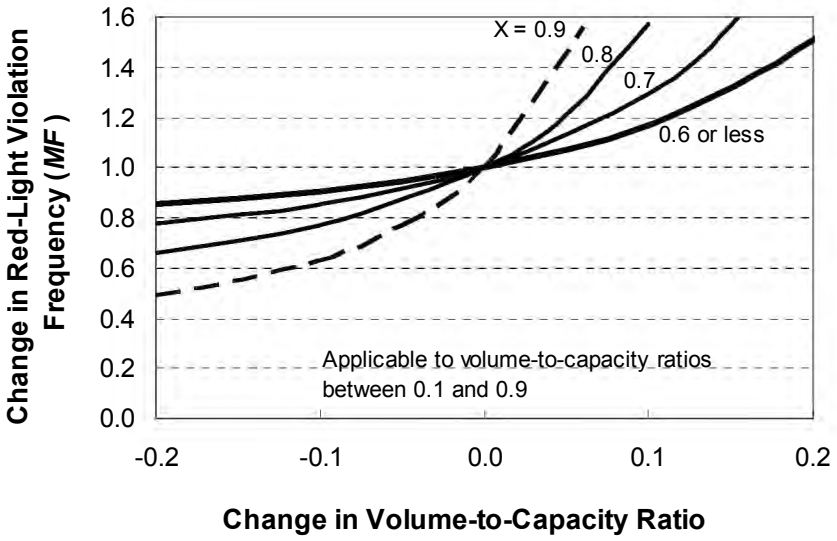

Figure 4-16. Effect of a Change in Volume-to-Capacity Ratio on Red-Light Violations.

In some situations, the change in volume-to-capacity ratio may be due to a change in cycle length. Further examination of the combined effect of a change in cycle length and volume-to-capacity ratio revealed the existence of a range of volume-to-capacity ratios for which red-light violations were minimal. This effect is shown in Figure 4-17.

As shown in Figure 4-17, red-light violations were found to be at their lowest level when the volume-to-capacity ratio was in the range of 0.6 to 0.7. This range was found to yield minimal violations, regardless of speed, path length, yellow duration, heavy-vehicle percentage, cycle length, phase duration, or traffic volume. Volume-to-capacity ratios below this range resulted in an increase in violations due primarily to shorter cycle lengths. Volume-to-capacity ratios above this value resulted in an increase in violations due primarily to an increase in overflow delay.

Use of Back Plates

An analysis of Equation 35, relative to the use of back plates, suggests that back plates are associated with a lower frequency of red-light violation. The modification factor for adding back plates is 0.75, which corresponds to a reduction of 25 percent. This reduction is lower than the 47 percent value found in the examination of the red-light-violation database (as noted in the discussion of Figure 4-9); however, it is a more reliable estimate because the effects of other factors are removed through the use of Equation 35. The modification factor for removing back plates is 1.33, which corresponds to an increase of 33 percent.

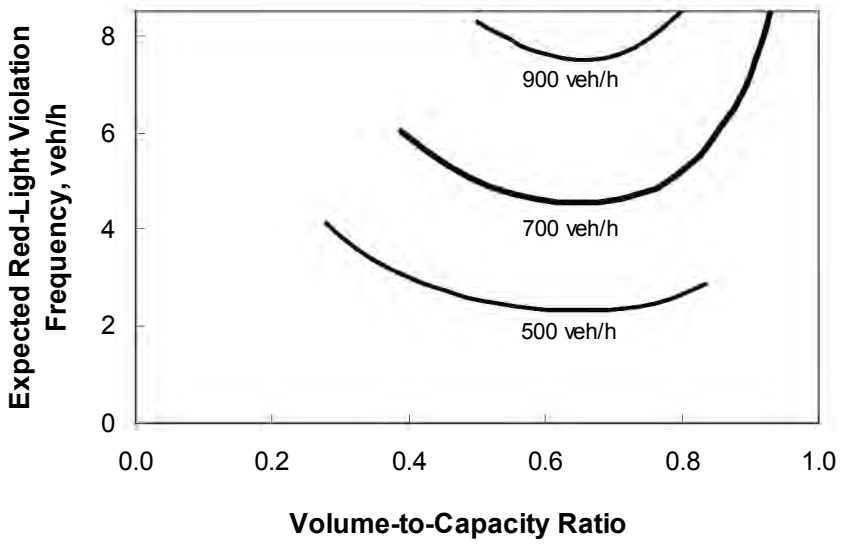

Figure 4-17. Volume-to-Capacity Ratios Associated with Minimal Red-Light Violations.

MODEL EXTENSIONS

This section describes the findings from an application of the calibrated model to a range of input values. Initially, the application is in the context of a sensitivity analysis, where the relative effect of each variable is evaluated in terms of the increase or decrease in red-light violations caused by a change in the variable's value. Then, a commonly used equation for computing the yellow interval duration is examined in terms of the expected red-light violation frequency associated with the durations obtained from the equation. The implications of these findings are discussed.

Examination of a Common Yellow Interval Equation

This section examines the relationship between red-light violation frequency and the yellow interval duration computed using Equation 1. The approach taken in this examination was to compare the observed violation frequency on an approach with the difference between the yellow duration observed at the approach and that computed for it using Equation 1. The results are shown in Figure 4-18.

The data in Figure 4-18 indicate that there is a trend toward more red-light violations when the observed yellow duration is shorter than the computed duration. A regression analysis of the relationship between yellow interval difference and red-light violation frequency indicated that the relationship is statistically significant (i.e., $p = 0.001$). A similar finding was previously reported by Retting and Greene (*15*) in an examination of red-light violations at several intersections. A similar trend with respect to red-light-related crashes was shown in Figure 2-11.

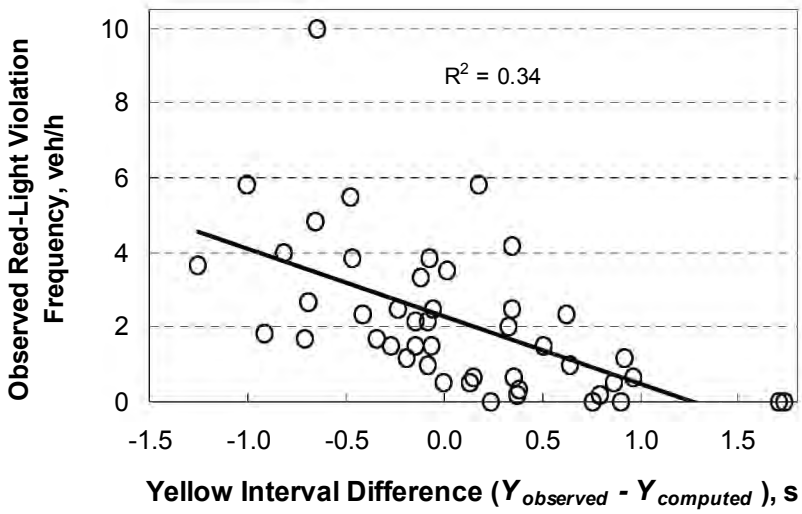

Figure 4-18. Red-Light Violation Frequency as a Function of Yellow Interval Difference.

Figure 4-19 illustrates the effect of yellow interval duration and 85th percentile speed on the frequency of red-light violations. The trend lines are based on the prediction model described previously (i.e., Equation 35). They indicate that the frequency of red-light violations decreases with an increase in yellow interval duration. They also indicate that, for the same yellow duration, the number of violations is higher on higher-speed approaches.

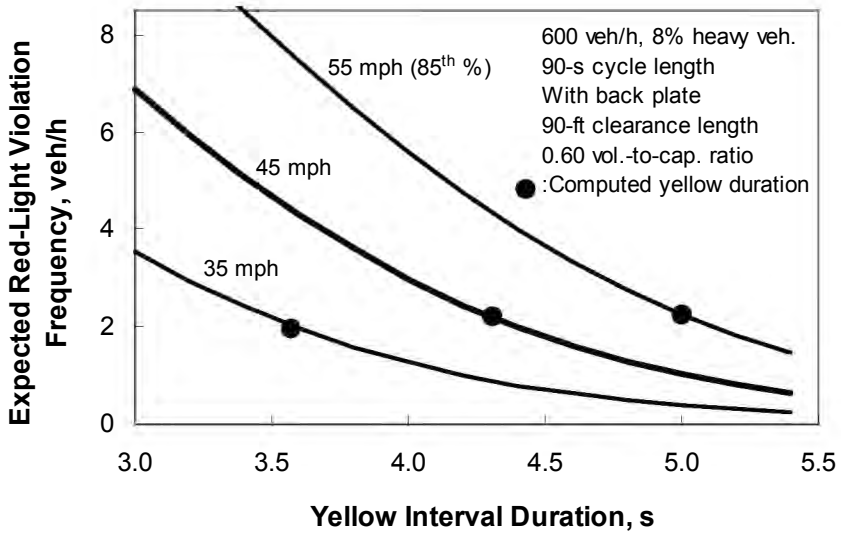

Figure 4-19. Predicted Effect of Yellow Duration and Speed on Red-Light Violation Frequency.

The black dots in Figure 4-19 indicate the value of the yellow interval duration computed using Equation 1 for the corresponding speed. The location of the dots suggests that use of this equation yields about 2.0 red-light violations per hour (or 0.8 red-light violations per 10,000 vehicle-cycles) for the "typical" conditions represented in the figure.

Identify Sites with Potential for Red-Light-Related Safety Improvement

As discussed in Chapter 2, Hauer *(9)* and others have observed that intersections selected for safety improvement are often in a class of "high-crash" locations. As a consequence of this selection process, these intersections tend to exhibit significant crash reductions after specific improvements are implemented. While the observed reduction is factual, it is not typical of the benefit that could be derived from the improvement if it were applied to other locations. Hauer *(9)* advocates the use of the empirical Bayes method to more accurately quantify the true crash reduction potential of a specific improvement or countermeasure. This source of bias is also present when using red-light violation frequency to identify problem intersections. Hence, the methods developed in Chapter 2 are extended in this section to the identification of truly problem intersections based on the observation of violation frequency.

The empirical Bayes method can be used to obtain an unbiased estimate of the red-light violation frequency for a specific intersection approach. This estimate is based on a weighted combination of the observed frequency of red-light violations x on the subject approach and the predicted red-light violation frequency $E[R]$ for similar approaches. The unbiased estimate (i.e., $E[R|x]$) is a more accurate estimate of the expected red-light violation frequency on the subject approach than either of the individual values (i.e., $E[R]$ or x). The following equations can be used to compute $E[R|x]$:

$$E[R|x] = E[R] \times weight + \frac{x}{H} \times (1 - weight) \quad \textbf{(37)}$$

with,

$$weight = \left(1 + \frac{E[R]\,H}{k}\right)^{-1} \quad \textbf{(38)}$$

where,

$E[R|x]$ = expected red-light violation frequency given that x violations were observed in H hours, veh/h;
x = observed red-light violation frequency, veh;
H = time interval during which x violations were observed, h; and
$weight$ = relative weight given to the prediction of expected red-light violation frequency.

The estimate obtained from Equation 37 can also be used (with Equation 35) to identify problem intersection approaches. Initially, Equation 35 is used to compute the expected red-light violation frequency for a "typical" approach. Then, Equation 37 is used to compute the expected red-light violation frequency *given* that x violations were observed on the subject approach. These two estimates are then used to compute the following index:

$$Index = \frac{E[R|x] - E[R]}{\sqrt{\sigma_{R|x}^2 + \sigma_R^2}} \quad \textbf{(39)}$$

with,

$$\sigma_{R|x}^2 = (1 - weight)\ \frac{E[R|x]}{H} \quad \textbf{(40)}$$

$$\sigma_r^2 = \frac{E[R]^2}{k\ n_o} \quad \textbf{(41)}$$

where,

$\sigma_{R|x}^2$ = variance of $E[R|x]$;
σ_R^2 = variance of $E[R]$ for the typical intersection approach; and
n_o = number of observations used in the development of the model used to predict $E[R]$.

The values of k and n_o are provided in Table 4-6.

If the observed red-light violation frequency x, when expressed on an hourly basis (i.e., as the quotient of x/H), is less than the expected crash frequency $E[R]$, then the index will be negative. If this situation occurs, the subject approach is not likely to have a red-light violation problem. However, the red-light-related crash frequency should also be evaluated to confirm this finding.

The index value is an indicator of the extent of the red-light violation problem for a given intersection approach. It is consistent with the "scaled difference in frequency" statistic identified in Table 2-1. In general, intersection approaches associated with a positive index value have more red-light violations than the "typical" approach. An approach with an index of 2.0 is likely to have a greater problem than an approach with an index of 1.0. Greater certainty in the need for treatment can be associated with higher index values.

Occasionally, an intersection approach may not have its yellow interval or approach speed limit in conformance with agency policy. When this occurs, the computed index value should reflect the deviation from agency policy. In this situation, two values of $E[R]$ should be computed (i.e., $E[R, existing]$ and $E[R, policy]$. The first value (i.e., $E[R, existing]$) is obtained using Equation 35 with variable values that reflect conditions on the subject intersection approach. This value is also used in Equations 37 and 38 to estimate $E[R|x]$ and *weight*, respectively.

The second value (i.e., *E[R, policy]*) represents the expected red-light violation frequency of the typical intersection approach having yellow intervals, back plates, and (if applicable) an advance detection design established in accordance with agency policy. If agency policy does not address yellow interval timing, then Equation 1 should be used to compute the value of *Y* used in Equation 31. The value of *E[R, policy]* is then used in Equations 39 and 41 to estimate the *index* and σ_R^2, respectively.

CHAPTER 5. RED-LIGHT VIOLATION CAUSES AND COUNTERMEASURES

OVERVIEW

This chapter examines the characteristics of red-light violations and related crashes for the purpose of identifying the most appropriate set of countermeasures to use in treating problem locations. The characteristics considered include crash type and the duration of time the signal indication was red prior to the crash or violation. This latter characteristic is defined herein as "time-into-red." As described in the next section, there is evidence that both the time-into-red of the typical violation and the manner of collision of the typical red-light-related crash provide important clues to the selection of countermeasures.

The remainder of this chapter is divided into four sections. Initially, the literature is reviewed as it relates to the characteristics of red-light violations and related crashes. Then, a data collection plan is developed for the purpose of analyzing the relationship between these characteristics and various causal factors. Next, the data are analyzed and the underlying trends quantified. Finally, the findings are used to develop guidelines for countermeasure selection.

LITERATURE REVIEW

This section reviews the literature related to red-light violation causes and their characteristics. It also examines the reported relationships between time-into-red and both red-light violations and red-light-related crashes. With regard to crashes, it is likely that crash type is related to the time-into-red that the crash occurs. The literature on various engineering countermeasures that have been used to reduce red-light violations are also examined. The findings from this review provide the foundation for a data collection plan that will lead to the development of countermeasure selection guidelines.

Causes of Red-Light Violations

Several thousand crash reports were collected and reviewed by Bonneson et al. (*11*) for the purpose of identifying red-light-related crash trends and costs. A review of these reports revealed that several reasons were frequently cited by drivers involved in red-light-related crashes. The more frequently cited reasons are summarized in Table 5-1. They reflect some generalization by the authors and are intended to illustrate the range of causes typically cited.

Many of the "causes" listed in Table 5-1 are self-explanatory; however, a couple are worthy of added clarification. "Judged safe as driver < 2 s ahead violated the red" means that the driver has judged it safe to run the red indication because he or she is closely following (i.e., has a headway less than 2.0 s with) another red-light runner. This situation occurs most frequently when a succession of vehicles pass through the intersection after the onset of red. This sequence of red-running

vehicles is quite visible to drivers in conflicting movements and rarely leads to a crash. "Expectation of green when in platoon" means that the driver was traveling along a street with a coordinated signal system. Drivers in a through movement platoon tend to develop an expectation of continued receipt of the green indication as long as they stay in the platoon. Such drivers are prone to run the red indication in order to stay within the platoon.

Table 5-1. Red-Light Violation Characterizations and Possible Causes.

Cause Category	Cause of Red-Light Violation [1]	Violation Type	Driver Intent	Time of Violation
Unnecessary delay	Disregard for red (unnecessary delay)	Avoidable	Intentional	Any time during red
	Judged safe due to low conflicting volume			
Congestion, dense traffic	Congestion or excessive delay			First few seconds of red
	Judged safe as driver < 2 s ahead violated the red			
	Expectation of green when in platoon			
Incapable of stop	Downgrade steeper than expected	Unavoidable		
	Speed higher than posted limit			
	Unable to stop (yellow seemed too short)			
Inattentive	Unexpected, first signal encountered		Unintentional	Any time during red
	Distracted and did not see traffic signal			
	Not distracted, just did not see signal (e.g., drowsy)			
	Restricted view of signal due to sight obstruction			
	Confusing signal display (looked at wrong signal)			

Note:
1 - Causes listed reflect the driver's point of view.

Characterizations of a Red-Light Violation

Shown in Table 5-1 are several characterizations of the red-light violation. These characterizations include "violation type," "driver intent," and "time of violation." Violation type describes whether the violation was perceived as "avoidable" or "unavoidable." Driver intent describes whether the violation was "intentional" or "unintentional." Time of violation describes when the violation occurs relative to the onset of the red indication.

Avoidable Violations

An "avoidable" violation is committed by a driver who believes that it is possible to safely stop but decides it is in his or her best interest to run the red indication. Frequent avoidable red-light violations may be an indication of congestion, dense traffic, or unnecessary delay. Avoidable violations are also characterized as "intentional."

Congestion. Violations due to congestion reflect driver frustration after experiencing lengthy delay. The violation is likely to occur in the first few seconds of red. Short of significant capacity improvements, this violation may be most effectively treated by enforcement.

Dense Traffic. Violations attributed to "dense traffic" are likely found in coordinated signal systems where the progression band is constrained at its trailing edge by the signal timing of the subject approach. In this situation, drivers in platoons have an expectation of continued receipt of green because they are in the progression band and are "surprised" at the onset of yellow. This violation is likely to occur in the first few seconds of red. Signal timing modifications may mitigate this problem. Enforcement may also be appropriate if engineering countermeasures are ineffective.

Unnecessary Delay. Violations due to "unnecessary delay" reflect a perception that there is: (1) no need to stop because the conflicting movements are vacant, or (2) previous stops led to lengthy waits at the intersection that seem unnecessary because there were numerous breaks in the crossing traffic during which the green could have been returned to the waiting driver. This perception often leads to a degradation in driver respect for traffic signals. The violation can occur any time during the red. Signal removal or timing modifications may mitigate this problem. Enforcement may also be appropriate if engineering countermeasures are ineffective.

Unavoidable Violations

An "unavoidable" violation is committed by a driver who either: (1) believes that he or she is unable to safely stop and consciously decides to run the red, or (2) is unaware of the need to stop. Frequent unavoidable violations may be caused by driver inability to stop or inattention. The former "cause" represents an intentional violation; the latter represents an unintentional violation.

Incapable of Stop. This violation occurs when a driver sees the yellow signal indication but determines that it is impossible to stop safely before reaching the intersection. This determination could be the result of a lengthy reaction time to the yellow onset, steep downgrade, high speed, or a low tolerance for high deceleration. Frequent violations may be an indication of an inconspicuous yellow indication, inadequate yellow interval duration, or excessive speed. This violation is likely to occur in the first few seconds of red. Signal timing modifications or improvements to enhance the conspicuity of the yellow indication should mitigate this problem.

Inattentive. This violation occurs when the driver is inattentive and does not see the signal (or sees it too late to respond appropriately). Frequent violations may be an indication of poor signal visibility or conspicuity. This violation can occur at any time during the red. Improvements to signal visibility or conspicuity should mitigate this problem to some degree.

Time of Violation

The time of violation (or time-into-red) relates to the time that the driver enters the intersection after the onset of the red indication. When a driver enters late into the red, it may be an

indication of deficiencies in signal visibility or sight distance along the intersection approach. When drivers enter during the first few seconds of red, it may be an indication of frustration due to excessive delay, an inadequate yellow interval duration, or excessive speed.

Analysis of Time-Into-Red

This section examines the reported relationships between time-into-red and both red-light violations and red-light-related crashes. The time of the crash would depend on the time of the red-light violation and on the time of entry of the second vehicle involved in the crash. Some recent research on these topics is briefly discussed in the remainder of this section.

Time of Red-Light Violations

Researchers have investigated the time after the start of red when a red-light violator enters an intersection. In one of the more recent studies, Bonneson et al. (*13*) examined 541 signal phases in which at least one through vehicle entered the intersection after the start of red. The results of this examination are shown in Figure 5-1. The median entry time was less than 0.5 s. About 98 percent of drivers entered the intersection within 4 s after the start of red (i.e., end of yellow).

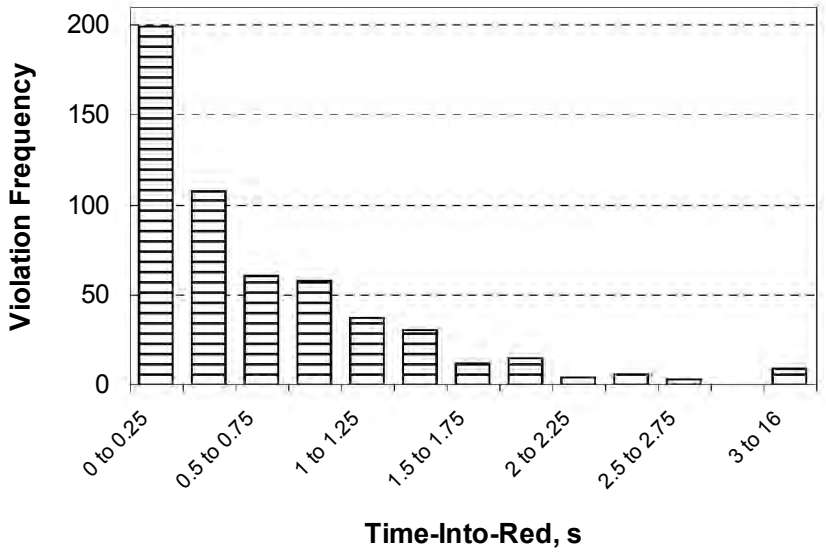

Figure 5-1. Frequency of Red-Light Violations as a Function of Time-Into-Red.

Milazzo et al. (*7*) noted that there are two common types of red-light-related crashes: right-angle and left-turn-opposed. Unlike right-angle crashes, left-turn-opposed crashes are likely to occur soon after the start of red (possibly prior to the end of the all-red interval). This statement is especially true when the left-turn movement is permitted to turn through gaps in the opposing through traffic stream. Drivers of left-turning vehicles waiting in the intersection at the end of the

phase may unintentionally turn in front of an opposing through vehicle, believing that its driver will stop for the red indication. If this through driver violates the red indication, he or she may collide with the left-turning driver. This situation is not likely to occur when protected-only left-turn phasing is provided.

Figure 5-2 illustrates the time of entry of the opposing left-turn and crossing through movements that conflict with the subject through movement. These times are illustrated in terms of the probability of a headway less than 2.5 s in the respective traffic streams. The threshold value of 2.5 s was selected for this illustration based on the assumption that a red-light violator is not able to avoid conflict with a stream of vehicles when their headway is less than 2.5 s.

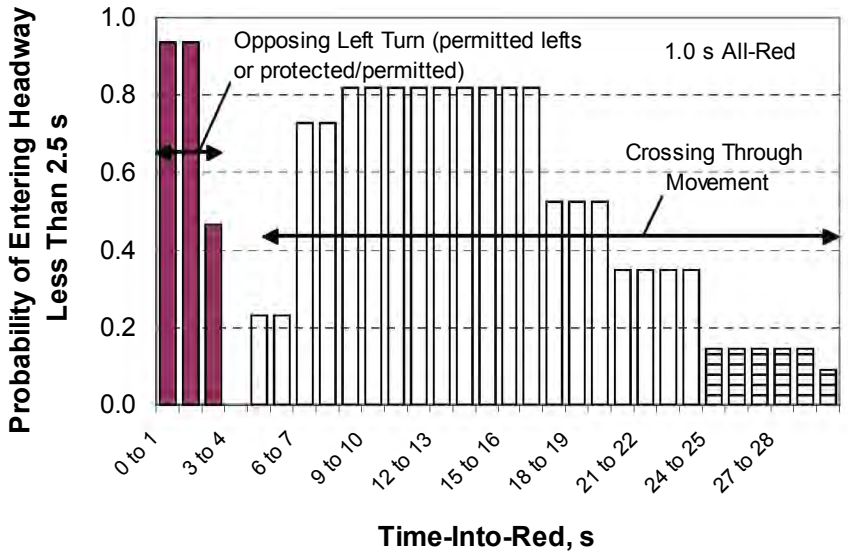

Figure 5-2. Probability of Entering Intersection as a Function of Time-Into-Red.

Both conflicting traffic movements identified in Figure 5-2 are in queue as the subject phase ends. The probability associated with the crossing through movement increases more gradually than the left-turn movement and reflects the slightly longer start-up reaction time of the crossing through driver to the change in signal indication. The probability for the through movement decreases after about 20 s of red reflecting the transition from queue service to random arrivals during green. The probabilities shown in Figure 5-2 suggest that permitted left-turn vehicles clear the intersection within the first 3 s of red. Given a 1.0-s all-red interval, the probabilities also suggest that crossing through vehicles will not start to enter until after about 4 s have lapsed.

Figure 5-3 illustrates how the time of violation and the time of entry combine to create the potential for a red-light-related conflict. It represents the combination of Figures 5-1 and 5-2 in terms of the joint probability of a red-light violation during a specific time interval and the probability of a conflicting vehicle entering the intersection during the same time interval.

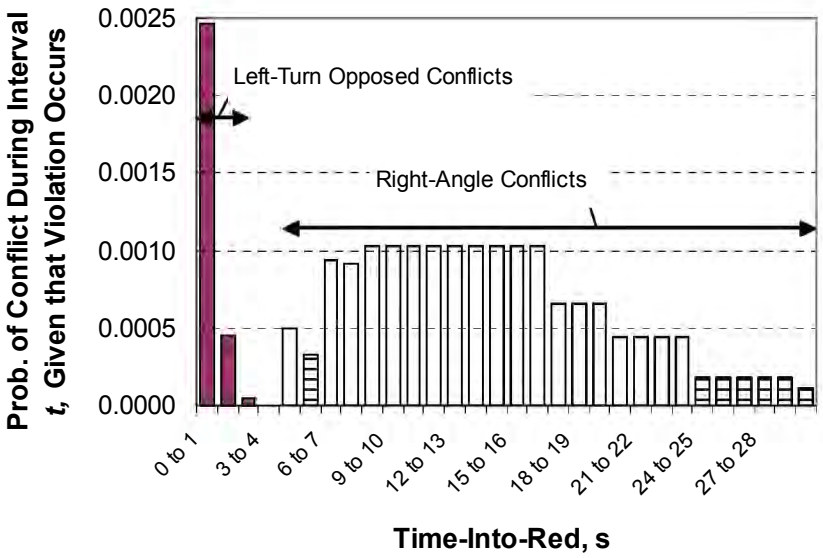

Figure 5-3. Probability of a Red-Light-Related Conflict as a Function of Time-Into-Red.

The trends in Figure 5-3 indicate that the potential for conflict is very high in the first second of red. This conflict would be between a through vehicle violating the red and an opposing left-turn vehicle attempting to clear the intersection. The trend drops rapidly for the second and third seconds of red reflecting the decreasing probability of violation and of left-turn presence. After the fourth second, the probability of conflict increases in a manner consistent with the probability of a through vehicle having a headway less than 2.5 s (shown in Figure 5-2). These trends suggest that the red-light-related crash type is likely to be highly correlated with the time of the crash.

The likelihood of a left-turn-opposed crash is represented as the area under the associated "curve" (i.e., the sum of the first three probabilities). Similarly, the likelihood of a right-angle conflict is obtained by summing the area under its curve. These two sums for the curves shown in Figure 5-3 suggest that there are five to six times as many right-angle conflicts as there are left-turn-opposed conflicts. This ratio is consistent with the findings reported by Bonneson et al. (*11*) in their analysis of 502 red-light-related crashes in three Texas cities.

The points made in this, and previous, sections are summarized in Table 5-2 as they relate to red-light violations. The information in this table indicates that most of the violations occur in the first 4 s of red. If the frequency of violations is excessive, the violations are most likely caused by congestion, dense traffic streams, or conditions that make it difficult for drivers to stop. Also, it is likely that permitted left-turn movements will be most at risk to experience conflict. These findings suggest that countermeasures that address violations in the first few seconds of red are likely to significantly reduce left-turn-opposed crashes, should such crashes be over-represented at the treated intersection.

Table 5-2. Relationship between Time of Violation and Violation Characteristics.

Time of Violation, s	Percent of Violations, %	Left-Turn Phasing	Most Likely Conflict	Cause of Violation
0.0 to 4.0	98	Protected-only	None	--
		Permitted or Prot./Perm.	Left-turn-opposed	Congestion, dense traffic, incapable of stop
4.0 to end of green	2	Any	Right-angle	Unnecessary delay, inattentive

Time of Red-Light-Related Crashes

Milazzo et al. (7) investigated the relationship between time-into-red and crash type. To perform their study, they obtained 34 photographs of red-light-related crashes taken by enforcement cameras. All photos were obtained from Internet websites hosted by enforcement agencies. The crashes in the photos were then classified by crash type. The right-angle crashes were further classified by their time-into-red. Milazzo et al.'s findings are shown in Table 5-3.

Table 5-3. Red-Light-Related Crash Summary Statistics.

Crash Type	Range of Time-Into-Red, s	Number of Crashes	Average Time-Into-Red, s	Median Time-Into-Red, s
Right-angle	0.0 to 2.9	0	No crashes	No crashes
	3.0 to 21.8	27	8.7	6.7
Left-turn-opposed	1.0 to 26.9	7	6.0	1.9
	Overall:	34	8.1	6.4

The trends in the data in Table 5-3 are consistent with those noted for Figure 5-3. First, right-angle crashes do not appear likely to occur in the first 3 or 4 s of red. Second, the median time-into-red for the left-turn-opposed crashes of 1.9 s suggests that most of these crashes occur as a result of permitted left-turning activity at the end of the phase. Finally, it is likely that the majority of red-light-related crashes are of the right-angle type.

The reported average time-into-red for the left-turn movement of 6.0 s, when compared with the median time of 1.9 s, suggests that there is one left-turn crash that occurred well into the red. It is likely that this crash was due to driver inattention rather than a misjudged gap at the end of a permitted left-turn movement.

The points made in this, and previous, sections are summarized in Table 5-4 as they relate to red-light-related crashes. The information in this table is consistent with that previously offered in Table 5-2. Specifically, over-represented left-turn-opposed crashes are a likely indication that the violations that occur in the first few seconds of red should be the focus of countermeasure selection.

These violations are most likely related to congestion, dense traffic streams, or conditions that make it difficult for drivers to stop. On the other hand, if right-angle crashes are over-represented at the intersection but left-turn-opposed crashes are not over-represented, then the violations occurring later into the red should be the focus of countermeasure selection. These violations are most likely related to driver desire to avoid unnecessary delay or the inability of drivers to detect the controlling signal indications in a timely manner.

Table 5-4. Relationship between Time of Crash and Crash Characteristics.

Time of Crash	Left-Turn Phasing	Most Likely Crash	Cause of Violation Leading to Crash
Early in red	Protected-only	None	--
	Permitted or Prot./Perm.	Left-turn-opposed	Congestion, dense traffic, incapable of stop
Any time in red	Any	Right-angle	Unnecessary delay, inattentive

Countermeasures

This section describes countermeasures that are likely to reduce red-light-related crashes. Initially, engineering countermeasures are described. Then, the public awareness campaign as a countermeasure is described. Enforcement countermeasures were previously discussed in Chapter 3.

Engineering Countermeasures

Table 5-5 lists most of the engineering countermeasures cited in the literature as having some ability to reduce red-light violations, related crashes, or both. The reported effectiveness of many of these factors is also presented in the table. These reduction factors reflect the findings from several research projects, as identified in the last column of the table. The effectiveness of education and enforcement are also shown and will be discussed in subsequent sections.

A reduction factor is not provided for some countermeasures listed in Table 5-5. Any such omission reflects the fact that some countermeasures have not been formally studied. Nevertheless, their ability to reduce red-light violations and related crashes is intuitive and widely recognized, especially when operations or visibility are improved by their implementation. A fairly detailed discussion of many of these countermeasures is provided in the ITE report, *Making Intersections Safer: A Toolbox of Engineering Countermeasures to Reduce Red-Light Running* (*38*).

Public Awareness Campaign

There are generally three main themes of an effective public awareness campaign. These themes and their associated objectives are:

Table 5-5. Red-Light Violation Countermeasure Effectiveness.

Category	Countermeasure	Reported Reductions, % [1, 2, 3]		
		Violations	Crashes	Reference [4]
Traffic char.	Reduce approach speed by 5 mph	30	25 to 30	Chap. 4, 2
Signal operation	Increase signal cycle length by 10 s, if *v/c* ratio < 0.60	15	--	Chap. 4
	Increase yellow interval duration by 0.5 s	40	20 to 25	Chap. 4, 2
	Provide green extension (advance detection) [5]	65	--	*29*
	Add protected-only left-turn phasing [6]	--	70	*34*
Motorist information	Improve signal visibility via better signal head location	--	--	--
	Improve signal visibility via additional signal head	--	47	*35*
	Improve signal visibility by clearing sight lines to signal	--	--	--
	Improve signal conspicuity by upgrading to 12" lenses	--	47	*35*
	Improve signal conspicuity by using yellow LEDs	13	--	*13*
	Improve signal conspicuity by using red LEDs	--	--	--
	Improve signal conspicuity by using back plates	25	32	Chap. 4, *35*
	Improve signal conspicuity by using dual red indications	--	33	*35*
	Add advance warning signs (no active flashers) [7]	--	44	*35*
	Add advance warning signs with active flashers [7]	29	--	*36*
Traffic operation	Reduce delay through re-timing if *v/c* ratio > 0.70	10 to 50	--	Chap. 4
	Reduce unnecessary delay through signal re-timing	--	--	--
	Improve signal coordination [8]	--	--	--
Geometry	Remove unneeded signals	100	100	--
	Add capacity with additional lanes or turn bays	--	--	--
Education	Implement public awareness campaign	--	--	--
Enforcement	Implement officer enforcement program [9]	16 (--)	-- (6.4)	*23*, Chap. 3
	Implement camera enforcement [10]	40 (--)	36 (10)	*37*, *6*

Notes:

1 - Values listed are for the specific intersection approach to which the countermeasure is applied.

2 - Values in parentheses apply to the entire city or area influenced by the enforcement program.

3 - Underlined factors are based on a simple before-after study without comparison. Hence, values listed may overstate the true effect of the countermeasure. They are shown only to illustrate the potential benefit of the countermeasure.

4 - When two references are listed, they are listed in the order of "violation reference," "crash reference." Chapter references refer to chapters in this report. Numbers in italics identify published reports listed in Chapter 7.

5 - Green extension using advance detection should reduce red-light violations provided it does not max-out frequently.

6 - Crash reduction factor applies only to left-turn-opposed crashes.

7 - Active flashers accompany the advance warning sign and are activated during the last few seconds of green.

8 - Improvements to signal coordination will be most effective in reducing red-light violations if they result in: (1) lower delay, (2) longer cycle lengths, and (3) progression bands that are not constrained by the end of the phase such that platoons traveling through the intersection are repeatedly caught by the change to red.

9 - A citywide officer enforcement program should emphasize the enforcement of intersection traffic control violations. Enforcement should be repeated for 1 or 2 hours each day to retain its effectiveness. The 16 percent reduction listed is based on 28 percent reduction for continuous officer presence but adjusted to represent a daily average for the situation where enforcement is applied only 1 hour each day. Adjustment is based on reported data (*23*).

10- Camera enforcement is generally recognized to result in an increase in rear-end crashes; however, most studies indicate that this increase does not negate the greater reduction in red-light-related crashes (*26*).

"--" - data not available.

- Educate drivers on red-light-running hazards (objective: stimulate a voluntarily change in the driver's behavior).
- Use the media to open communications between elected officials and the public about the extent of the problem and the need for treatment (objective: gain public support for treatment).
- Provide advance warning that additional enforcement is being implemented to improve traffic safety (objective: minimize negative public reaction and avoid accusations of deception).

A wide range of methods are often used to convey the campaign message and heighten motorist awareness. Some of the more commonly used methods include: posters, mass mailings, hand outs, electronic media commercials, billboards, warning signs, and bumper stickers (*39*). Methods less commonly used, but recommended, include: (1) outreach efforts to schools, driver education, and community groups; (2) maintenance of a website with program information and answers to frequently-asked questions; and (3) regular surveys of public opinion, support, and awareness of the program.

A review of the literature indicates that the effectiveness of public awareness campaigns is rarely quantified and reported. This limitation is likely due to the fact that campaigns are almost always conducted in parallel with heightened enforcement. In this situation, it is difficult to separate the effect of the public awareness campaign from that of the enforcement program.

DATA COLLECTION PLAN

Based on the review of red-light-related crash trends, it was determined that data were needed to further investigate the relationship between time-into-red and crash type. The specific objectives of this investigation were:

- to show when crashes occur after the start of red,
- to determine the effect of time-into-red on crash type and severity,
- to determine if other factors are correlated with time-into-red, and
- to show how this information can be used to select countermeasures to reduce red-light-related crashes.

Site Selection Process

A database containing a minimum of 100 crashes was established as needed to achieve the objectives of this investigation. The establishment of this minimum was intended to ensure statistical stability in any trends found in the data. To achieve this minimum, it was rationalized that 2 to 3 years of crash data for 3 to 5 intersections (each with camera enforcement) in each of 2 cities would be needed.

Several agencies known to have camera enforcement were contacted to solicit their participation in this investigation. Those agencies having the most cameras in operation for the

greatest length of time were contacted first. A key criterion used in selecting these agencies was the availability of archived photos of red-light violations that resulted in a crash.

Fifteen individuals representing nine city (or county) transportation departments in four states were contacted for the purpose of obtaining their assistance with this investigation. Of these agencies, only four indicated a willingness to assist with the data collection process. From these four agencies, two city agencies were ultimately selected based primarily on their level of interest in this research project. These two agencies are located in Arizona.

Database Attributes

The database assembled for this investigation includes crash-related data, traffic control settings, traffic volume, and geometric conditions for several camera-enforced intersections. The crash-related data consisted of the information that was recorded on the crash report or in the photographed image of a red-light violation. The attributes in the database for the Arizona cities are listed in column 3 of Table 5-6.

The crash-related data included in the database for the Arizona sites were acquired from a combination of the enforcement photolog and the crash report archives maintained by the respective cities. Practical limitations on data archiving and storage capacity limited the number of years for which crash data were available. Volume data were obtained from each city's transportation department. Traffic control and geometry data were gathered by means of a field survey conducted during the visit to each city.

Adjustments to Accommodate Sample Size

An initial review of the crash records at the two Arizona cities indicated that the minimum desired sample size would not be achieved by considering only three to five intersections in each city. This realization was a result of three factors. First, the presence of enforcement cameras had a significant effect on reducing the frequency of red-light-related crashes in the selected cities. Second, it was revealed that the cameras oftentimes did not photograph the actual crash. This finding was due to several causes (e.g., the red-light violator did not travel in a lane monitored by the camera, the camera was located at a different intersection on the day of the crash, etc.). Third, many of the enforcement cameras in the two cities studied had been in service for 18 months or less.

Based on the aforementioned challenges to achieving the desired sample size, two approaches were undertaken to maximize the amount of data collected for this investigation. First, the number of intersections included in the database was expanded to include all of the intersections for which the city had enforcement camera equipment in operation during the previous 3 years. This approach expanded the database to include 12 intersections in Arizona. Data for a total of 27 crashes were obtained from these intersections.

Table 5-6. Database Attributes–Time-Into-Red Analysis.

Data Type	Attribute	Data Availability by Resource			
		Arizona	Maryland	Milazzo (7)	Internet
Crash	Time-into-red of crash	✔	✔	✔	✔
	Speed of red-light-running vehicle	✔	✔	✔	✔
	Travel direction at intersection (e.g., left-turn)	✔	--	--	--
	Date & time of crash	✔	✔	✔	✔
	Crash type (right-angle or left-turn-opposed)	✔	✔	✔	✔
	Severity	✔	--	--	--
	Number of injuries	✔[1]	--	--	--
	Contributing factor(s)	✔	--	--	--
Traffic control	Left-turn phasing	✔	✔[2]	✔[2]	✔[2]
	Yellow interval duration	✔	✔	--	--
	All-red interval duration	✔	--	--	--
	Approach speed limit	✔	✔	--	--
Volume	Annual average daily traffic (AADT)	✔	--	--	--
Number of lanes	Left, through, & right-turn lanes on subject street	✔	✔[3]	✔[3]	✔[3]
	Left, through, & right-turn lanes on cross street	✔	✔[3]	✔[3]	✔[3]
	Total Crashes: 63	27	18	7	11
	Data Sources:	Crash reports, agency files, field survey	Photo	Photo	Photo

Notes:
1- Number of injuries known only for a portion of the crashes.
2- Left-turn signal heads not always visible in camera field of view.
3- All lanes not always visible in camera field of view.

A second approach used to maximize the amount of crash data gathered involved the acquisition of crash photos from other agencies and individuals. These additional data resources are identified in columns 4 through 6 of Table 5-6 (a description of these resources is provided in the next section). As indicated by the dashes in this table, the sole use of crash photos as the only data source precluded the collection of some attributes. This fact limited the examination of crash severity, contributing factors, all-red interval duration, and traffic volume to only the "Arizona" data. A total of 36 crash photos were obtained from resources other than Arizona. The combined database represents information on 63 red-light-related crashes.

Data Sources

Arizona

Data describing 27 crashes at 12 intersections were obtained from two cities in Arizona. The distribution of these crashes among the two cities is listed in Table 5-7. For legal reasons, photos of

the crashes could not be obtained from either city. Instead, city personnel reviewed the photos and associated crash reports and documented their findings. These findings were made available to the research team.

Table 5-7. Distribution of Crashes by Source and Crash Type.

Source	Number of Intersection Approaches	Number of Crashes by Crash Type		
		Left-Turn-Opposed	Right-Angle	Total
Arizona, City 1	3	4	2	6
Arizona, City 2	9	12	9	21
Maryland	11	3	15	18
Milazzo et al. (7)	3	1	4	5
Various Other	9	2	11	13
Total:	35	22	41	63

With a couple of exceptions, all of the crash data identified in column 3 of Table 5-6 were obtained from city personnel. Information about the severity of each crash was limited to simply an indication of whether one or more persons involved were injured or killed. Levels of injury extent were not provided. Also, the number of injured persons was often not reported. As a result, an investigation of the number of injuries by time-into-red was not possible.

Maryland

An agency in Maryland provided 18 photos of red-light-related crashes. These crashes occurred at 11 intersections collectively located in four counties in central Maryland. The distribution of these crashes is shown in Table 5-7.

All of the photos obtained indicated the time-into-red, vehicle speed, date and time, crash type, left-turn phasing, yellow duration, and approach speed limit. No information was available about travel direction, crash severity, contributing factor, all-red duration, or traffic volume. Information about the approach geometry was available in some photos. Ten of the 11 intersections were subsequently identified using Internet-based street maps. From this identification, aerial photos were obtained and used to provide missing information about the geometry of each intersection approach.

Milazzo Research

The report by Milazzo et al. (7) contained five photos of red-light-related crashes. These photos had the following distribution:

- two crashes in Charlotte, North Carolina, representing one intersection;
- one crash in Oxnard, California; and
- two crashes in Washington, D.C., representing one intersection.

The distribution of these crashes is shown in Table 5-7.

The photos provided by Milazzo et al. (*7*) tended to contain less information than those provided by Maryland. Specifically, they only provided data for time-into-red, vehicle speed, date and time, crash type, and left-turn phasing. No information was available about travel direction, crash severity, contributing factor, yellow duration, all-red duration, approach speed limit, or traffic volume. Geometric information for each approach was obtained from a combination of the crash photo and aerial photos obtained from the Internet.

Other Crash Photos

Thirteen photos of red-light-related crashes were obtained from various Internet sources. Collectively, these photos represent nine intersections. The locations of eight intersections were identified using the photo and Internet-based street maps; however, the location of one intersection could not be determined. The photos of three crashes were obtained from various red-light-violation-related Internet websites. Three other photos were obtained from a prominent magazine. The remaining crash photos were obtained from individuals affiliated with various enforcement agencies. Collectively, the photos represent locations in Washington D.C., North Carolina, and Australia. The distribution of these crashes is shown in Table 5-7.

The data obtained from these photos varied. Most of them contained the types of information available in the Maryland photos. However, some of them contained less information–more consistent with that found in the photos provided by Milazzo et al. (*7*).

DATA ANALYSIS

This section describes a summary of key database statistics and an examination of correlations between crash frequency and various factors (including time-into-red).

Database Summary

Selected database attributes are summarized in Table 5-8. Collectively, the statistics demonstrate that the data reflect a wide range of typical traffic control and volume conditions. They also show that, with one exception, there is no practical difference between the conditions present in the left-turn-opposed and the right-angle crash photos. Specifically, the percent injury crashes, speed of violator, speed limit, and volume are almost invariant among the two crash types.

Table 5-8. Database Summary–Time-Into-Red Analysis.

Crash Type	Attribute	Statistic					
		Obs.	Average	Std. Dev.	Median	Minimum	Maximum
Left-turn-opposed	Time-into-red, s	22	0.9	0.6	**0.9**	0.1	3.1
	Yellow duration, s	19	4.0	0.2	4.0	3.5	4.5
	Percent injury crashes [1]	16	56	--	--	--	--
	Speed of violator, mph	21	32.8	10.1	32	16	52
	Speed limit, mph	19	40.8	3.8	40	35	45
	AADT, veh/d [1]	16	18,100	4600	18,400	9800	32,100
Right-angle	Time-into-red, s	41	14.1	12.0	**8.9**	0.6	44.2
	Yellow duration, s	33	4.3	0.4	4.0	3.9	5.0
	Percent injury crashes [1]	11	55	--	--	--	--
	Speed of violator, mph	40	33.5	7.8	32	17	55
	Speed limit, mph	26	40.4	6.0	40	35	55
	AADT, veh/d [1]	11	17,800	2500	18,900	14,800	23,300

Note:
1 - Based on data from the two cities in Arizona.

The median time-into-red for left-turn-opposed crashes is 0.9 s whereas that for right-angle crashes is 8.9 s. This trend is consistent with that reported by Milazzo et al. (*7*), as discussed previously with regard to Table 5-3. It could be argued that this consistency is due, in part, to the five photos that are common to both databases. To test this argument, the five photos were deleted from the database; however, the aforementioned median statistics did not change in value. From this test, it was concluded that the effect of crash type on time-into-red exists independently in both databases.

The number of crashes for each crash type is indicated in column 3 of Table 5-8 for the "time-into-red" attribute. These statistics indicate that right-angle crashes exceed left-turn-opposed crashes by a factor of two (= 41/22). This factor is much smaller than the "five to six" reported by Bonneson, et al. (*11*), as discussed in a previous section. It suggests that the number of left-turn crashes are over-represented in the database. However, this finding should not be construed to mean that there is any bias in the time-into-red or other statistics included in the database.

Analysis and Interpretation

The relationship between time-into-red and the attributes listed in Table 5-8 was investigated more thoroughly using statistical techniques. This investigation found that crash type was the only attribute related to time-into-red. Discernable trends relating to the other factors were not found.

Figure 5-4 shows the frequency of crashes as a function of time-into-red. The trends in this figure confirm the tendency for left-turn-opposed crashes to occur in the first few seconds of red.

With one exception, all of the right-angle crashes occurred after 5 s or more of red. Closer inspection of the one exception revealed that it occurred very late at night with *both* vehicles violating their respective red indications at about the same time.

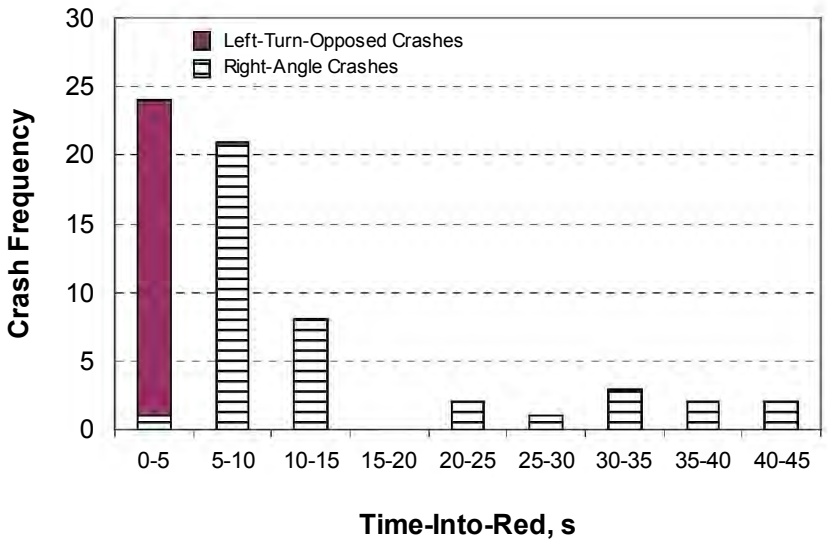

Figure 5-4. Crash Frequency by Time-Into-Red.

The trends in Figure 5-4 indicate that the frequency of red-light-related crashes tends to be highest in the first 5 s of red. Crash frequency declines thereafter, reaching a nominally small but constant frequency after 20 s of red. Based on the discussion associated with Figure 5-3, this pattern was expected. The high frequency of right-angle crashes in the range of 5 to15 s into red is due to the discharge of the cross street through movement queue. Red-light violations during queue discharge have a high likelihood of conflict. The potential for conflict after queue discharge is invariant, reflecting the random occurrence of cross street arrivals and red-light violations during the latter part of the red interval.

The distribution of crashes during the first 15 s of red was more closely examined to determine how the distribution of crashes varied over time for the left-turn-opposed and right-angle crashes. For this examination, the data shown in Figure 5-4 were used to develop Figure 5-5. The only difference between the figures is in the time interval used for each vertical bar.

The trends in Figure 5-5 are very similar to the hypothetical trends shown in Figure 5-3. These trends confirm the hypothesized effect of the joint probabilities of violation and conflicting vehicle presence on crash occurrence. From these trends, it is logical that enforcement efforts are likely to reduce violations in the first few seconds of red and, therefore, significantly reduce left-turn-opposed crashes. In contrast, engineering countermeasures are most likely to reduce violations throughout the red and, therefore, reduce both right-angle and left-turn-opposed crashes in somewhat

equal proportion. Increasing the all-red interval is likely to reduce the portion of right-angle crashes that occur in the first few seconds of red. However, these crashes are relatively infrequent, so increasing the all-red interval may not significantly reduce the total number of right-angle crashes.

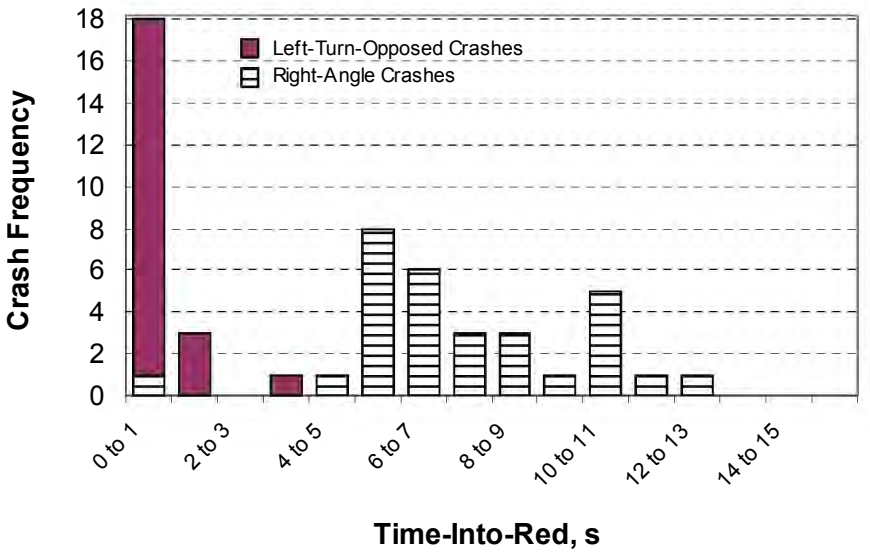

Figure 5-5. Crash Frequency in the First Few Seconds of Red.

GUIDELINES FOR COUNTERMEASURE SELECTION

The findings from the data analysis are used in this section to develop guidelines for selecting countermeasures to reduce red-light violations. Initially, the characteristics of the red-light violator are used to identify whether engineering or enforcement countermeasures are appropriate. Then, these characteristics are pooled with time-into-red and crash-type distribution statistics to develop guidelines for determining when enforcement or engineering countermeasures will be most effective.

Red-Light Violation Characteristics and Related Countermeasures

The characterizations offered previously with regard to the discussion associated with Table 5-1 are combined with the findings from the previous section to identify the most appropriate countermeasure category. These characterizations are repeated in columns 1 through 4 of Table 5-9.

As indicated in Table 5-9, time of violation is correlated with crash type. Specifically, about 98 percent of all red-light violations occur within the first 4 s of red. The red-light-related crash that occurs within the first few seconds of red almost always includes a permitted left-turning vehicle and an opposing through vehicle (i.e., a left-turn-opposed crash). In this situation, the left-turning driver is attempting to clear the intersection at the end of the adjacent through phase and an opposing through driver runs the red indication (this scenario exists when protected-only left-turn phasing is

not provided). After the first few seconds of red, the right-angle crash is the more common red-light-related crash.

Table 5-9. Red-Light Violation Characterizations and Related Countermeasures.

Cause Category	Violation Type	Driver Intent	Time of Violation	Most Likely Crash	Countermeasure Category
Unnecessary delay	Avoidable	Intentional	Any time during red	Right-angle	Enforcement (unless engineering can be used to reduce delay or eliminate signal)
Congestion, dense traffic			First few seconds of red	Left-turn-opposed	
Incapable of stop	Unavoidable				Engineering (to increase probability of stopping)
Inattentive		Unintentional	Any time during red	Right-angle	Engineering (to improve signal visibility or conspicuity)

As noted in a previous section, the various "causes" of a red-light violation (as reflect the driver's point of view) offer important clues to identifying the countermeasures that would be most appropriate in certain specific situations. For example, violations due to congestion reflect driver frustration after experiencing lengthy delay. This violation is likely to be most effectively treated by enforcement unless significant improvements in capacity can be made through intersection reconstruction. This, and similar, relationships are illustrated in Table 5-9. The various relationships shown in this table between "cause category," "most likely crash," and "countermeasure category" are used in the next section to develop countermeasure selection guidelines.

Countermeasure Selection Guidelines

Based on the characterizations offered in the previous section, guidelines have been developed to help engineers determine when enforcement or engineering countermeasures are likely to be most beneficial. These guidelines are presented in the form of a flow chart where the various decisions that need to be made are identified as a series of steps. These steps ultimately lead to the identification of a viable set of countermeasures. This flow chart is shown in Figure 5-6.

In general, countermeasure selection to address a problem location should be based on a comprehensive engineering study of traffic conditions, traffic control device visibility, crash history, and intersection sight distance. The findings from the engineering analysis can then be used with the guidelines in Figure 5-6 to determine the most beneficial countermeasure category.

As a first step in the use of Figure 5-6, the crash history should be examined to determine if red-light-related crashes are over-represented in terms of crash frequency. Red-light-related crashes include right-angle and left-turn-opposed crashes. The index value described in Chapter 2 (i.e., Equation 10) can be used for this purpose. An index of 1.0 or larger indicates over-representation of crashes. If these crashes are over-represented, then the analysis proceeds to the next step.

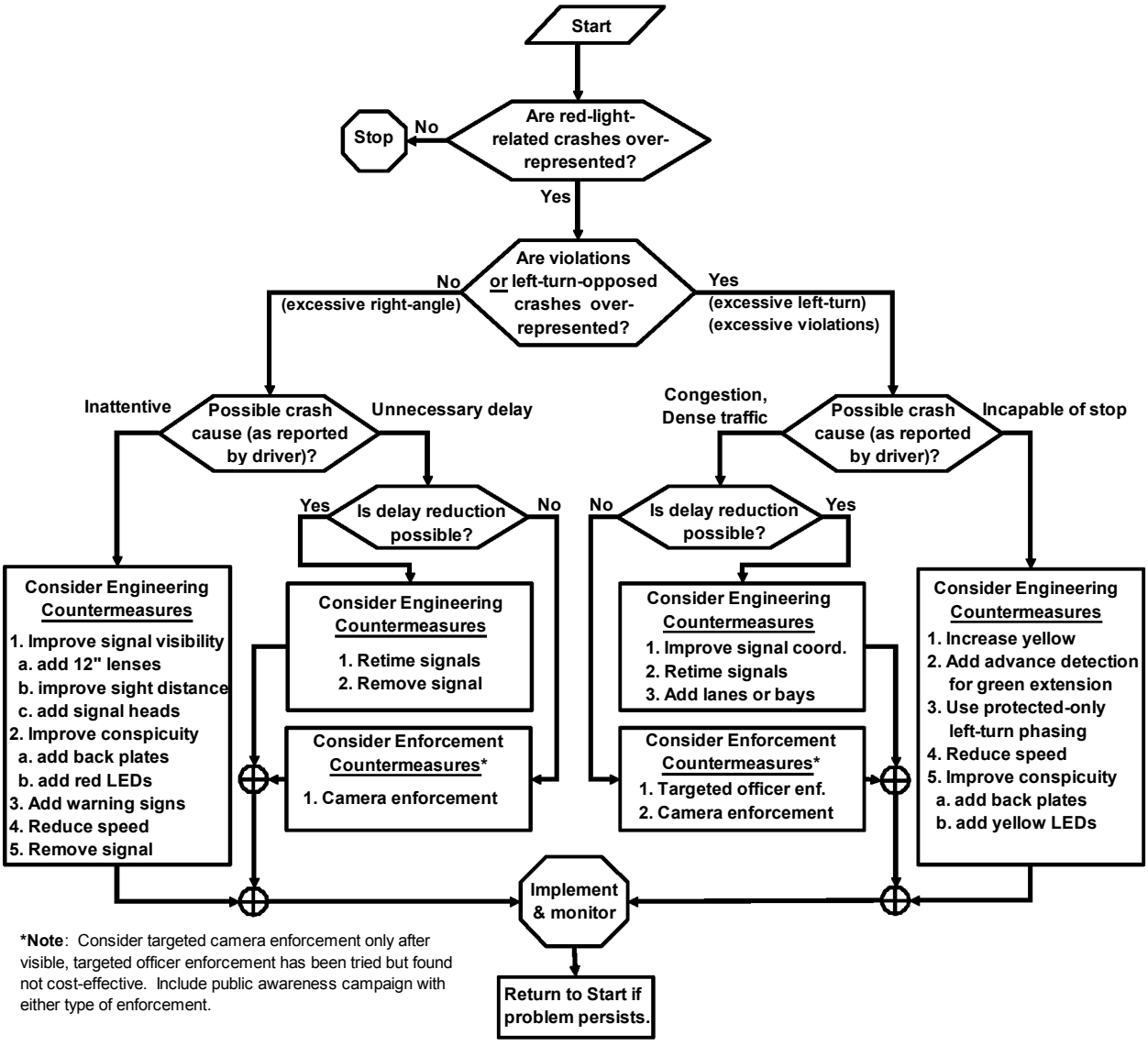

Figure 5-6. Guidelines for Countermeasure Selection.

The next step is to determine whether red-light violations or red-light-related left-turn-opposed crashes are over represented. The index value described in Chapter 4 can be used to evaluate red-light violations. A procedure is described in the Appendix for extending the equations in Chapters 2 and 3 to the estimation of an index value for left-turn-opposed crashes. Again, an index of 1.0 or larger is an indication of over-representation for the purpose of countermeasure selection. Excessive violations or left-turn-opposed crashes are an indication that countermeasure selection should focus on treatment of violations occurring during the first few seconds of red.

As a third step, the engineer should determine the probable cause of the typical crash, from the perspective of the driver. This determination should be based on both a review of the crash reports and the findings from a field visit to the subject intersection. During the field visit, the engineer should use a videotape recorder to record traffic events on the subject intersection approach. While this recording is underway, the engineer should evaluate intersection operation, signal visibility, signal timing, and traffic speed. When the field visit is completed, the engineer should review the videotape and study the characteristics of the red-light violations that occurred. Based on a review of all data sources, the engineer should determine the probable cause of the typical red-light-related crash. Possible causes include: driver inattention, congestion, unnecessary delay, and incapable of stop.

If the crash cause is a result of congestion or unnecessary delay, then the engineer should determine if there are viable capacity or signal timing improvements that can be made to reduce the congestion or delay. It should be noted that "unnecessary" delay is any delay that appears unreasonable to the driver. This type of delay can occur for a variety of reasons. For example, unnecessary delay often occurs for minor movements at an intersection where the major street through movement is held in green for coordination purposes. The unnecessary delay occurs after the platoon has passed and no vehicles are arriving on the major street, even though the signal remains green. Drivers on the minor movements can become impatient when they are delayed for no apparent reason. A capacity analysis of this intersection may indicate that this minor movement incurs a relatively short average delay so the engineer may not believe there is a problem. However, unnecessary delay may still occur and promote disrespect for the signal.

Once the typical crash cause is determined, the engineer should select the class of countermeasures that is appropriate for the typical crash characteristics found at the subject intersection. This category and a range of appropriate countermeasures are listed in each of the rectangular boxes in Figure 5-6. The countermeasures listed are tailored to the considerations that led to the selection of the specific box.

CHAPTER 6. CONCLUSIONS

OVERVIEW

A recent review of the Fatality Analysis Reporting System database by the Insurance Institute for Highway Safety indicated that an average of 95 motorists die each year on Texas streets and highways as a result of red-light violations (*2*). A ranking of red-light-related fatalities on a "per capita" basis indicates that Texas has the fourth highest rate in the nation. Moreover, the cities of Dallas, Corpus Christi, Austin, Houston, and El Paso were specifically noted to have an above-average number of red-light-related crashes (on a "per capita" basis) relative to other U.S. cities with populations over 200,000.

An examination of the Texas Department of Public Safety crash database by Quiroga et al. (*3*) revealed that the reported number of persons killed or injured in red-light-related crashes in Texas has grown from 10,000 persons/yr in 1975 to 25,000 persons/yr in 1999. They estimate that these crashes currently impose a societal cost on Texans of $1.4 to $3.0 billion annually.

The problem of red-light-running is widespread and growing; its cost to society is significant. A wide range of potential countermeasures to the red-light-running problem exist. These countermeasures are generally divided into two broad categories: engineering countermeasures and enforcement countermeasures. A study by Retting et al. (*4*) has shown that countermeasures in both categories are effective in reducing the frequency of red-light violations.

The objectives of this research project were to: (1) quantify the safety impact of red-light-running at intersections in Texas, and (2) provide guidelines for identifying truly "problem" intersections and whether enforcement or engineering countermeasures are appropriate.

SUMMARY OF FINDINGS

The findings from the research are presented in this section. The headings in this section are consistent with the four main chapters of this report and follow their order of presentation.

Intersection Red-Light-Related Crash Frequency

A database was assembled for the purpose of evaluating the various factors that are correlated with, or have an effect on, the frequency of red-light-related crashes. The database includes the traffic volume, geometry, traffic control, and crash data for 47 intersections in three Texas cities. A total of 181 intersection approaches are represented in the database.

A review of peace officer crash reports revealed that 296 red-light-related crashes were reported on the 181 approach study sites during a 3-year period. These crashes represent 29 percent

of all the crashes that occurred at the 47 intersections. The average crash rate is 0.55 red-light-related crashes per year per approach.

The data were used to examine the relationship between crash frequency and the yellow interval duration computed using Equation 1. This equation is referenced in several authoritative engineering reference documents (*14*). The approach taken in this examination was to compare the reported crash frequency with the difference between the yellow duration observed at the approach and that computed for it using Equation 1. The results of the examination indicate that there is a trend toward fewer red-light-related crashes when the observed yellow duration is longer than the computed duration.

A regression model was developed relating crash frequency to various volume, geometry, and traffic control factors. The findings from this development indicated that the following factors are correlated with red-light-related crash frequency: approach leg AADT, yellow interval duration, speed limit, and clearance time. The results of a sensitivity analysis using the calibrated crash prediction model are summarized in Table 6-1.

Table 6-1. Predicted Effect of Selected Factors on Red-Light-Related Crash Frequency.

Factor	Effect of a Reduction in the Factor Value [1]		Effect of an Increase in the Factor Value [1]	
	Factor Change	Crash Freq. Change	Factor Change	Crash Freq. Change
Approach flow rate	-1.0 %	-0.5 %	+1.0 %	+0.5 %
Yellow interval duration	-1.0 s	+125 to +225 %	+1.0 s	-35 to -40 %
Approach speed limit	-10 mph	0 to -60 %	+10 mph	+83 to +123 %
Clearance path length	-40 ft	+40 to +50 %	+40 ft	-30 to +50 %

Note:
1 - Negative changes represent a reduction in the associated factor.

The trends shown in Table 6-1 indicate that crashes decrease with an increase in yellow interval duration and a reduction in speed limit. The effect of clearance path length is less obvious. In general, an increase in path length is associated with a decrease in crashes provided that the corresponding clearance time is less than 2.5 s. This trend reflects increasing driver reluctance to violate the red indication at wider intersections. Path length and speed combinations that exceed 2.5 s travel time are associated with an increase in crashes. This trend reflects the greater likelihood of a red-light-related crash at wider intersections.

The aforementioned “breakpoint” clearance time of 2.5 s effectively defines an optimal intersection width for a given approach speed (or, alternatively, an optimum speed limit for a given width). These optimal widths are 110, 120, 150, and 165 ft for speed limits of 30, 35, 40, and

45 mph, respectively. Theoretically, red-light-related crashes will be minimized at these optimum width and speed combinations.

A procedure was developed for identifying intersections with the potential for red-light-related safety improvement (i.e., "problem" intersections). The application of this procedure is intended to identify intersections that are likely to need some type of safety improvement and for which the treatment is likely to be cost-effective. To this end, the procedure can be used to identify, and rank, intersections with an above average frequency of red-light-related crashes.

The procedure combines the empirical Bayes method with the calibrated crash prediction model to estimate the expected crash frequency for the subject intersection approach. This estimate is then used to compute an index value that serves as an indicator of the extent of the red-light-related crash problem for the subject approach. In general, approaches associated with a positive index value have more red-light-related crashes than the "typical" approach. An approach with an index of 2.0 is likely to have a greater problem than an approach with an index of 1.0. Greater certainty in the need for treatment can be associated with higher index values.

Area-Wide Red-Light-Related Crash Frequency and Enforcement Effectiveness

A database was assembled for the purpose of evaluating the effectiveness of an officer enforcement program that targets intersection traffic control violations. In this program, the enforcement agency uses a heightened level of enforcement relative to that otherwise employed. The program is sustained for a period of time that can range from several months to 1 year. The objective of the program is to encourage drivers to be compliant with traffic control laws and more aware of traffic control devices; the overarching goal is to make the road safer, as evidenced by fewer crashes. This type of targeted enforcement is often coupled with a public awareness campaign that is intended to inform drivers and garner public support for the program.

Citywide crash data were assembled for eight Texas cities that participated in TxDOT's Intersection Traffic Control-Selective Traffic Enforcement Program. Each city implemented a citywide heightened enforcement program and public awareness campaign for 1 or 2 years in the period 1997 to 2000. A total of 33,769 officer-hours were expended by these cities as part of the ITC-STEP, and a total of 31,615 citations for red-light violation were issued.

A before-after evaluation method was used to evaluate the effectiveness of the ITC-STEP at reducing red-light-related crashes. The empirical Bayes-based method described by Hauer (*9*) was used for the analysis. The results of the analysis revealed that crashes were reduced at six of the eight cities during the time that they participated in the ITC-STEP. The program is estimated to have reduced red-light-related crashes by 6.4 percent during the time of its implementation.

A procedure was developed to identify cities that have an exceptionally high frequency of red-light-related crashes. The application of this procedure is intended to identify cities for which area-wide enforcement is likely to be cost-effective.

Intersection Red-Light Violation Frequency

A database was assembled for the purpose of evaluating the various factors that are correlated with, or have an effect on, the frequency of red-light violations. The database includes traffic volume, geometry, traffic control, and violation data for 13 intersections. Two approaches were studied at each intersection.

More than 11,266 signal cycles were observed at the 26 intersection approaches. During these cycles, 595 vehicles entered the intersection after the change in signal indication from yellow to red. An examination of vehicle-type revealed that heavy vehicle operators are more than twice as likely to run the red indication as passenger car drivers. This finding was previously noted by Zegeer and Deen (*29*).

The data were used to examine the relationship between violation frequency and the yellow interval duration computed using Equation 1. The approach taken in this examination was to compare the observed violation frequency with the difference between the yellow duration observed at the approach and that computed for it using Equation 1. The results of the examination indicate that there is a trend toward more violations when the observed yellow duration is shorter than the computed duration.

A regression model was developed relating violation frequency to various volume, geometry, and traffic control factors. The findings from this development indicated that the following factors are correlated with red-light violation frequency: yellow interval duration, use of signal head back plates, speed, clearance path length, heavy-vehicle percentage, and volume-to-capacity ratio. The results of a sensitivity analysis using the calibrated prediction model are summarized in Table 6-2.

The trends shown in Table 6-2 indicate that violations decrease with an increase in cycle length, yellow interval duration, clearance path length, and the addition of back plates. Violations also decrease with a decrease in 85th percentile speed, heavy-vehicle percentage, and volume-to-capacity ratio. The effect of heavy vehicles on violation frequency is likely a result of the greater propensity of heavy-vehicle operators to run the red light.

An examination of the combined effect of a change in cycle length and volume-to-capacity ratio revealed that red-light violations were at their lowest level when the volume-to-capacity ratio was in the range of 0.6 to 0.7. This range of ratios was found to yield minimal violations, regardless of speed, path length, yellow duration, heavy-vehicle percentage, cycle length, phase duration, or traffic volume. Volume-to-capacity ratios below this range resulted in an increase in violations due primarily to shorter cycle lengths. Volume-to-capacity ratios above this value resulted in an increase in violations due primarily to an increase in delay.

Table 6-2. Predicted Effect of Selected Factors on Red-Light Violation Frequency.

Factor	Effect of a Reduction in the Factor Value [1]		Effect of an Increase in the Factor Value [1]	
	Factor Change	Violation Freq. Change	Factor Change	Violation Freq. Change
Approach flow rate	-1.0 %	-1.0 %	+1.0 %	+1.0 %
Cycle length	-20 s	+20 to +50 %	+20 s	−17 to -23 %
Yellow interval duration	-1.0 s	+100 %	+1.0 s	−60 %
85th Percentile speed	-10 mph	-50 %	+10 mph	+70 %
Clearance path length	-40 ft	+38 %	+40 ft	−30 %
Heavy-vehicle percentage	-5.0 %	-19 %	+5.0 %	+20 %
Volume-to-capacity ratio	-0.1	-10 to -40 %	+0.1	+10 to +100 %
Use of back plates	remove back plates	+33 %	add back plates	−25 %

Note:
1 - Negative changes represent a reduction in the associated factor.

A procedure was developed for identifying intersections with the potential for red-light-related safety improvement. The procedure combines the empirical Bayes method with the calibrated violation prediction model to estimate the expected violation frequency for the subject intersection approach. This estimate is then used to compute an index value that serves as an indicator of the extent of the violation problem for the subject approach. In general, approaches associated with a positive index value have more violations than the "typical" approach. An approach with an index of 2.0 is likely to have a greater problem than an approach with an index of 1.0. Greater certainty in the need for treatment can be associated with higher index values.

Red-Light Violation Causes and Countermeasures

A database was assembled to examine the characteristics of red-light-related crashes for the purpose of identifying the most appropriate set of countermeasures to use in treating problem locations. The characteristics considered include crash type and the duration of time the signal indication was red prior to the crash. This latter characteristic is defined herein as "time-into-red."

The database assembled for this investigation includes the time of crash and crash type for each of 63 red-light-related crashes representing intersections in five states. Photos from enforcement cameras were the primary source of these data.

Analysis of the data indicated that the median time-into-red for left-turn-opposed crashes is only 0.9 s whereas that for right-angle crashes is 8.9 s. This trend is consistent with that reported by Milazzo et al. (7). An examination of the distribution of crash frequency and type by time-into-red indicates that the frequency of red-light-related crashes tends to be highest in the first 5 s of red. Crash frequency declines thereafter, reaching a nominally small but constant frequency after 20 s of red.

CONCLUSIONS

Several conclusions are reached based on the findings of this research. These conclusions are summarized in this section.

The objective of a red-light-running treatment program should be the reduction of red-light-related crashes (as opposed to red-light violations). Countermeasures that reduce red-light-related crashes will likely also reduce violations.

The identification of intersections with the potential for safety improvement (i.e., "problem" locations) should be based on an evaluation of individual intersection approaches. The need for treatment at a specific approach should be based on the difference between expected crash frequency for that approach and that for the "typical" approach. Intersection approaches that have an expected crash frequency that exceeds that of the typical approach have the greatest potential for improvement.

To ensure reasonable certainty in the identification of problem locations, the aforementioned difference in crash frequency should be divided by its standard deviation. The resulting quotient represents a dimensionless "index" that serves as an indicator of the extent of the red-light-related crash problem for the subject approach. In general, approaches associated with a positive index value have more red-light-related crashes than the "typical" approach. An approach with an index of 2.0 is likely to have a greater problem than an approach with an index of 1.0. Greater certainty in the need for treatment can be associated with higher index values.

Any treatment of a problem intersection approach should be intended to return the approach's expected crash frequency to a level that is consistent with that of the typical approach. The implementation of countermeasures with the intent to reduce crashes below that of the typical approach represents "over treatment." Over treatment is not likely to be cost-effective.

Treatment programs for locations with red-light-related problems should follow a sequential process that includes the following steps:

1. Conduct an engineering study to confirm the nature and extent of the problem.
2. Identify and implement viable enforcement countermeasures.
3. Evaluate the effectiveness of the implemented countermeasures.
4. If red-light-related problems still exist, consider implementation and evaluation of additional (or other) engineering countermeasures until all viable countermeasures have been tried.
5. If red-light-related problems still exist, consider the implementation of an officer enforcement program that targets intersection traffic control violations and includes a public awareness campaign.
6. If officer enforcement is determined to be unsuccessful or ineffective, then camera enforcement can be considered. If camera enforcement is implemented, it should be

accompanied by a public awareness campaign. Also, rear-end crashes should be monitored and remedial action taken if a sustained increase in rear-end crashes is observed.

In general, countermeasure selection to address a problem location should be based on a comprehensive engineering study of traffic conditions, traffic control device visibility, crash history, and intersection sight distance. The findings from the engineering analysis can then be used with the procedure outlined in Figure 5-6 to determine the most viable set of countermeasures.

The following specific conclusions are reached as a result of the analysis of the data collected for this research:

- Red-light-related crashes represent about 30 percent of all crashes that occur at signalized intersections in Texas.
- Red-light-related crashes are influenced by, or correlated with, several intersection factors. These relationships were exploited in the development of a crash prediction model. This model can be used to predict the expected crash frequency for an intersection approach based on the following factors: approach leg AADT, yellow interval duration, speed limit, and clearance time.
- The calibrated crash prediction model indicates that red-light-related crashes tend to be at a minimum value when the clearance time is about 2.5 s. This time corresponds to clearance path widths of 110, 120, 150, and 165 ft for speed limits of 30, 35, 40, and 45 mph, respectively.
- Area-wide officer enforcement of intersection traffic control devices will reduce red-light-related crashes by 6.4 percent during the time of the enforcement activity.
- Heavy vehicle operators are more than twice as likely to run the red indication as passenger car drivers.
- Red-light violations are influenced by, or correlated with, several intersection factors. These relationships were exploited in the development of a violation prediction model. This model can be used to predict the expected violation frequency for an intersection approach based on the following factors: yellow interval duration, use of signal head back plates, 85th percentile speed, clearance path length, heavy-vehicle percentage, and volume-to-capacity ratio.
- Red-light violations are at their lowest level when the volume-to-capacity ratio is in the range of 0.6 to 0.7. This range of ratios yields minimal violations, regardless of speed, path length, yellow duration, heavy-vehicle percentage, cycle length, phase duration, or traffic volume.
- Enforcement efforts are likely to reduce violations occurring primarily in the first few seconds of red and, therefore, should significantly reduce left-turn-opposed crashes. In an indirect manner, these efforts should also reduce some right-angle crashes by encouraging driver compliance with the signal. In contrast, engineering countermeasures are most likely to reduce violations throughout the red and, therefore, reduce both right-angle and left-turn-opposed crashes in somewhat equal proportion.
- Increasing the all-red interval is likely to reduce the portion of right-angle crashes that occur in the first few seconds of red. However, right-angle crashes are relatively infrequent in the

first few seconds of red, so increasing the all-red interval may not significantly reduce the total number of right-angle crashes.

CHAPTER 7. REFERENCES

1. Retting, R.A., R.G. Ulmer, and A.F. Williams. "Prevalence and Characteristics of Red-Light-Running Crashes in the United States." *Accident Analysis and Prevention*. Vol. 31, 1999, pp. 687-694.

2. "Red-Light-Running Factors into More than 800 Deaths Annually." News Release. Insurance Institute for Highway Safety, Arlington, Virginia, July 13, 2000.

3. Quiroga, C., E. Kraus, I. van Schalkwyk, and J. Bonneson. *Red Light Running–A Policy Review.* Report No. TX-02/150206-1. Texas Transportation Institute, Texas A&M University System, College Station, Texas, March 2003.

4. Retting, R.A., A.F. Williams, and M.A. Greene. "Red-Light Running and Sensible Countermeasures." *Transportation Research Record 1640.* Transportation Research Board, National Research Council, Washington, D.C., 1998, pp. 23-26.

5. *The Red Light Running Crisis: Is It Intentional?* Office of the Majority Leader, U.S. House of Representatives, May 2001.

6. California State Auditor. *Red Light Camera Programs: Although They Have Contributed to a Reduction in Accidents, Operational Weaknesses Exist at the Local Level*. Report 2001-125, Bureau of State Audits, Sacramento, California, July 2002.

7. Milazzo, J.S., J.E. Hummer, and L.M. Prothe. *A Recommended Policy for Automated Electronic Traffic Enforcement of Red Light Running Violations in North Carolina.* Final Report. Institute for Transportation Research and Education, North Carolina State University, Raleigh, North Carolina, June 2001.

8. Hauer, E. "Identification of Sites with Promise." *Transportation Research Record 1542*. Transportation Research Board, Washington, D.C., 1996, pp. 54-60.

9. Hauer, E. *Observational Before-After Studies in Road Safety.* Pergamon Press, Elsevier Science Ltd., Oxford, United Kingdom, 1997.

10. Persaud, B., C. Lyon, and T. Nguyen. "Empirical Bayes Procedure for Ranking Sites for Safety Investigation by Potential for Safety Improvement." *Transportation Research Record 1665*. Transportation Research Board, Washington, D.C., 1999, pp. 7-12.

11. Bonneson, J., K. Zimmerman, and C. Quiroga. *Review and Evaluation of Enforcement Issues and Safety Statistics Related to Red-Light-Running.* Report No. FHWA/TX-04/4196-1. Texas Department of Transportation, Austin, Texas, September 2003.

12. Mohamedshah, Y.M., L.W. Chen, and F.M. Council. "Association of Selected Intersection Factors with Red Light Running Crashes." *Proceedings of the 70th Annual ITE Conference.* (CD-ROM). Institute of Transportation Engineers, Washington, D.C., August 2000.

13. Bonneson, J., K. Zimmerman, and M. Brewer. *Engineering Countermeasures to Reduce Red-Light-Running.* Report No. FHWA/TX-03/4027-2. Texas Department of Transportation, Austin, Texas, August 2002.

14. "Determining Vehicle Change Intervals (proposed recommended practice)." ITE Technical Committee 4A-16. *ITE Journal*, Vol. 57, No. 7. Institute of Transportation Engineers, Washington, D.C., 1989, pp. 21-27.

15. Retting, R.A., and M.A. Greene. "Influence of Traffic Signal Timing on Red-Light Running and Potential Vehicle Conflicts at Urban Intersections." *Transportation Research Record 1595*. Transportation Research Board, Washington D.C., 1997, pp. 1-7.

16. McCullagh, P., and J.A. Nelder. *Generalized Linear Models*, Chapman and Hall, New York, New York, 1983.

17. Abbess, C., D. Jarrett, and C.C. Wright. "Accidents at Black-Spots: Estimating the Effectiveness of Remedial Treatment, with Special Reference to the 'Regression-to-the-Mean' Effect." *Traffic Engineering and Control*, Vol. 22, No. 10, October 1981, pp. 535-542.

18. *SAS/STAT User's Guide, Version 6*, 4th ed., SAS Institute, Inc., Cary, North Carolina, 1990.

19. Sawalha, Z., and T. Sayed. "Statistical Issues in Traffic Accident Modeling." Paper No. 03-2137. Presented at the 82nd Annual Meeting of the Transportation Research Board, Washington, D.C., 2003.

20. Miaou, S.P. *Measuring the Goodness-of-Fit of Accident Prediction Models.* Report No. FHWA-RD-96-040. Federal Highway Administration, Washington, D.C., 1996.

21. *Stop on Red = Safe on Green: A Guide to Red Light Camera Programs.* National Campaign to Stop Red-Light Running. Washington, D.C. www.stopredlightrunning.com, 2002.

22. Maccubbin, R.P., B.L. Staples, and A.E. Salwin. *Automated Enforcement of Traffic Signals: A Literature Review.* Federal Highway Administration, Washington, D.C., August 2001.

23. Cooper, P.J. "Effects of Increased Enforcement at Urban Intersections on Driver Behavior and Safety." *Transportation Research Record 540*. Transportation Research Board, National Research Council, Washington, D.C., 1975, pp. 13-21.

24. Krulikowski, E.C., and T. Holman. "Supplemental Red Light Photo Enforcement with RAT Lights in the City of El Cajon." *Westernite* Newsletter. Vol. 56, No. 3. District 6 of the Institute of Transportation Engineers, May/June 2002, pp. 2-3.

25. Newstead, S.V., M.H. Cameron, and M.W. Leggett. "The Crash Reduction Effectiveness of a Network-Wide Traffic Police Deployment System." *Accident Analysis and Prevention*, Vol. 33, 2001, pp. 393–406.

26. Retting, R.A., S.A. Ferguson, and A.S. Hakkert. "Effects of Red Light Cameras on Violations and Crashes: A Review of the International Literature." *Traffic Injury Prevention,* Vol. 4, 2003, pp 17-23.

27. *2000 Census: Population of Texas Cities.* Texas State Library and Archives Commission. Austin, Texas, August 2003. www.tsl.state.tx.us

28. *Highway Capacity Manual.* 4th ed. Transportation Research Board, Washington, D.C., 2000.

29. Zegeer, C.V., and R.C. Deen. "Green-Extension Systems at High-Speed Intersections." *ITE Journal*, Institute of Transportation Engineers, Washington, D.C., November 1978, pp. 19-24.

30. Kamyab, A., T. McDonald, J. Stribiak, and B. Storm. *Red Light Running in Iowa: The Scope, Impact, and Possible Implications.* Final Report. Center for Transportation Research and Education, Iowa State University, Ames, Iowa, December 2000.

31. Baguley, C.J. "Running the Red at Signals on High-Speed Roads." *Traffic Engineering & Control.* Crowthorne, England, July/August 1988, pp. 415-420.

32. Van der Horst, R., and A. Wilmink. "Drivers' Decision-Making at Signalized Intersections: An Optimization of the Yellow Timing." *Traffic Engineering & Control.* Crowthorne, England, December 1986, pp. 615-622.

33. Bonneson, J.A., and P.T. McCoy. "Average Duration and Performance of Actuated Signal Phases." *Transportation Research: Part A–Administrative.* Vol. 29A, No. 6. Elsevier Science Ltd., Great Britain, November/December 1995, pp. 429-443.

34. Hauer, E. "Left-Turn Protection, Safety, Delay, and Guidelines: A Literature Review." Draft. Available at: http://members.rogers.com/hauer/, October 2004.

35. Polanis, S. "Improving Intersection Safety Through Design and Operations." *Compendium of Papers for the ITE Spring Conference*. (CD-ROM) Institute of Transportation Engineers, Washington, D.C., March 2002.

36. Farraher, B.A., R. Weinholzer, and M.P. Kowski. "The Effect of Advanced Warning Flashers on Red Light Running–A Study Using Motion Imaging Recording System Technology at Trunk Highway 169 and Pioneer Trail in Bloomington, Minnesota." *Compendium of Technical Papers for the 69th Annual ITE Meeting.* (CD-ROM) Institute of Transportation Engineers, Washington, D.C., 1999.

37. Retting, R.A., A.F. Williams, C.M. Farmer, and A.F. Feldman. "Evaluation of Red Light Camera Enforcement in Oxnard, California." *Accident Analysis and Prevention*, Vol. 31, 1999, pp. 169-174.

38. McGee, H.W. *Making Intersections Safer: A Toolbox of Engineering Countermeasures to Reduce Red-Light Running*. Institute of Transportation Engineers, Washington, D.C., 2003.

39. PB Farradyne. *City of San Diego Photo Enforcement System Review.* Final Report. City of San Diego Police Department, San Diego, California, January 2002.

40. Harwood, D.W., F.M. Council, E. Hauer, W.E. Hughes, and A. Vogt. *Prediction of the Expected Safety Performance of Rural Two-Lane Highways.* Report No. FHWA-RD-99-207. Federal Highway Administration, Washington, D.C., 2000.

41. McGee, H., T. Sunil, and B. Persaud. *NCHRP Report 491: Crash Experience Warrant for Traffic Signals*. Transportation Research Board, National Research Council, Washington, D.C., 2003.

42. Hauer, E., D.W. Harwood, F.M. Council, and M.S. Griffith. "Estimating Safety by the Empirical Bayes Method: A Tutorial." *Transportation Research Record 1784*. Transportation Research Board, National Research Council, Washington, D.C., 2002, pp. 126-131.

APPENDIX

ESTIMATION OF EXPECTED LEFT-TURN CRASH FREQUENCY

ESTIMATION OF EXPECTED LEFT-TURN CRASH FREQUENCY

OVERVIEW

This appendix describes the development of a method for estimating the expected crash frequency of a specified subset of crashes for which the only prediction model available is that for predicting total crash frequency. In this situation, a prediction model is not available for directly estimating the frequency of the crash subset. For example, a model for predicting the expected severe red-light-related crash frequency is developed in Chapter 2 (and Chapter 3); however, the frequency of severe red-light-related, left-turn-opposed crashes is a sufficiently small subset of all crashes as to frustrate the development of an accurate left-turn-opposed crash prediction model.

Initially, the need for a subset crash estimation method is described. Then, a method developed by Harwood et al. (*40*) for FHWA is reviewed and its underlying assumptions identified. Next, a variation of the FHWA method is described that overcomes some specified weaknesses. Finally, the method is illustrated in an example application.

LITERATURE REVIEW

Background

The empirical Bayes method is used in Chapter 2 to obtain an unbiased estimate of the red-light-related crash frequency for a specific intersection approach (it is also used in Chapter 3 for area-wide crash estimation). The unbiased estimate is based on a weighted combination of the reported frequency of red-light-related crashes x on the subject approach and the predicted red-light-related crash frequency $E[r]$ of similar approaches. The unbiased estimate (i.e., $E[r|x]$) is a more accurate estimate of the expected red-light-related crash frequency on the subject approach than either of the individual values (i.e., $E[r]$ or x). The following equations were offered in Chapter 2 to compute $E[r|x]$:

$$E[r|x] = E[r] \times weight + \frac{x}{y} \times (1 - weight) \quad \textbf{(A-1)}$$

with,

$$weight = \left(1 + \frac{E[r]\,y}{k}\right)^{-1} \quad \textbf{(A-2)}$$

where,

$E[r|x]$ = expected red-light-related crash frequency given that x crashes were reported in y years, crashes/yr;

$E[r]$ = expected severe red-light-related crash frequency for the subject approach, crashes/yr;
x = reported red-light-related crash frequency, crashes;
y = time interval during which x crashes were reported, yr;
k = dispersion parameter; and
weight = relative weight given to the prediction of expected red-light-related crash frequency.

The equations developed in Chapters 2 and 3 apply to severe (i.e., injury or fatal) crashes. However, Equation A-1 is not restricted to this specific category of crashes. It can also be used to estimate the expected crash frequency for other crash categories and types, such as the expected number of total crashes (i.e., property-damage-only, injury, and fatal) or the expected number of left-turn-opposed crashes. The only caveats to these applications are: (1) x must represent the reported number of crashes of the specified type, and (2) the equation used to compute $E[r]$ must be calibrated to estimate the expected frequency of crashes of the specified type.

The second caveat mentioned in the previous paragraph often poses a significant challenge because the development of models applicable to only a subset of the crash population (e.g., a model for predicting only severe crashes or a model for predicting only left-turn-opposed crashes) is based on only a portion of the available crash database. Such partitioning of the database reduces the sample size for model calibration and, given the extreme randomness in crash data, can severely limit the accuracy of the resulting "subset" model.

FHWA Subset Crash Estimation Method

In recognition of the aforementioned limitations of "subset" model development, Harwood et al. (*40*) developed a method for estimating severe crash frequency $E[c]_{fi}$ using a model that predicts total crash frequency $E[c]$. The method begins with the use of the following equation to estimate severe crash frequency:

$$E[c]_{fi} = E[c] \times p_{fi} \quad \textbf{(A-3)}$$

where,
$E[c]_{fi}$ = expected severe crash frequency, crashes/yr;
p_{fi} = portion of severe crashes; and
$E[c]$ = expected total crash frequency, crashes/yr.

As a second step, Harwood et al. recommend the use of Equation A-1 and the estimate from Equation A-3 to obtain the expected severe crash frequency for a specific location $E[c|x]_{fi}$. This method is based on two assumptions. Each assumption is discussed in the following sections.

Assumption 1: Dispersion Parameter Equality

Harwood et al. (*40*) recommend that value of *weight* computed using Equation A-2 should be based on the dispersion parameter k for the "total crash" model. The use of this parameter

represents an assumption that the dispersion parameter associated with Equation A-3 for the severe crash data is the same as that for the total crash data (i.e., $k_{fi} = k$).

The accuracy of the aforementioned assumption was investigated using data reported by McGee et al. (*41*). They developed models for four crash-type categories: total severe crashes, severe left-turn crashes, severe rear-end crashes, and severe right-angle crashes. A crash-type model was developed for each combination of three- and four-leg intersections at stop-controlled and at signal-controlled intersections. A total of 32 prediction models were developed. Each model was associated with a unique dispersion parameter.

The reported dispersion parameters for the "total severe crash" models were compared with the parameters obtained for the three crash-type subset models. The results are shown in Figure A-1. The y-axis in this figure represents the ratio of the dispersion parameter k_i for crash-type category i to the dispersion parameter for the "total severe crash" model k.

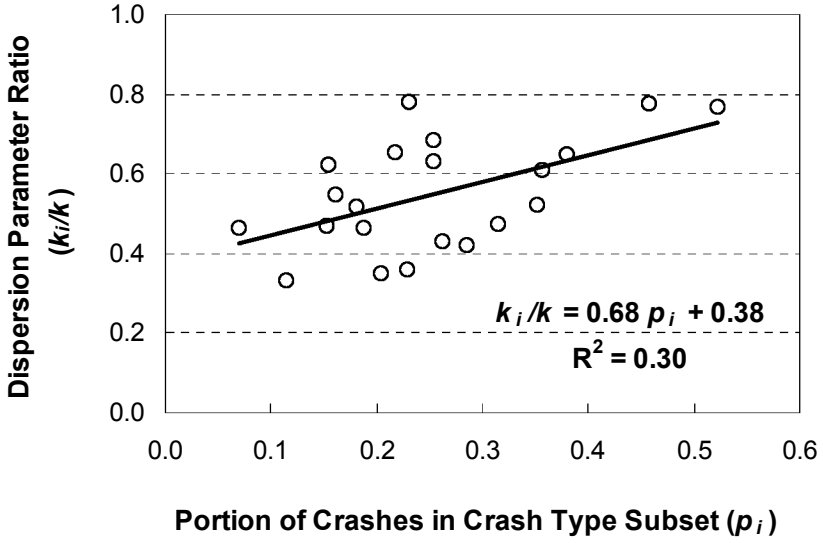

Figure A-1. Relationship between Portion Crashes in Subset and Dispersion Parameter Ratio.

The data in Figure A-1 indicate that the dispersion parameters for the crash-type subset models is not equal to the dispersion parameter of the "total severe crash" model (i.e., $k_{fi} \neq k$). Equality of these two parameters would have been evidenced by the data being clustered about the ratio of 1.0 and independent of the portion of crashes in the subset. Rather, the subset dispersion parameters k_i range from 35 to 80 percent of k, the amount being correlated with the portion of crashes in the subset p_i. A more detailed analysis did not indicate any correlation between crash type and the dispersion parameter ratio. These findings suggest that the assumption by Harwood et al. (*40*) is relatively weak.

Assumption 2: Bias Correction

The method recommended by Harwood et al. (*40*) for estimating severe crash frequency consists of several steps. First, Equation A-1 is used for each crash subset (i.e., once for property-damage-only crashes, once for severe crashes). Then, it is used to estimate "total crash" frequency. This application yields three crash frequency estimates: $E[c|x]_{pdo}$, $E[c|x]_{fi}$, and $E[c|x]$.

At this point in the method, Harwood et al. (*40*) note that the sum of the estimates for the individual subsets do not add to that obtained for total crashes (i.e., $E[c|x]_{pdo} + E[c|x]_{fi} \neq E[c|x]$) but that they theoretically should add to this value. To overcome this bias, they recommend a third step that involves a bias correction. In this step, the following equation is used to estimate the "corrected" severe crash frequency:

$$E[c|x]_{fi}^{*} = E[c|x]\left(\frac{E[c|x]_{fi}}{E[c|x]_{fi} + E[c|x]_{pdo}}\right) \qquad \textbf{(A-4)}$$

where,

$E[c|x]_{fi}^{*}$ = expected severe crash frequency (corrected) given that x severe crashes were reported, crashes/yr; and

$E[c|x]$ = expected total crash frequency given that x crashes were reported, crashes/yr.

A similar equation is offered for correcting the property-damage-only crash estimate. The corrected estimates thus obtained sum to equal $E[c|x]$ and are offered as unbiased estimates of $E[c|x]_{pdo}$ and $E[c|x]_{fi}$.

The basis for development of the bias correction step is not described by Harwood et al. (*40*). However, it is discussed by Hauer et al. (*42*) in a subsequent publication and appears to be based on an ad hoc method of correcting for the bias in the component terms. The correct way of removing the bias is noted by Hauer et al. to be available but would add additional parameters and complexity.

The accuracy of the bias correction step described by Harwood et al. (*40*) has not been documented in other literature. It is likely to be sufficiently accurate to yield reasonable estimates of $E[c|x]$ for subset crash types. However, the step does not specify how to obtain an accurate estimate of *weight* for each subset. An accurate estimate of this variable is needed when the empirical Bayes method is extended to the identification of problem locations (i.e., when using Equations 10 and 23).

METHOD DEVELOPMENT

An alternative subset crash estimation method is developed in this section that can be used to estimate the expected crash frequency of crash category i (e.g., left-turn-opposed crashes) and corresponding values of k_i and $weight_i$. The approach is based on the availability of a crash

prediction model that has been previously developed for estimating "total" crashes. The expected crash frequency for a specified subset of crashes using this model is obtained by multiplying the total crash estimate from the prediction model by the portion of crashes represented by the specified subset category (i.e., consistent with Equation A-3). The advantage of this method is that it does not share the limitations associated with the method described in the previous section.

The remainder of this section describes the development of a method for predicting severe red-light-related, left-turn-opposed crashes. However, the method can be extended to the prediction of crash frequency for other crash categories. The development is based on the severe red-light-related crash prediction model developed in Chapter 2 for local intersection analysis (i.e., Equation 6). The modeling approach can also be extended to area-wide analyses using the crash prediction model described in Chapter 3 (i.e., Equation 16). The following equation is used to estimate the expected left-turn-opposed crash frequency:

$$E[r]_{lt} = E[r] \times p_{lt} \quad \textbf{(A-5)}$$

where,

$E[r]_{lt}$ = expected severe red-light-related, left-turn-opposed, crash frequency, crashes/yr;
p_{lt} = portion of severe red-light-related crashes that are defined as "left-turn-opposed" (use 0.15); and
$E[r]$ = expected severe red-light-related crash frequency for the subject approach, crashes/yr.

An analysis of the distribution of red-light-related crash types by Bonneson et al. (*11*) indicates that left-turn-opposed crashes represent 15 percent of all red-light-related crashes.

The trend line in Figure A-1 indicates that the dispersion parameter associated with Equation A-5 can be estimated using a linear equation. However, the equation shown in the figure does not comply with a necessary boundary condition. Specifically, the subset dispersion factor k_i should converge to the dispersion parameter for total crashes k as the portion of crashes in the subset p_i approaches 1.0 (i.e., the dispersion parameter ratio should equal 1.0 when $p_i = 1.0$).

A second boundary condition was also established during the investigation regarding the relationship among k, k_i, and p_i. Specifically, the value of k_i used in Equation A-2 should yield estimates of the expected subset crash frequency from Equation A-1 that add to the value estimated for total crashes (i.e., $E[c|x]_{lt} + E[c|x]_{other} = E[c|x]$).

Several functional forms for the relationship among k, k_i, and p_i were evaluated. The form that provides compliance with the aforementioned boundary conditions, overcomes the aforementioned limitations of the method described by Harwood et al. (*40*), and is reasonably consistent with the trends in Figure A-1 is:

$$k_{lt} = k \times p_{lt} \quad \textbf{(A-6)}$$

where,

k_{lt} = estimated dispersion parameter for left-turn-opposed crashes; and
k = dispersion parameter for total-crash prediction model.

The form of Equation A-6 implies a linear relationship between p_i and the dispersion parameter ratio k_i/k with an intercept of 0.0 and a slope of 1.0. These values compare with the 0.38 and 0.68 shown in Figure A-1. Alternative forms of Equation A-6 that included these parameters, or similar, were all found to have undesirable features. Specifically, use of the linear equation shown in Figure A-1 violated both boundary conditions. A slight modification of the slope and intercept values was found to yield compliance with the first boundary condition and yield an equally good fit to the data in Figure A-1. However, an additional adjustment factor was needed in Equation A-1 to ensure compliance with the second boundary condition. Solutions that included the additional adjustment factor were found to be unduly complex in their mathematical representation, relative to the simplicity and fit obtained with Equation A-6.

The implication of Equation A-6 is that the *weight* variable is the same for the "total crash" estimate as it is for any one crash-type subset. The use of identical *weight* variables for each crash subset ensures that the sum of the expected crash frequencies will equal the total crash frequency.

METHOD APPLICATION

The estimation method developed in the previous section is illustrated in this section in terms of an example application. Consider an intersection approach for which three severe red-light-related crashes were reported in the previous year. One of these crashes was identified as left-turn-opposed. The traffic, signal timing, and geometric conditions for the intersection approach were input to Equation 6 to find that the expected severe red-light-related crash frequency for similar approaches *E[r]* is 0.60 crashes/yr. Table 2-6 indicates that this model has a dispersion parameter of 4.0. These data are shown in Table A-1.

Equation A-5 is used to estimate the expected crash frequency for the "left-turn-opposed" and "other" crash categories. The results are shown in the third row of computations in Table A-1. Equation A-6 is used to estimate the dispersion parameter for each crash category. These results are shown in the fourth row. Equation A-2 is used to compute the *weight* variable. It should be noted that the value of this variable is identical for all crash categories. Finally, Equation A-1 is used to compute the expected crash frequency given that *x* crashes were reported.

In this example application, as with any application of the recommended method, the data in the first six rows of the crash-type columns (i.e., columns 2 and 3) add to the values shown in the total-crash column (i.e., column 4). The bias correction step recommended by Harwood et al. (*40*) is not necessary with the proposed estimation method.

The last three rows of Table A-1 illustrate the application of the problem location identification procedures (i.e., Equations 10, 11, and 12 of Chapter 2; and Equations 23, 24, and 25

of Chapter 3). The index values for the two crash types do not exceed 1.0, which is offered as the threshold for identifying locations with a likely red-light-related crash problem. Hence, it can be concluded that neither left-turn-opposed or total red-light-related crashes are over-represented at this intersection.

Table A-1. Application of Left-Turn-Opposed Crash Frequency Estimation Method.

Statistic	Crash Type Category		Total Severe Red-Light-Related Crashes
	Left-Turn-Opposed	Other	
Portion of total crashes (p) [1]	0.15	0.85	1.00
Reported crashes (x), crashes/yr	1	2	3
Expected crash freq. ($E[r]$), crashes/yr	0.09	0.51	0.60
Dispersion parameter (k)	0.6	3.4	4.0
weight	0.87	0.87	0.87
Expected crash freq. given that x crashes were reported ($E[r\|x]$), crashes/yr	0.21	0.70	0.91
Variance of $E[r]$	0.0001	0.0004	0.0005
Variance of $E[r\|x]$	0.0273	0.0910	0.1183
Index	0.73	0.63	0.90

Note:
1 - Portion of red-light-related, left-turn-opposed crashes is based on data reported by Bonneson et al. (*11*).